UNIVERSITÄT AUGSBURG
Universitätsbibliothek

OPEN ACCESS
OPUS AUGSBURG

Coherent control of currents through molecular wires

Jörg Lehmann

Angaben zur Veröffentlichung / Publication details:

Lehmann, Jörg. 2003. "Coherent control of currents through molecular wires." Aachen: Shaker.

Nutzungsbedingungen / Terms of use:

licgercopyright

Dieses Dokument wird unter folgenden Bedingungen zur Verfügung gestellt: / This document is made available under these conditions:
Deutsches Urheberrecht
Weitere Informationen finden Sie unter: / For more information see:
https://www.uni-augsburg.de/de/organisation/bibliothek/publizieren-zitieren-archivieren/publiz/

Coherent control of currents through molecular wires

Zur Erlangung des akademischen Grades eines
Doktors der Naturwissenschaften
der Mathematisch-Naturwissenschaftlichen Fakultät
der Universität Augsburg vorgelegte

Dissertation

von
Dipl.-Phys. Jörg Lehmann
aus
Augsburg

Augsburg, im Mai 2003

published by Shaker Verlag, Aachen, ISBN 3-8322-1979-X

Erstberichterstatter:	Prof. Dr. Peter Hänggi
Zweitberichterstatter:	Prof. Dr. Ulrich Eckern
Drittberichterstatter:	Dr. habil. Volkhard May
Tag der mündlichen Prüfung:	8. Juli 2003

published by Shaker Verlag, Aachen, ISBN 3-8322-1979-X

Contents

1 Introduction **1**

2 Floquet theory **5**
2.1 Floquet's theorem and basic observations 5
2.2 Sambe space 6
2.2.1 Definition 6
2.2.2 Floquet theory in Sambe space 7
2.3 Numerical methods 8
2.4 Space-time symmetries of a system driven by a dipole field 10
2.4.1 Generalised parity 11
2.4.2 Time-inversion parity 11
2.5 Example: The driven two-level system 12
2.5.1 Perturbation theory in the limit of fast external driving 12
2.5.2 Coherent destruction of tunnelling 14
2.5.3 Dynamical symmetry breaking 17
2.6 Summary 17

3 Dynamics of a driven molecular wire **21**
3.1 The wire and its environment 21
3.1.1 Coupling to electronic leads 23
3.1.2 Coupling to phonon baths 24
3.2 Kinetic equation approach 25
3.2.1 Coherent dynamics 27
3.2.2 Incoherent dynamics 28
3.3 Rotating-wave approximation 33
3.4 Analytical solutions for two special cases 35
3.4.1 Thermal equilibrium 35
3.4.2 Equal coupling to all leads in the wide-band limit without electron-phonon coupling 35
3.5 Numerical solution of the kinetic equation 36

published by Shaker Verlag, Aachen, ISBN 3-8322-1979-X

3.6 Summary . . . 37

4 Electrical current through the wire 39
4.1 Time-dependent electrical current . . . 39
4.2 Time-averaged current . . . 41
4.2.1 Equal coupling to all leads . . . 42
4.2.2 Rotating-wave approximation . . . 42
4.3 Summary . . . 43

5 Coherent current control 45
5.1 Tight-binding model for the wire . . . 45
5.2 Current spectroscopy . . . 47
5.2.1 Average current at resonant excitations . . . 48
5.3 Rectification of driving induced currents . . . 51
5.3.1 Symmetries . . . 52
5.3.2 Rectification in two-level systems . . . 55
5.3.3 Rectification in long wires . . . 59
5.4 Current switches . . . 67
5.4.1 Current gate . . . 67
5.4.2 Current router: molecular transistor . . . 70

6 Summary and outlook 77

A Perturbation theory for the driven two-level system 81
A.1 General expression . . . 81
A.2 Application to the two-level system . . . 82

B Rotating-wave approximation 85

C Equilibrium solution of the kinetic equation 91

References 93

Acknowledgement 103

published by Shaker Verlag, Aachen, ISBN 3-8322-1979-X

Why cannot we write the entire 24 volumes of the Encyclopedia Brittanica on the head of a pin?

—Richard Feynman, There is plenty of room at the bottom

1 Introduction

Over the last decades, the ongoing miniaturisation of electronic circuits has been the principal driving force behind the technological progress. Indeed we have been witnessing an even exponential decrease of the typical structure sizes of integrated circuits with time, just as has already been predicted by Gordon E. Moore in the mid '60s of the last century [1]. According to the current roadmap of the semiconductor industry [2], this trend should last for at least one more decade with the current silicon semiconductor-based technology. Interestingly enough, the miniaturisation process will most probably not be limited by the laws of physics but by the fact—known as Rock's law—that the cost of capital equipment for the fabrication of semiconductors doubles every four years. By contrast, from a physical point of view, there is still "plenty of room at the bottom", to quote from the title of Richard Feynman's visionary lecture, which already in 1959 anticipated a new era of nanotechnology [3]. In his lecture, Feynman asked the "final question, whether, ultimately—in the great future—we can arrange atoms the way we want; the very atoms, all the way down!" But it should take about a quarter of a century, until this question was answered positively. Then, using the scanning tunnelling microscope (STM) technique [4], for the first time the selective manipulation of matter at the nanoscale was demonstrated in an experiment [5].

Feynman pointed out another important fact, namely that "atoms on a small scale behave like nothing on a large scale, for they satisfy the laws of quantum mechanics." A particularly prominent example for this is the discreteness of the energy of electronic levels in molecules. The intriguing idea to use this fact for the realisation of an electronic device came up in 1974, when Aviram and Ratner proposed to build a diode from an individual organic molecule [6]. Since then, the vision of completely molecule-based electronic circuits ("molecular electronics") has inspired a huge body of scientific research [7–9].

Starting from 1997, first experimental results for the measurement of electrical currents across one or a few organic molecules have been reported. The typical setup consists of a self-assembled monolayer (SAM) formed by the molecules binding to a gold surface via thiol end-groups. The contact to the other end of the molecule can then either be formed by an STM tip [10, 11] or by another gold surface. In the latter case, a mechanically controllable break-junction technique [12], known from atomic

published by Shaker Verlag, Aachen, ISBN 3-8322-1979-X

point contact experiments [13–15], is used to control the distance between the two metal surfaces. As a third possibility, a small patch of molecules may be created in a nanopore [16]. All these early experiments shared the problem that it was not clear whether only one single molecule—as opposed to a few ones—had been contacted. In order to definitely measure the conductance of individual molecules, it was necessary to dilute the concentration of conducting molecules on the surface, either by using a sub-monolayer coverage of the metal surface or by attaching the conducting thiol end-groups to only a small fraction of the molecules. For the first convincing realisation of the former variant, the break-junction technique was used [17, 18]. At about the same time, an experiment based upon the latter method was carried through [19]. Thereby, the contact on the top-side of the SAM was established indirectly via previously applied gold nanoparticles, which then have been addressed by a gold-coated atomic force microscope (AFM) tip. In the experiment, one then observes an ensemble of current voltage curves, which turn out to be quantised as integer multiples of a fundamental curve, corresponding to single-molecule conductance.

Both from an experimental and a practical point of view, it would be desirable to have an additional handle on the molecule. Since the typical electronic excitation energies of molecules are of the order of an eV, corresponding to light quanta from the optical and infrared spectral range, it is conceivable to act upon the molecules by optical means. This would be especially favourable, because most of today's lasers operate in this very spectral regime. Optimally, a selective laser control of the electronic currents through single molecules would then be possible. That there exist indeed prospects for the practical realisation of such a setup, was shown very recently for the transport through a quantum dot, i.e., an artificial molecule, which was irradiated by a pulsed laser [20]. The measured photocurrent in this system showed the signatures of a coherent Rabi oscillation induced in the two-level system by the external laser field. A further promising candidate for quantum control is the so-called coherent destruction of tunnelling (CDT), i.e., the dynamical suppression of the tunnelling effect in an isolated bistable potential under the influence of a strong time-periodic external bias [21–26].

A different, widely studied phenomenon in strongly driven systems, is the so-called ratchet effect [27–32], i.e., the emergence of directed transport even though the net bias of all external forces vanishes. This effect, originally discovered for the overdamped classical Brownian motion in spatially periodic, but asymmetric systems far from thermal equilibrium, subsequently has also been put forward for dissipative, incoherent quantum Brownian motion [33–36]. In particular, an inversion of the ratchet current upon changing the temperature was predicted [33] and later on experimentally verified using semiconductor superlattices in GaAs-AlGaAs heterostructures [37]. More recently, the appearance of a ratchet current was also discussed in the opposite limit of a purely coherent, Hamiltonian dynamics [38–40]. Related to ratchets, which require a periodic potential, are electron pumps [41–44], which in fact may be regarded as a

published by Shaker Verlag, Aachen, ISBN 3-8322-1979-X

localised version of a ratchet.

The theoretical description of transport through nanosystems commonly relies on a scattering approach, which views conductance as transmission [45–47]. This initially purely phenomenological picture, known as Landauer formula, was subsequently derived from first principles in the linear-response regime [48]. In its original form, the Landauer formula is only applicable to transport in a static case. The extension of the formalism to the transport in the presence of oscillating fields was not obvious, although quite general results have already been obtained [49–51]. Not making use of Floquet theory, their practical relevance was, however, rather limited. On the other hand, the usefulness of the Floquet picture in the context of laser assisted molecular conduction has been realised for instance in the recent works [52–54]. Yet, by calculating the current through the system via an *ad hoc* extension of the Landauer formula, the theoretical basis of these approaches remained rather weak. Furthermore, the corresponding results are only valid in the linear-response regime; either implicitly in Refs. [52, 53] due to the use of an "independent channel approximation" or explicitly in Ref. [54]. A completely different description of the driven transport problem is possible in a situation with a weak wire-lead coupling. Then, the system dynamics can very efficiently be described within a master equation formalism [55, 56]. In this thesis, we will put forward a generalisation of this approach.

The outline of this thesis is as follows. In Chapter 2, we introduce basic concepts of the description of time-periodically driven systems within a Floquet theory—the theoretical groundwork for the rest of this work. Included is a discussion of symmetries occurring in driven systems and some remarks on the numerical methods, that have been employed. As an exemplary application serves the driven two-level system, to which we shall come back in the sequel of this work. In Chapter 3, we extend the description of the wire dynamics by taking into account the contact between the molecular environment consisting of macroscopic electronic leads and phonon modes of the surroundings. In a weak-coupling limit, this will lead to a description in terms of a kinetic equation. In the presence of electron-phonon coupling, this kinetic equation no longer assumes a linear form but, within a mean-field approximation, acquires nonlinear terms. Chapter 4 concludes the formal part of this thesis. Based upon the results from Chapters 2 and 3, we develop explicit formulae for the current flowing across the different molecule-lead contacts.

The application of the general formalism is demonstrated in Chapter 5 for three qualitatively different situations: (i) The resonant amplification of a small current flowing through the molecule when a small voltage between the leads is applied. (ii) The generation of a directed current in the absence of an external bias, i.e., a molecular ratchet or pump. (iii) The externally controllable switching and routing of currents in two- and three-terminal devices, based on the coherent control of the tunnelling dynamics, discussed above. Concluding remarks and perspectives for further work are given in Chapter 6. Finally, the appendices collect some more technical points.

published by Shaker Verlag, Aachen, ISBN 3-8322-1979-X

published by Shaker Verlag, Aachen, ISBN 3-8322-1979-X

2 Floquet theory

In this work, we investigate molecules that are under the influence of a strong external laser field. Within a semiclassical approximation for the laser field, its action can be described by a periodic time-dependence in the molecular Hamiltonian $H(t) = H(t+T)$, where T is the driving period [57]. Then, the standard way for the solution of the corresponding Schrödinger equation

$$\mathrm{i}\hbar \frac{\mathrm{d}}{\mathrm{d}t} |\Psi(t)\rangle = H(t)|\Psi(t)\rangle \tag{2.1}$$

via the separation ansatz $|\Psi(t)\rangle = \exp(-\mathrm{i}Et/\hbar)|\Phi\rangle$, where E is the eigenenergy of a state $|\Phi\rangle$, is no longer applicable. Moreover, we will consider below field strengths for which a perturbative treatment of the time-dependence is ruled out. Yet, the time-periodicity of the Hamiltonian allows to apply Floquet theory, a powerful tool, which we briefly review in the present chapter.

2.1 Floquet's theorem and basic observations

The basis of Floquet theory consists in the observation that for a time-periodic Hamiltonian, $H(t) = H(t+T)$, there exists a complete set $\{|\Psi_\alpha(t)\rangle\}$ of solutions of the Schrödinger equation (2.1) of the form

$$|\Psi_\alpha(t)\rangle = \mathrm{e}^{-\mathrm{i}\epsilon_\alpha t/\hbar} |\Phi_\alpha(t)\rangle \ , \quad |\Phi_\alpha(t)\rangle = |\Phi_\alpha(t+T)\rangle \ . \tag{2.2}$$

The time-periodic functions $|\Phi_\alpha(t)\rangle$ are called Floquet modes or Floquet states and the quantities ϵ_α are referred to as quasienergies. As one can verify by insertion of the ansatz (2.2) into (2.1), they obey the eigenvalue equation

$$\left(H(t) - \mathrm{i}\hbar \frac{\mathrm{d}}{\mathrm{d}t}\right) |\Phi_\alpha(t)\rangle = \epsilon_\alpha |\Phi_\alpha(t)\rangle \ . \tag{2.3}$$

Different methods can be used to prove Floquet's theorem. Here, we present a constructive argument. Diagonalising the one-period propagator $U(T,0)$, where $U(t,t')$ is the time-evolution operator corresponding to the Schrödinger equation (2.1), we

published by Shaker Verlag, Aachen, ISBN 3-8322-1979-X

obtain

$$U(T,0)|\Phi_\alpha(0)\rangle = \mathrm{e}^{-\mathrm{i}\epsilon_\alpha T/\hbar}\,|\Phi_\alpha(0)\rangle\ . \tag{2.4}$$

Here, we have used that all eigenvalues of a unitary operator have unit modulus and hence can be written in the given form for some real ϵ_α. Next, we use the eigenstates $|\Phi_\alpha(0)\rangle$ as initial states for the quantum mechanical time-evolution according to Eq. (2.1), yielding the solutions $|\Psi_\alpha(t)\rangle = U(t,0)|\Phi_\alpha(0)\rangle$ of the Schrödinger equation (2.1). This allows us to define the Floquet modes $|\Phi_\alpha(t)\rangle := \exp(\mathrm{i}\epsilon_\alpha t/\hbar)|\Psi_\alpha(t)\rangle$, which are indeed T-periodic functions:

$$\begin{aligned}|\Phi_\alpha(t+T)\rangle &= \mathrm{e}^{\mathrm{i}\epsilon_\alpha(t+T)/\hbar}U(t+T,0)|\Phi_\alpha(0)\rangle\\ &= \mathrm{e}^{\mathrm{i}\epsilon_\alpha(t+T)/\hbar}U(t,0)U(T,0)|\Phi_\alpha(0)\rangle\\ &= \mathrm{e}^{\mathrm{i}\epsilon_\alpha t/\hbar}|\Psi_\alpha(t)\rangle = |\Phi_\alpha(t)\rangle\ .\end{aligned} \tag{2.5}$$

In the second line, we have used that owing to the time-periodicity of the Hamiltonian, the relation $U(t+T,T) = U(t,0)$ holds true for arbitrary times t. Finally, the completeness of the set of solutions $|\Psi_\alpha(t)\rangle$ follows, if we assume the completeness of the eigenstates of $U(T,0)$.

It is worthwhile to remark that the conceptual importance of Floquet theory lies in the fact that it allows to separate the long-time dynamics, governed by the quasienergies ϵ_α, from the dynamics within one driving period, determined by Floquet modes $|\Phi_\alpha(t)\rangle$ [cf. Eq. (2.2)]. Note also that the quasienergies and the Floquet states in Eq. (2.2) are not uniquely defined. In fact, the replacement

$$\epsilon_\alpha \to \epsilon_\alpha + k_\alpha\hbar\Omega\ , \quad |\Phi_\alpha(t)\rangle \to \mathrm{e}^{\mathrm{i}k_\alpha\Omega t}\,|\Phi_\alpha(t)\rangle\ , \tag{2.6}$$

where $\Omega := 2\pi/T$ is the angular frequency of the driving and $\{k_\alpha\}$ is an arbitrary sequence of integers, yields a new set of quasienergies and Floquet states corresponding to the same solution $|\Psi_\alpha(t)\rangle$ of the Schrödinger equation (2.1). In other words, the quasienergies and Floquet modes come in classes, out of which one is allowed to select a single representative, usually with quasienergy in a single "Brillouin zone" $E-\hbar\Omega/2 \le \epsilon_\alpha < E+\hbar\Omega/2$, where E is an arbitrary but fixed energy.[1]

2.2 Sambe space

2.2.1 Definition

According to the basic postulates of quantum mechanics, the state of a system is described by a vector $|\psi\rangle$ in a Hilbert space $\mathcal{R}$ equipped with a inner product $\langle\psi'|\psi\rangle$.

[1] The term "Brillouin zone" is borrowed from the theory of electrons moving in a periodic potential [58]. There, Bloch's theorem, the spatial analogue of Floquet's theorem, facilitates an efficient description by reducing the problem to one Brillouin zone.

published by Shaker Verlag, Aachen, ISBN 3-8322-1979-X

Let us assume without restriction of the generality that there exists a countable, complete set $\{|n\rangle\}$ of orthonormal states, i.e.,

$$\langle n|n'\rangle = \delta_{nn'} \ , \quad \sum_n |n\rangle\langle n| = 1 \ . \tag{2.7}$$

Here, $\delta_{nn'}$ is the Kronecker delta and 1 is the unity operator in the space $\mathcal{R}$.

Well known from the mathematical theory is the Hilbert space $\mathcal{T}$ of all T-periodic, complex valued functions with inner product

$$(u,v) := \frac{1}{T}\int_0^T \mathrm{d}t\, u^*(t)v(t) \ . \tag{2.8}$$

The functions $\exp(\mathrm{i}k\Omega t)$ with $k = 0, \pm1, \pm2, \ldots$ form a complete, orthonormal set in this Hilbert space. The decomposition of an arbitrary T-periodic, complex-valued function in this basis yields the standard Fourier series.

As first noted by Sambe [59], the time-periodicity of the Floquet modes suggests their description in the composite Hilbert space $\mathcal{R}\otimes\mathcal{T}$. Its elements, for which we adopt the notation $|\Phi\rangle\rangle$ [59], are the T-periodic state vectors $|\Phi(t)\rangle = |\Phi(t+T)\rangle$. Introducing the inner product in this space in the canonical way via

$$\langle\langle\Phi'|\Phi\rangle\rangle := \frac{1}{T}\int_0^T \mathrm{d}t\, \langle\Phi'(t)|\Phi(t)\rangle \ , \tag{2.9}$$

an orthonormal basis of $\mathcal{R}\otimes\mathcal{T}$ is given by the set of states $\{|\Phi_n^k\rangle\rangle\}$ defined by

$$|\Phi_n^k(t)\rangle := \mathrm{e}^{\mathrm{i}k\Omega t}\,|n\rangle \ . \tag{2.10}$$

The arbitrary integer k is sometimes called the sideband index.

2.2.2 Floquet theory in Sambe space

The usefulness of Sambe space for the present problem lies in the fact that the so-called Floquet Hamiltonian

$$\mathcal{H}(t) := H(t) - \mathrm{i}\hbar\frac{\mathrm{d}}{\mathrm{d}t} \tag{2.11}$$

is a Hermitian operator in the vector space $\mathcal{R}\otimes\mathcal{T}$. Consequently, in the composite Hilbert space, Eq. (2.3) corresponds to the formally "time-independent", Hermitian eigenvalue problem

$$\mathcal{H}(t)|\Phi_\alpha\rangle\rangle = \epsilon_\alpha|\Phi_\alpha\rangle\rangle \ . \tag{2.12}$$

Note that, as above, there exists for each Floquet mode $|\Phi_\alpha\rangle\rangle$ with quasienergy ϵ_α an equivalent mode

$$|\Phi_\alpha^k(t)\rangle := \mathrm{e}^{\mathrm{i}k\Omega t}\,|\Phi_\alpha(t)\rangle \tag{2.13}$$

published by Shaker Verlag, Aachen, ISBN 3-8322-1979-X

with quasienergy

$$\epsilon_{\alpha,k} := \epsilon_\alpha + k\hbar\Omega \ . \tag{2.14}$$

Thus, we can restrict ourselves to states with eigenvalues in one Brillouin zone, $E - \hbar\Omega/2 \leq \epsilon_\alpha < E + \hbar\Omega/2$.

Eigenstates belonging to the same Brillouin zone obey the following useful relation:

$$\langle \Phi_\alpha(t)|\Phi_\beta(t)\rangle = \langle\langle \Phi_\alpha|\Phi_\beta\rangle\rangle \ . \tag{2.15}$$

In particular, orthonormalisation in $\mathcal{R}\otimes\mathcal{T}$ implies orthonormalisation in $\mathcal{R}$ at *equal times*. For the proof of Eq. (2.15), we first note that $\langle \Phi_\alpha(t)|\Phi_\beta(t)\rangle$ is at most a periodic function of the time t. Moreover, it satisfies

$$\frac{1}{T}\int_0^T \mathrm{d}t\, \mathrm{e}^{\mathrm{i}k\Omega t}\, \langle \Phi_\alpha(t)|\Phi_\beta(t)\rangle = \frac{1}{T}\int_0^T \mathrm{d}t\, \langle \Phi_\alpha(t)|\Phi_\beta^k(t)\rangle = \langle\langle \Phi_\alpha|\Phi_\beta^k\rangle\rangle \tag{2.16}$$

for an arbitrary integer k. Since the Floquet modes $|\Phi_\alpha\rangle\rangle$ and $|\Phi_\beta\rangle\rangle$ are by construction from the same Brillouin zone, the right-hand side of the last equation vanishes for all $k \neq 0$. This means that $\langle \Phi_\alpha(t)|\Phi_\beta(t)\rangle$ is in fact time-independent and we can carry out the integral on the left-hand side of Eq. (2.16) to eventually obtain relation (2.15).

For later use, we introduce the decomposition of the time-dependence of a Floquet mode $|\Phi_\alpha\rangle\rangle$ in terms of the functions $\exp(\mathrm{i}k\Omega t)$, i.e., the Fourier representation

$$\begin{aligned} |\Phi_\alpha(t)\rangle &= \sum_k \mathrm{e}^{-\mathrm{i}k\Omega t}|\Phi_k\rangle \ , \\ |\Phi_{\alpha,k}\rangle &:= \frac{1}{T}\int_0^T \mathrm{d}t \mathrm{e}^{\mathrm{i}k\Omega t}|\Phi(t)\rangle \ . \end{aligned} \tag{2.17}$$

It is important, however, to always keep in mind that the states $|\Phi_{\alpha,k}\rangle$ are not orthonormal, because the Floquet modes are only mutually orthogonal at equal times [cf. Eq. (2.15)].

2.3 Numerical methods

In literature, many different computational methods for the determination of Floquet modes and quasienergies have been described. The basic idea behind one class of methods follows directly from our constructive proof of Floquet's theorem [see Eq. (2.4)]: First one computes the time-evolution operator after one driving period $U(T,0)$, for instance by means of a Runge-Kutta integration method. A numerical diagonalisation of the resulting $N \times N$-matrix, N being the dimension of the spatial Hilbert space $\mathcal{R}$, then yields both the Floquet states at time $t = 0$ and the respective quasienergies. The Floquet states at a later time $t < T$ are again obtained by a numerical propagation

published by Shaker Verlag, Aachen, ISBN 3-8322-1979-X

according to the Schrödinger equation (2.1).

Alternatively, one can start from the Hermitian eigenvalue problem (2.12) in the Sambe space. Then a numerical propagation of Eq. (2.1) is no longer necessary but instead one has to deal with the higher dimensionality of the composite Hilbert space. Yet, the numerical effort can often be reduced by choosing a particular adapted set of basis states. Let us, in order to illustrate this point, consider a Floquet Hamiltonian of the form

$$\mathcal{H}(t) = H_0 + \sum_{l=1}^{\infty} A_l \sin(l\Omega t + \varphi_l) H_l - \mathrm{i}\hbar \frac{\mathrm{d}}{\mathrm{d}t} \; . \tag{2.18}$$

In the canonical basis (2.10) of $\mathcal{R} \otimes \mathcal{T}$, the eigenvalue problem (2.12) then can be written as

$$\sum_{n'k'} \mathcal{H}^{kk'}_{nn'} \, \phi^{k'}_{n'} = \epsilon \, \Phi^{k}_{n} \; , \tag{2.19}$$

where we have introduced the Floquet matrix

$$\mathcal{H}^{kk'}_{nn'} := \left(\langle n|H_0|n'\rangle + n\hbar\Omega \, \delta_{nn'} \right) \delta_{kk'} + \sum_{l=1}^{\infty} \frac{A_l}{2\mathrm{i}} \, \langle n|H_l|n'\rangle \left(\mathrm{e}^{\mathrm{i}\varphi_l} \, \delta_{k,k'+l} - \mathrm{e}^{-\mathrm{i}\varphi_l} \, \delta_{k,k'-l} \right) . \tag{2.20}$$

For notational brevity, the index α of the quasienergies and the Floquet modes $\Phi^k_n := \langle\langle \Phi^k_n | \Phi_\alpha \rangle\rangle$ has been dropped. In passing, we note that if $A_l = 0$ for all $l > 1$, $\mathcal{H}^{kk'}_{nn'}$ is of block tridiagonal structure, and thus, for instance, matrix continued-fraction methods can be applied for the efficient computation of the eigenvalues [60]. For numerical computations, it is of course only possible to take into account a finite number of k- and n-values. However, as noted above, a basis set which is particularly well adapted for a certain problem achieves convergence already for a small number of basis states. For moderate driving strengths A_l, the decomposition (2.20) with arbitrary basis states $|n\rangle$ is *a priori* optimal. For weak driving, however, it is worthwhile to diagonalise the undriven Hamiltonian H_0 first, and to use the resulting eigenbasis for the states $|n\rangle$. On the other hand, in the strongly driven regime, on which we put the main focus in the following, the Floquet modes of the time-dependent contribution to the Hamiltonian (2.18) form a particularly suitable basis set. Let us consider for instance the special case $A_1 = A$ and $A_l = 0$ for all $l > 1$, where the time-dependent contribution to Eq. (2.18) is given by the Floquet Hamiltonian

$$\mathcal{H}_1(t) := A \sin(\Omega t) H_1 - \mathrm{i}\hbar \frac{\mathrm{d}}{\mathrm{d}t} \; , \tag{2.21}$$

which is readily diagonalised by the states

$$|\bar{\Phi}^k_n(t)\rangle = \mathrm{e}^{\mathrm{i}k\Omega t + \mathrm{i}A\bar{E}_n \cos(\Omega t)/\hbar\Omega} \, |\bar{n}\rangle \tag{2.22}$$

with quasienergies $k\hbar\Omega$ (independent of n). Here, $|\bar{n}\rangle$ and $\bar{E}_n$ denote the eigenstates

published by Shaker Verlag, Aachen, ISBN 3-8322-1979-X

and the eigenenergies, respectively, of H_1, i.e., $H_1|\bar{n}\rangle = \bar{E}_n|\bar{n}\rangle$. Using the standard identity

$$\mathrm{e}^{\mathrm{i}a\cos\varphi} = \sum_k \mathrm{i}^k J_k(a)\,\mathrm{e}^{-\mathrm{i}k\varphi} \tag{2.23}$$

for Bessel functions [61], we obtain the new Floquet matrix [62]

$$\bar{\mathcal{H}}^{kk'}_{nn'} := (-\mathrm{i})^{k-k'} J_{k-k'}\big(A\,(\bar{E}_n - \bar{E}_{n'})/\hbar\Omega\big)\,\langle\bar{n}|H_0|\bar{n}'\rangle + k\hbar\Omega\,\delta_{kk'}\,\delta_{nn'}\ . \tag{2.24}$$

2.4 Space-time symmetries of a system driven by a dipole field

Typically, the time-dependence of the Hamiltonian $H(t)$ results from the coupling of a quantum mechanical system to an external electromagnetic field. Within a semi-classical description and in the electric dipole approximation, such a situation can be described by a Hamiltonian of the form [57]

$$H(x,p,t) = H_0(x,p) + xa(t)\ . \tag{2.25}$$

Here, $H_0(x,p)$ is the static Hamiltonian of the system, x and p are the position and momentum operators, respectively, and $a(t) = eE(t)$ is a real-valued function describing the time-dependent driving by the external electromagnetic field $E(t)$.

Let us now consider a Hamiltonian $H_0(x,p)$ that is an even function of x and, thus, is invariant under the parity transformation

$$\mathsf{P} : x \mapsto -x\ . \tag{2.26}$$

Then, its eigenstates $|\varphi_\alpha\rangle$ can be divided into two classes: even and odd ones, according to the sign in $\varphi_\alpha(x) = \pm\varphi_\alpha(-x)$.

Adding a periodically time-dependent dipole force $xa(t)$ to such a Hamiltonian evidently breaks the parity symmetry since P changes the sign of the interaction with the radiation. The Floquet description in the extended space $\mathcal{R}\otimes\mathcal{T}$, however, allows to generalise the parity transformation such that the Floquet Hamiltonian

$$\mathcal{H}(x,p,t) = H_0(x,p) + xa(t) - \mathrm{i}\hbar\frac{\mathrm{d}}{\mathrm{d}t}\ , \tag{2.27}$$

remains invariant. This requires that the shape of the driving $a(t)$ is such that an additional time transformation "repairs" the acquired minus sign. We consider two types of transformations: generalised parity and time-reversal parity. Both occur for purely harmonic driving, $a(t) = \sin(\Omega t)$. In the following two sections, we derive their impact on the Fourier coefficients (2.17) of the Floquet modes, which in the present

published by Shaker Verlag, Aachen, ISBN 3-8322-1979-X

context are functions of the position variable x, i.e.,

$$\Phi_k(x) := \frac{1}{T}\int_0^T \mathrm{d}t\, e^{\mathrm{i}k\Omega t}\,\Phi(x,t) \;\text{ with }\; \Phi(x,t) := \langle x|\Phi(t)\rangle \;. \tag{2.28}$$

For notational brevity, we have suppressed the index α distinguishing the different Floquet modes.

2.4.1 Generalised parity

It has been noted previously [21,22,63] that a Floquet Hamiltonian of the form (2.27) with $a(t) = \sin(\Omega t)$ may possess degenerate quasienergies due to its symmetry under the so-called generalised parity transformation

$$\mathsf{S}_{\mathrm{GP}}: \quad (x,t) \to (-x, t+\pi/\Omega) \;, \tag{2.29}$$

which consists of a spatial parity transformation plus a time shift by half a driving period. This symmetry is present in the Floquet Hamiltonian (2.27), if the driving field obeys $a(t) = -a(t+\pi/\Omega)$, since then S_{GP} leaves the Floquet equation (2.12) invariant. Owing to $\mathcal{S}_{\mathrm{GP}}^2 = 1$, we find that the corresponding Floquet states are either even or odd, $\mathsf{S}_{\mathrm{GP}}\Phi(x,t) = \Phi(-x,t+\pi/\Omega) = \pm\Phi(x,t)$. Consequently, the Fourier coefficients (2.28) obey the relation

$$\Phi_k(x) = \pm(-1)^k\,\Phi_k(-x) \;. \tag{2.30}$$

2.4.2 Time-inversion parity

A further symmetry is found if $a(t)$ is an odd function of time, $a(t) = -a(-t)$. Then, time inversion transforms the Floquet Hamiltonian (2.27) into its complex conjugate so that the corresponding symmetry is given by the anti-linear transformation

$$\mathsf{S}_{\mathrm{TP}}: \quad (\Phi,x,t) \to (\Phi^*,-x,-t) \;. \tag{2.31}$$

This transformation represents a further generalisation of the parity P; we will refer to it as *time-inversion parity* since in literature the term generalised parity is mostly used in the context of the transformation (2.29).

Let us now assume that the Floquet Hamiltonian is invariant under the transformation (2.31), $\mathcal{H}(x,t) = \mathcal{H}^*(-x,-t)$, and that $\Phi(x,t)$ is a Floquet state, i.e., a solution of the eigenvalue equation (2.12) with quasienergy ϵ. Then, $\Phi^*(-x,-t)$ is also a Floquet state with the same quasienergy. In the absence of any degeneracy, both Floquet states must be identical and, thus, we find as a consequence of the time-inversion parity S_{TP} that $\Phi(x,t) = \Phi^*(-x,-t)$. This is not necessarily the case in the presence of degeneracies, but then we are able to choose linear combinations of the (degenerate) Floquet states which fulfil the same symmetry relation. Again we are interested in the

published by Shaker Verlag, Aachen, ISBN 3-8322-1979-X

Fourier decomposition (2.28) and obtain

$$\Phi_k(x) = \Phi_k^*(-x) \ . \tag{2.32}$$

The time-inversion discussed here can be generalised by an additional time-shift to read $t \to t_0 - t$. Then, we find by the same line of argumentation that $\Phi_k(x)$ and $\Phi_k^*(-x)$ differ at most by a phase factor. However, for convenience one may choose already from the start the origin of the time axis such that $t_0 = 0$.

2.5 Example: The driven two-level system

The driven two-level system represents a simple, yet non-trivial example for the application of the Floquet formalism. Two-level systems are abundant in many areas of physics. Prominent representatives are the states $|\uparrow\rangle$ and $|\downarrow\rangle$ of a spin-1/2 particle, the ground state $|\mathrm{g}\rangle$ and the excited state $|\mathrm{e}\rangle$ of an atom/ion, and the ground-state doublet of a bistable potential. Related to the latter system and particularly important for the present work, is a two-level system consisting of two localised atomic orbitals $|\mathrm{L}\rangle$ and $|\mathrm{R}\rangle$ of a molecule (see Sects. 5.3.2 and 5.4.1). Let us thus consider a Hamiltonian of the form

$$H(t) = \begin{pmatrix} E_\mathrm{b}/2 & -\Delta \\ -\Delta & -E_\mathrm{b}/2 \end{pmatrix} + \frac{a(t)}{2} \begin{pmatrix} 1 & 0 \\ 0 & -1 \end{pmatrix} = -\Delta\sigma_x + \frac{1}{2}\left[E_\mathrm{b} + a(t)\right]\sigma_z \ . \tag{2.33}$$

Here, E_b and Δ are the static bias and the tunnelling coupling, respectively, between the two states. The external driving is specified by the T-periodic, but for the moment otherwise arbitrary function $a(t)$, which, in contrast to Eq. (2.25), has dimension energy. In the last equation, the Hamiltonian has also been written in an alternative, pseudo-spin form with the Pauli matrices $\sigma_x = -|\mathrm{L}\rangle\langle\mathrm{R}| - |\mathrm{R}\rangle\langle\mathrm{L}|$ and $\sigma_z = |\mathrm{L}\rangle\langle\mathrm{L}| - |\mathrm{R}\rangle\langle\mathrm{R}|$.

2.5.1 Perturbation theory in the limit of fast external driving

Quasienergies and Floquet states of the two-level system (2.33) cannot be expressed in analytically closed form. Yet, perturbational methods allow to describe the system dynamics reasonably well in certain limiting cases. Here, extending an approach put forward in Ref. [64], we focus on the high-frequency regime of the external driving: $\hbar\Omega \gg |\Delta|, |E_\mathrm{b}|$. In this limit, the static contribution to Eq. (2.33) can be treated as a perturbation. Hence, we start from the Hamiltonian

$$\mathcal{H}_0(t) = \frac{a(t)}{2}\,\sigma_z - \mathrm{i}\hbar\frac{\mathrm{d}}{\mathrm{d}t} \tag{2.34}$$

published by Shaker Verlag, Aachen, ISBN 3-8322-1979-X

and consider the static Hamiltonian operator

$$\mathcal{H}_1 = \frac{E_\mathrm{b}}{2}\,\sigma_z - \Delta\,\sigma_x \tag{2.35}$$

to act as a perturbation.

In each Brillouin zone, the eigenvalue problem (2.12) for $\mathcal{H}_0(t)$ has one degenerate eigenvalue $\epsilon_{1,k} = \epsilon_{2,k} = k\hbar\Omega$ with eigenspace spanned by the states

$$|\phi_1^k(t)\rangle := \mathrm{e}^{-\mathrm{i}A(t)/2\hbar + \mathrm{i}k\Omega t}\,|\mathrm{L}\rangle\ , \quad |\phi_2^k(t)\rangle := \mathrm{e}^{\mathrm{i}A(t)/2\hbar + \mathrm{i}k\Omega t}\,|\mathrm{R}\rangle\ , \tag{2.36}$$

where $A(t) = \int_0^t \mathrm{d}t' a(t')$. Next, we diagonalise $\mathcal{H}_1$ in each degenerate subspace, yielding the Floquet modes

$$\begin{aligned} |\phi_+^k\rangle\rangle &= \cos(\Theta/2)\mathrm{e}^{\mathrm{i}\Xi/2}\,|\phi_1^k\rangle\rangle - \sin(\Theta/2)\mathrm{e}^{-\mathrm{i}\Xi/2}\,|\phi_2^k\rangle\rangle\ , \\ |\phi_-^k\rangle\rangle &= \sin(\Theta/2)\mathrm{e}^{\mathrm{i}\Xi/2}\,|\phi_1^k\rangle\rangle + \cos(\Theta/2)\mathrm{e}^{-\mathrm{i}\Xi/2}\,|\phi_2^k\rangle\rangle \end{aligned} \tag{2.37}$$

with corresponding quasienergies

$$\epsilon_{\pm,k} = \pm\frac{1}{2}\sqrt{E_\mathrm{b}^2 + 4|\Delta_0|^2} + k\hbar\Omega\ . \tag{2.38}$$

The angles Θ and Ξ are defined implicitly by

$$\tan\Theta = \frac{2|\Delta_0|}{E_\mathrm{b}} \quad (0 \le \Theta < \pi)\ , \tag{2.39}$$

$$\Delta_0 = |\Delta_0|\mathrm{e}^{\mathrm{i}\Xi} \quad (0 \le \Xi < 2\pi)\ , \tag{2.40}$$

and we have denoted the tunnelling matrix element renormalised by the Fourier coefficients of $\exp(\mathrm{i}A(t)/\hbar)$ by

$$\Delta_k := \frac{\Delta}{T}\int_0^T \mathrm{d}t\,\mathrm{e}^{\mathrm{i}k\Omega t + \mathrm{i}A(t)/\hbar}\ . \tag{2.41}$$

Note that for a driving field with $a(t) = -a(-t)$, one finds $A(t) = A(-t)$, yielding the relation $\Delta_{-k} = \Delta_k$. Similarly, one finds for $a(t+\pi/\Omega) = -a(t)$ that $\Delta_{-k} = (-1)^k\Delta_k^*$. In particular, Δ_0 is then real and thus $\Xi = 0$. For the important example of a sinusoidal driving force $a(t) = A\sin(\Omega t)$, the Bessel function identity (2.23) yields the renormalised tunnelling matrix elements $\Delta_k = (-\mathrm{i})^k J_k(A/\hbar\Omega)\,\Delta$.

With the expressions (2.37) and (2.38), we have already determined the Floquet modes to zeroth order and the first-order corrections to the quasienergies, respectively. For the rather technical details of the calculation of the first-order correction to the Floquet modes, we refer to Appendix A. Here, we only give the resulting expression for the matrix elements of the σ_z operator in the basis of the Floquet states, which is

published by Shaker Verlag, Aachen, ISBN 3-8322-1979-X

needed for the next two sections. Up to first order in $\mathcal{H}_0$, they follow from Eqs. (2.37) and (A.10) as

$$\langle\langle \Phi_\alpha|\sigma_z|\Phi_\beta\rangle\rangle_{\alpha,\beta=\pm} \approx \begin{pmatrix} \cos\Theta - 2\lambda\sin\Theta & \sin\Theta + 2\lambda\cos\Theta \\ \sin\Theta + 2\lambda\cos\Theta & -(\cos\Theta - 2\lambda\sin\Theta) \end{pmatrix} . \tag{2.42}$$

Here, we have introduced the dimensionless, real parameter

$$\lambda := \frac{|\Delta_0|}{4|\Delta_0|^2 + E_\mathrm{b}^2} \sum_{k\neq 0} \frac{|\Delta_k|^2 - |\Delta_{-k}|^2}{k\hbar\Omega} , \tag{2.43}$$

which vanishes for the two special driving forms $a(t) = -a(-t)$ or $a(t+\pi/\Omega) = -a(t)$, discussed after Eq. (2.41).

2.5.2 Coherent destruction of tunnelling

A prominent quantum effect occurring in strongly driven systems, is the so-called coherent destruction of tunnelling (CDT) [21–23], i.e., the dynamical suppression of the quantum mechanical tunnel effect. As a prototypical example, we will discuss CDT in a two-level system described by Eq. (2.33) [23, 65]. Thereby, we assume that the driving field fulfils $a(t+\pi/\Omega) = -a(t)$, implying $\lambda = 0$ and $\Xi = 0$ or $\Xi = \pi$.

CDT in an unbiased two-level system

Let us first consider the unbiased case $E_\mathrm{b} = 0$. We start with a particle that initially has been prepared in the state $|\Psi(t=0)\rangle = |\mathrm{L}\rangle$. From Eq. (2.39) we find $\Theta = \pi/2$, leading to the following expression of the initial state in terms of the adapted eigenstates of $\mathcal{H}_0$:

$$|\Psi(t=0)\rangle = \pm\frac{1}{\sqrt{2}}\left(|\phi_+(0)\rangle + |\phi_-(0)\rangle\right) \approx \pm\frac{1}{\sqrt{2}}\left(|\Phi_+(0)\rangle + |\Phi_-(0)\rangle\right) . \tag{2.44}$$

Here, the plus (minus) sign corresponds to $\Xi = 0$ ($\Xi = \pi$). Owing to the orthonormality of the states $|\Phi_\pm(0)\rangle$, the system evolves approximately according to

$$|\Psi(t)\rangle \approx \pm\frac{1}{\sqrt{2}}\left(\mathrm{e}^{-\mathrm{i}\epsilon_+ t/\hbar}\,|\phi_+(t)\rangle + \mathrm{e}^{-\mathrm{i}\epsilon_- t/\hbar}\,|\phi_-(t)\rangle\right) . \tag{2.45}$$

Thus, we find that the probability $P_\mathrm{L}(t)$ to find the system in the state $|\mathrm{L}\rangle$ oscillates with time t [66],

$$P_\mathrm{L}(t) \approx \cos^2\left(\frac{\epsilon_+ - \epsilon_-}{2\hbar}\,t\right) = \cos^2\left(\frac{\Delta_0}{\hbar}\,t\right) . \tag{2.46}$$

published by Shaker Verlag, Aachen, ISBN 3-8322-1979-X

This result corresponds to the well-known tunnel oscillations between the states $|\mathrm{L}\rangle$ and $|\mathrm{R}\rangle$ in the undriven situation. The only difference is that energies are substituted by quasienergies. Since the frequency of these oscillations is proportional to the renormalised tunnelling matrix element Δ_0, we expect for vanishing Δ_0 a standstill of the tunnelling dynamics, i.e., the CDT effect. Because Δ_0 is always a real number (remember that either $\Xi = 0$ or $\Xi = \pi$), we obtain only one equation from the CDT condition $\Delta_0 = 0$. Its solutions thus lie on one-dimensional manifolds in the two-dimensional parameter space of driving amplitude A and frequency Ω [67]. For a sinusoidal driving $a(t) = A\sin(\Omega t)$, Eq. (2.23) yields $\Delta_0 = J_0(A/\hbar\Omega)\Delta$. One therefore obtains the vanishing of the zeroth order Bessel function J_0 as condition for CDT.

Figure 2.1 shows exact results from a numerical solution of the quantum dynamics (2.33). In the upper panel, the probability $P_\mathrm{L}(t)$ is plotted for two different driving amplitudes A. Thereby one can confirm that for the driving amplitude corresponding to the first zero of J_0 the particle rests indeed in the state $|\mathrm{L}\rangle$, while for a slightly larger driving amplitude tunnel oscillations between the states $|\mathrm{L}\rangle$ and $|\mathrm{R}\rangle$ occur. Moreover, besides small oscillations within one driving period, the approximate result (2.46) describes the exact dynamics reasonably well.

CDT in a biased two-level system

Although in literature CDT is commonly discussed only for spatially symmetric systems, the effect is in fact stable against a small system bias, i.e., a situation with $E_\mathrm{b} \neq 0$ but still $|E_\mathrm{b}| \ll \hbar\Omega$. Then, we can already infer from the perturbative result (2.38) that the quasienergies cannot be degenerate any longer; they form avoided crossings. However, we will see that CDT still occurs whenever $\Delta_0 = 0$ is fulfilled. To see how this comes about, we expand again a localised initial state $|\Psi(t=0)\rangle = |\mathrm{L}\rangle$ in terms of the zeroth order Floquet modes (2.37),

$$|\Psi(0)\rangle = \pm\left(\cos^2(\Theta/2)\,|\phi_+(0)\rangle + \sin^2(\Theta/2)\,|\phi_-(0)\rangle\right) \ . \tag{2.47}$$

The same line of reasoning as above then yields the approximative result [68]

$$P_\mathrm{L}(t) \approx \frac{1}{4\Delta_0^2 + E_\mathrm{b}^2}\left[E_\mathrm{b}^2 + 4\Delta_0^2\cos^2\left(\frac{\epsilon_+ - \epsilon_-}{2\hbar}\,t\right)\right] \tag{2.48}$$

for the probability to find the system in state $|\mathrm{L}\rangle$ at time t [see also Eq. (2.39)]. For $\Delta_0 = 0$ the prefactor of the oscillating term vanishes and one obtains $P_\mathrm{L}(t) \approx 1$, i.e., again a suppression of the tunnelling dynamics. We point out that here the common explanation of CDT fails. It is no longer the frequency appearing in the cosine function that is zero at a *quasienergy* degeneracy, but the prefactor of the cosine that vanishes as a consequence of the form of *Floquet states* (2.37).

Again, for the special case of a sinusoidal driving, our conclusion from the approximate dynamics (2.48) are in accordance with numerically exact results (cf. Fig. 2.2).

published by Shaker Verlag, Aachen, ISBN 3-8322-1979-X

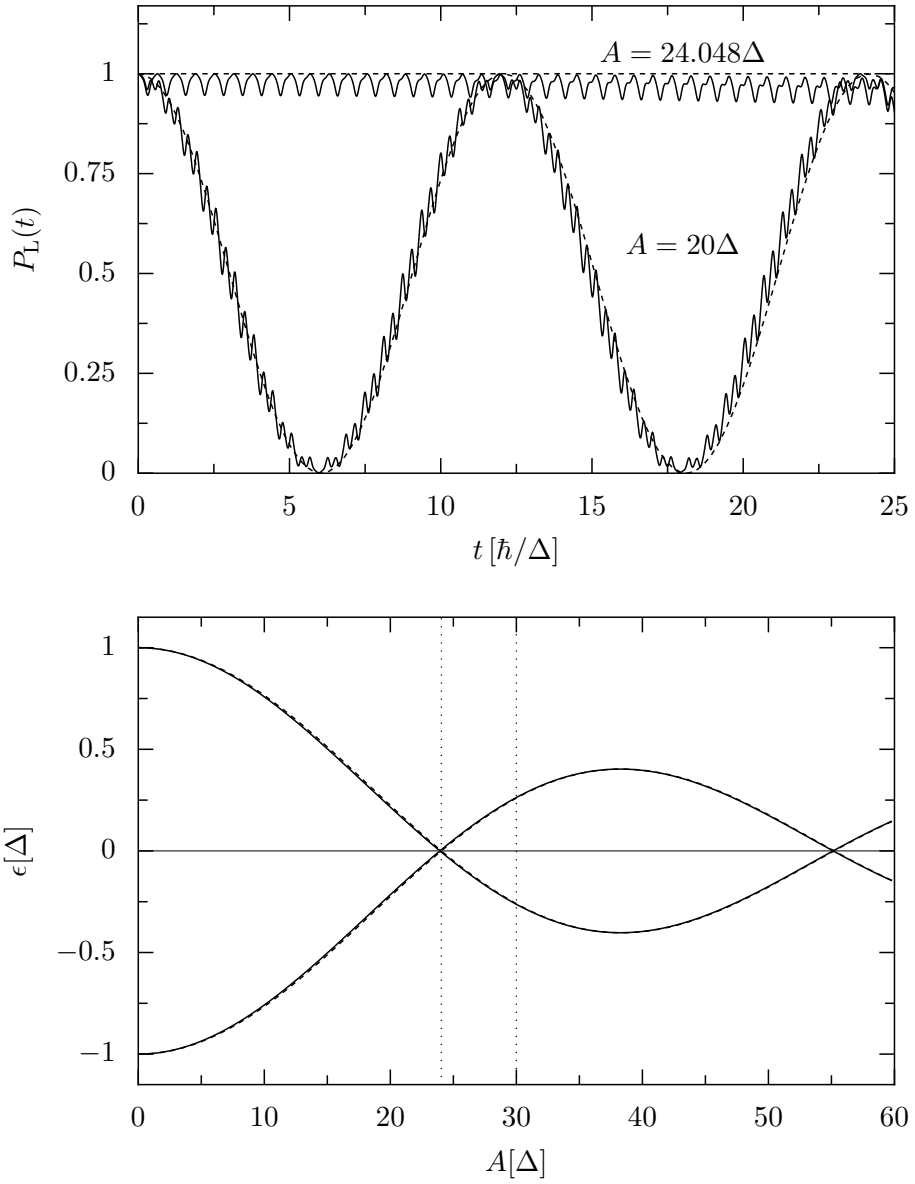

Figure 2.1: Unbiased two-level system (Eq. (2.33) with $E_{\mathrm{b}} = 0$) driven by a harmonic signal $a(t) = A\sin(\Omega t)$ with a driving frequency $\Omega = 10\Delta/\hbar$. Upper panel: probability $P_{\mathrm{L}}(t)$ of finding the system in the state $|\mathrm{L}\rangle$ at time t for two different driving amplitudes A. Shown are both exact results from a numerical diagonalisation of the Floquet equation (2.19) (solid lines) and the approximate results (2.46) (dashed lines). Lower panel: quasienergies as a function of the driving amplitude A. The two driving amplitudes used in the upper panel are indicated by a dotted vertical line.

published by Shaker Verlag, Aachen, ISBN 3-8322-1979-X

2.5.3 Dynamical symmetry breaking

The discussion of the space-time symmetries in Sect. 2.4 is exemplified nicely by the two-level dynamics (2.33) without bias, i.e. $\Theta = \pi/2$. For the moment, we do not impose any further restriction on the driving field—apart from its time-periodicity. Instead of looking at the dynamical time evolution of the two-level system, we focus on the spatial symmetry of the Floquet modes $|\Phi_\pm\rangle\rangle$. As indicator for the localisation properties of a Floquet mode, we choose the time-averaged expectation values of the Pauli matrix σ_z: For perfect localisation, the absolute value of this time-averaged expectation values would be unity, while they vanish in the opposite case with delocalised states. From the perturbative result (2.42), we find

$$\langle\langle \Phi_+|\sigma_z|\Phi_+\rangle\rangle \approx -\langle\langle \Phi_-|\sigma_z|\Phi_-\rangle\rangle \approx -2\lambda \ . \tag{2.49}$$

As discussed after Eq. (2.43), the effective parameter λ and, thus, the time-average of the expectation value is zero for a driving field obeying any of the two symmetries discussed in Sect. 2.4; then both Floquet modes $|\Phi_\pm\rangle$ are completely delocalised. On the other hand, a broken space-time symmetry leads in general to a non-vanishing λ and consequently to a driving-induced localisation of the Floquet states.

Note that a driving field of the form $a(t) = A_1 \sin(\Omega t) + A_2 \sin(2\Omega t + \varphi)$ allows to tune this localisation as a function of the phase difference φ. From the previous discussion it is clear, that λ has to vanish for both $\varphi = 0$ and $\varphi = \pi$, where $a(t) = -a(-t)$. For other values of φ, relation (2.23) may be used to obtain an expression for Δ_k in terms of a sum over a product of Bessel functions and an exponential factor containing the phase difference φ. Upon insertion into Eq. (2.43) this yields an expression for λ, which, however, cannot be written in a compact form.

2.6 Summary

In this chapter, we have reviewed some basic concepts of Floquet theory, a method that not only gives important insights in the properties of quantum mechanical systems with a time-periodic Hamiltonian but also permits their efficient numerical treatment. Most naturally, Floquet theory is discussed in Sambe space, i.e., in the composite Hilbert space $\mathcal{R} \otimes \mathcal{T}$, where $\mathcal{R}$ is the original Hilbert space of the spatial coordinates (including spin and other degrees of freedom of the particle) and $\mathcal{T}$ is the space of all T-periodic functions in time. In Sambe space, the time-dependent problem reduces to an effectively stationary one, a fact that allows the application of the standard methods known from time-independent quantum mechanics.

Symmetries in $\mathcal{R}$ possess generalisations in the composite space $\mathcal{R} \otimes \mathcal{T}$. The parity

published by Shaker Verlag, Aachen, ISBN 3-8322-1979-X

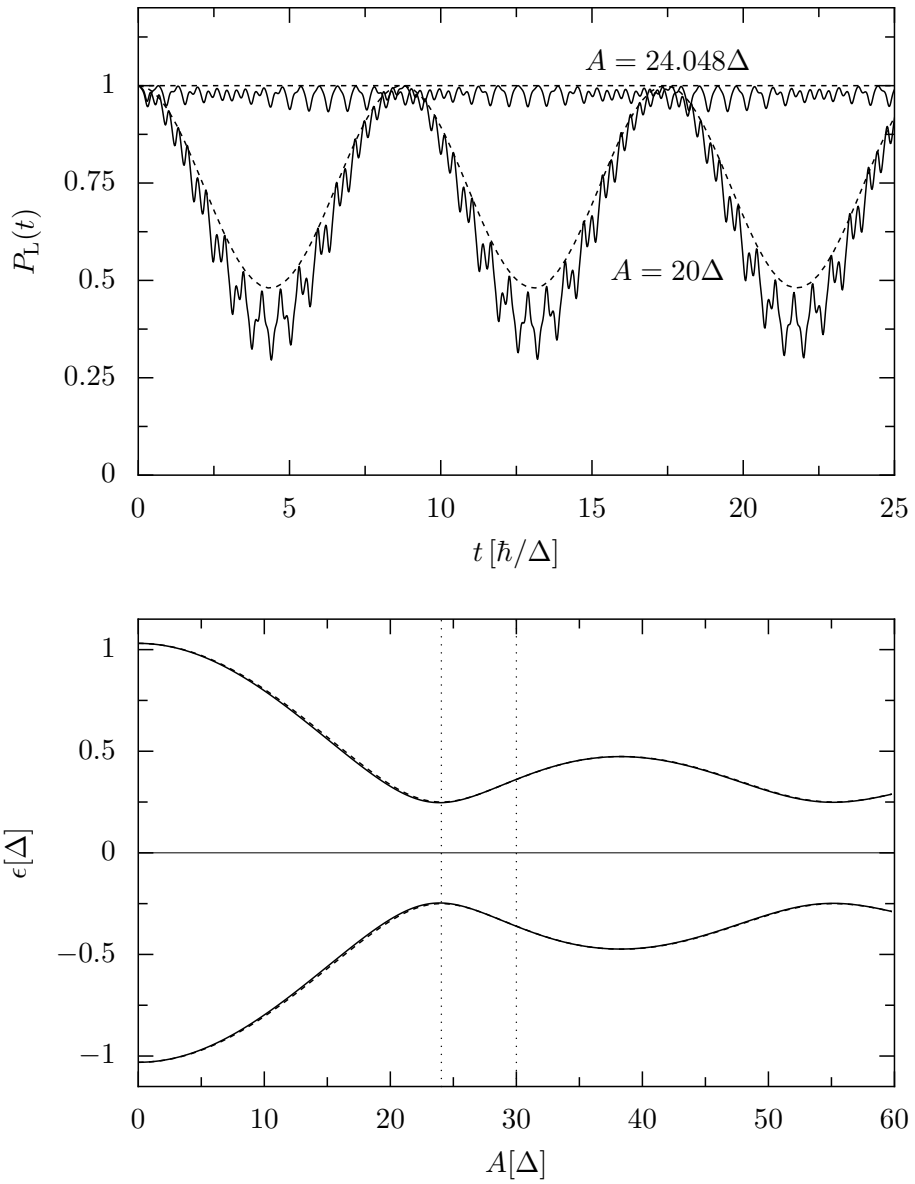

Figure 2.2: Probability $P_{\mathrm{L}}(t)$ (upper panel) and quasienergy spectrum (lower panel) for the biased two-level system (2.33) driven by a harmonic signal $a(t) = A\sin(\Omega t)$. All parameters and details are as in Fig. 2.1, except for the additional bias $E_{\mathrm{b}} = 0.5\Delta$.

published by Shaker Verlag, Aachen, ISBN 3-8322-1979-X

symmetry operation in $\mathcal{R}$, for instance, may be extended in a two-fold way, leading to either a time-inversion parity or a generalised parity operation. Such symmetries have consequences for the Fourier coefficients of the Floquet modes.

Finally, we have discussed aspects of the simplest, non-trivial application of the Floquet formalism, namely the driven two-level system. A perturbation theory in the static Hamiltonian already allows to explain two important effects occurring in such systems: (i) Coherent destruction of tunnelling, which for an unbiased system results from a quasienergy degeneracy and for a biased system comes from a localisation of the Floquet states. Later on, we will see that this effect permits a sensitive switching of the currents through nanosystems. (ii) Dynamical symmetry breaking appearing in spatially symmetric systems due to the action of a driving field with vanishing mean but non-vanishing higher moments. The discussed two-level situation will turn out to be a minimal example for the generation of currents in spatially symmetric systems by means of an external driving field, i.e., an electron pump based on harmonic mixing of different Fourier components of the driving field.

published by Shaker Verlag, Aachen, ISBN 3-8322-1979-X

published by Shaker Verlag, Aachen, ISBN 3-8322-1979-X

3 Dynamics of a driven molecular wire

While isolated systems can be described by a pure state $|\Psi(t)\rangle$, it is well-known that this is no longer the case when the system is coupled to environmental degrees of freedom. In the present context, such a coupling originates both from contacting the wire to macroscopic leads—this is indispensable for a transport experiment—and from the interaction of the wire electrons with the phononic degrees of freedom of the molecule itself and of its environment. Due to the presence of a coupling between wire and environment, the dynamics of the wire electrons is no longer unitary, and one has to formulate a theory in terms of a (reduced) density matrix. Then, two new important physical effects emerge: (i) decoherence, that is loss of the quantum mechanical phase information and (ii) dissipation, i.e., energy exchange with the environment, leading to a relaxation of the system towards an equilibrium state. In the case of a tunnelling coupling between wire and leads, particle exchange accompanies these processes.

Transport through systems which are merely coupled to electronic leads is commonly referred to as *coherent* transport [9, 47, 69, 70]. On the other hand, in the *incoherent* regime, transport is dominated by hopping processes, whereby an intermediate localisation on a wire site occurs due to the presence of electron-phonon interaction [9, 47, 71–73]. Most challenging from a theoretical point of view is the *intermediate* regime, where neither of these transport mechanisms is dominant. In the context of molecular wire transport, this regime was only recently addressed. Different methods ranging from a multichannel scattering approach [74–76], Liouville space pathway techniques [77] to a scattering approach combined with a Redfield formalism [78, 79] have been applied. In this chapter, we put forward a non-linear kinetic equation approach, which allows to efficiently include oscillating fields, but requires a weak coupling to both the leads and the phonons.

3.1 The wire and its environment

The total system consisting of the molecular wire, electronic leads, and phonon baths together with the wire-lead and the wire-phonon coupling (cf. Fig. 3.1) is described by a Hamiltonian of the form

$$H(t) = H_{\text{wire}}(t) + H_{\text{leads}} + H_{\text{wire-leads}} + H_{\text{phonons}} + H_{\text{wire-phonons}} \,. \tag{3.1}$$

published by Shaker Verlag, Aachen, ISBN 3-8322-1979-X

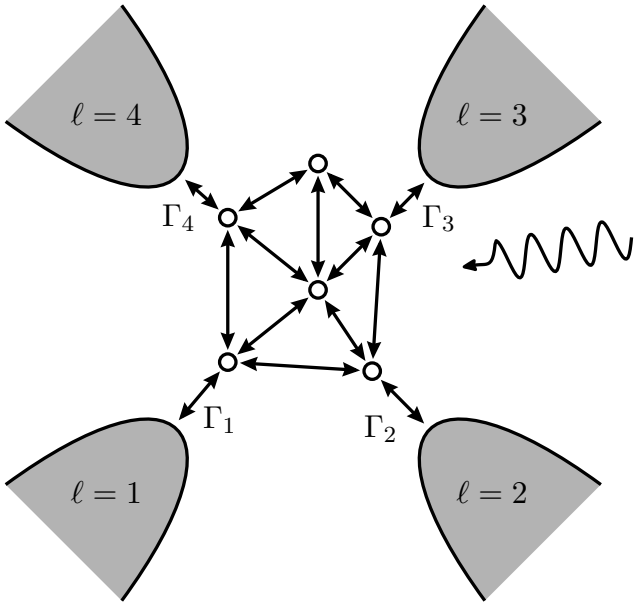

Figure 3.1: Molecular circuit consisting of $N = 6$ sites, of which the sites $1,\ldots,L$ are coupled to $L = 4$ leads. The molecule is under the additional influence of a laser field (wiggled line).

The wire itself, we model by a set of noninteracting electrons in a finite, N-dimensional Hilbert space,

$$H_{\text{wire}}(t) = \sum_{n,n'} H_{nn'}(t)\, c_n^\dagger c_{n'} \ , \tag{3.2}$$

where the sums over n and n' run over all wire sites $n = 1,\ldots,N$. The fermionic operators c_n and $c_n^\dagger$ annihilate and create, respectively, an electron in the wire orbital $|n\rangle$. Here, orthonormality $\langle n|m\rangle = \delta_{nm}$ of the orbitals $\{|n\rangle\}$ is presumed. The creation and annihilation operators hence obey the anticommutation relations $[c_n, c_m^\dagger]_+ = \delta_{nm}$ and $[c_n, c_m]_+ = [c_n^\dagger, c_m^\dagger]_+ = 0$, where $[A,B]_+ := AB + BA$.

The Hamiltonians (3.1) and (3.2) also account for a T-periodic external field acting upon the wire, $H_{nn'}(t+T) = H_{nn'}(t)$. We assume in our model that the field influences only the wire itself. This is physically motivated by the fact that typical laser frequencies are in the infrared or in the optical range. Since such frequencies lie well below typical plasma frequencies of metals [58, 80], the laser light is reflected at the metal surface and is not able to penetrate the leads. This justifies also our later assumption that the leads remain close to equilibrium. However, it is well-known that near the metal surface, and in particular near metallic tips, the electrical field may be enhanced drastically [81].[1] Note also that the energy of infrared light quanta is by

[1] A well-established application of this effect is the so-called Surface-Enhanced Raman Scattering [82, 83], where the response increases by several orders of magnitude if the molecule is adsorbed on a metal surface.

published by Shaker Verlag, Aachen, ISBN 3-8322-1979-X

far smaller than the work function of a common metal, which is of the order of 5 eV. Thus, photoelectrons do not play a role for the further considerations.

The environment comprises both the macroscopic electronic leads as well as phononic degrees of freedom of the molecule itself and of its surroundings. We will discuss both contributions in the next two sections.

3.1.1 Coupling to electronic leads

We assume that there are L electronic leads, described by grand-canonical ensembles of non-interacting electrons at a common temperature T and possibly different electrochemical potentials μ_ℓ, $\ell = 1,\ldots,L$. Thus, we describe the leads by the Hamiltonian

$$H_{\text{leads}} = \sum_{\ell=1}^{L} \sum_{q} \epsilon_{q\ell}\, c_{q\ell}^\dagger\, c_{q\ell} \ , \tag{3.3}$$

where the operators $c_{q\ell}$ and $c_{q\ell}^\dagger$ destroy and create, respectively, an electron with energy $\epsilon_{q\ell}$ in state q of lead ℓ. All lead states are mutually orthogonal and orthogonal to the wire states. Consequently, the anticommutation relations $[c_{q\ell}, c_{q'\ell'}^\dagger]_+ = \delta_{qq'}\,\delta_{\ell\ell'}$ and $[c_{q\ell}, c_n^\dagger]_+ = [c_n, c_{q\ell}^\dagger]_+ = 0$ are fulfilled. The equilibrium distribution of the leads is completely specified by the expectation values

$$\langle c_{q\ell}^\dagger c_{q'\ell'} \rangle_{\text{eq}} = \delta_{qq'}\,\delta_{\ell\ell'}\, f(\epsilon_{q\ell} - \mu_\ell) \ , \tag{3.4}$$

where $f(\epsilon) = (\mathrm{e}^{\epsilon/k_\mathrm{B}T} + 1)^{-1}$ denotes the Fermi function.

Furthermore, we presume that each lead is coupled to exactly one of the suitably labelled molecular orbitals via the tunnelling Hamiltonian

$$H_{\text{wire-leads}} = \sum_{\ell=1}^{L} \sum_{q} V_{q\ell}\, c_{q\ell}^\dagger\, c_\ell + \text{h.c.} \tag{3.5}$$

with $V_{q\ell}$ being the tunnelling matrix elements. As it will turn out, the effect of the coupling to the leads is completely characterised by the distribution (3.4) together with the spectral density of the coupling

$$\Gamma_\ell(\epsilon) := \frac{2\pi}{\hbar} \sum_{q} |V_{q\ell}|^2\, \delta(\epsilon - \epsilon_{q\ell}) \ , \tag{3.6}$$

which becomes a continuous function of the energy ϵ if the lead states are dense. It is frequently assumed that the attached leads can be described by a one-dimensional tight-binding chain with hopping matrix elements Δ'. Then, the spectral densities $\Gamma_\ell(\epsilon)$ of the lead-wire couplings are given by the Newns-Anderson model [84], i.e. they assume an semi-elliptical shape with a band width $4\Delta'$. However, since we are mainly

published by Shaker Verlag, Aachen, ISBN 3-8322-1979-X

interested in the behaviour of the molecule itself and not in the details of the lead-wire coupling [85], we will later on assume that the conduction band width of the leads is much larger than all remaining relevant energy scales. In this so-called wide-band limit, we assume constant spectral-densities

$$\Gamma_\ell(\epsilon) = \text{const.} = \Gamma_\ell \ . \tag{3.7}$$

3.1.2 Coupling to phonon baths

The coupling of the wire electrons to environmental degrees of freedom, like high-frequency molecular vibrational modes and low-frequency phonon modes of the surrounding medium, depends in principle on many microscopic details of the system. Here, we consider independent phonon baths, labelled by an index ν, each of which comprises phonon modes q with frequency $\omega_{q\nu}$,

$$H_{\text{phonons}} = \sum_\nu \sum_q \hbar\omega_{q\nu}\, b^\dagger_{q\nu} b_{q\nu} \ . \tag{3.8}$$

The corresponding canonical commutation relations take on the form $[b_{q\nu}, b^\dagger_{q'\nu'}] = \delta_{qq'}\,\delta_{\nu\nu'}$ and $[b_{q\nu}, b_{q'\nu'}] = [b^\dagger_{q\nu}, b^\dagger_{q'\nu'}] = 0$. Of course, all bosonic operators commute with all fermionic operators. A complete characterisation of the equilibrium Bose-distribution of the phonons is provided by the expectation values

$$\langle b^\dagger_{q\nu}\, b_{q'\nu'}\rangle_{\text{eq}} = \delta_{qq'}\,\delta_{\nu\nu'}\, n_{\text{B}}(\hbar\omega_{q\nu}) \tag{3.9}$$

with the Bose function $n_{\text{B}}(\epsilon) = (\mathrm{e}^{\epsilon/k_{\text{B}}T} - 1)^{-1}$.

Within our model, we describe the coupling between the wire electrons and the phonons by the Hamiltonian [75, 86]

$$H_{\text{wire-phonons}} = \sum_\nu \sum_{n,n'} X_{nn'\nu}\, c^\dagger_n c_{n'} \sum_q M_{q\nu}\,(b_{q\nu} + b^\dagger_{q\nu}) \ , \tag{3.10}$$

where the $X_{nn'\nu} = X^*_{n'n\nu}$ are Hermitian matrices and the $M_{q\nu}$ are real constants. Again, we introduce for the coupling the spectral density

$$D_\nu(\omega \geq 0) := \frac{\pi}{\hbar} \sum_q M_q^2\, \delta(\omega - \omega_{q\nu}) \ . \tag{3.11}$$

For the description within a kinetic equation approach, we have to require that $D_\nu(\omega)$ vanishes at least linearly for $\omega \to 0$ [cf. Eq. (3.48) below]:

$$D_\nu(\omega) \propto \omega^s \text{ with } s \geq 1 \ . \tag{3.12}$$

published by Shaker Verlag, Aachen, ISBN 3-8322-1979-X

Thus, we exclude the case of a subohmic damping. Furthermore, we extend the definition (3.11) of $D_\nu(\omega)$ to negative frequencies $\omega < 0$ by setting

$$D_\nu(\omega < 0) := -D_\nu(-\omega) \ . \tag{3.13}$$

In our numerical calculations, we will later employ a model, where each wire site couples locally to a separate bath with an Ohmic spectral density, thus

$$X_{nn'\nu} = \delta_{nn'}\,\delta_{n\nu} \quad \text{and} \quad D_\nu(\omega) = \kappa\hbar\omega \ , \tag{3.14}$$

where the dimensionless coupling strength κ is assumed to be identical for all sites. This model has been used previously to describe the effect of dephasing and relaxation in bridged molecular systems without time-dependent driving [78, 79]. The local form of the coupling disregards correlations between the baths at different wire sites and is therefore only valid, if these are well separated in space. Note that if each bath consists of only one single oscillator, the coupling (3.14) reduces to the standard Holstein Hamiltonian [87].

3.2 Kinetic equation approach

Because of the wire-environment coupling, a proper description of the wire electrons requires a formulation by means of a density operator (see also discussion in the introduction of this chapter). We therefore consider the total density matrix $\varrho(t)$ describing the wire and its environment. The dynamics is then fully specified by the Liouville-von Neumann equation

$$\dot{\varrho}(t) = -\frac{\mathrm{i}}{\hbar}[H(t), \varrho(t)] \tag{3.15}$$

together with an initial condition at time $t = t_0$. Since we will not be interested in any transient effects, we may safely assume that the long-time dynamics is independent of any initial correlations between the wire electrons and the environmental degrees of freedom and thus

$$\varrho(t_0) = \varrho_{\text{wire}}(t_0) \otimes \varrho_{\text{env,eq}} \ . \tag{3.16}$$

The environment is assumed to be in thermal equilibrium and $\varrho_{\text{wire}}(t) := \mathrm{Tr}_{\text{env}}\,\varrho(t)$ is the reduced density matrix of the wire electrons. Our aim is to eliminate the environmental degrees of freedom in the regime of a weak wire-environment coupling, yielding a complete description in terms of the reduced density matrix $\varrho_{\text{wire}}(t)$. An oft-used, systematic method to achieve this goal is the so-called projection operator technique [88, 89]. Here, we present a different, for the present purposes more direct derivation [90, 91]. To this end, we focus on the coupling Hamiltonian $H_{\text{coupl}} := H_{\text{wire-leads}} + H_{\text{wire-phonons}}$ by switching to the interaction picture with respect

published by Shaker Verlag, Aachen, ISBN 3-8322-1979-X

to the uncoupled dynamics, defined by the operators $\widetilde{O}(t,t') := U_0^\dagger(t,t')O(t)U_0(t,t')$, where $O(t)$ is an arbitrary operator in the Schrödinger picture and

$$U_0(t,t') = \overleftarrow{T}\exp\left(-\frac{\mathrm{i}}{\hbar}\int_{t'}^{t}\mathrm{d}t''\,[H_{\mathrm{wire}}(t'') + H_{\mathrm{leads}} + H_{\mathrm{phonons}}]\right)\ . \tag{3.17}$$

is the propagator of wire and environment in the absence of H_{coupl}. Here, $\overleftarrow{T}$ denotes the time-ordering operator, which sorts operators in such a way that those at the latest time appear farthest to the left. The Liouville-von Neumann equation then assumes the form

$$\dot{\widetilde{\varrho}}(t,t_0) = -\frac{\mathrm{i}}{\hbar}[\widetilde{H}_{\mathrm{coupl}}(t,t_0),\widetilde{\varrho}(t,t_0)]\ , \tag{3.18}$$

which reads after integration

$$\widetilde{\varrho}(t,t_0) = \widetilde{\varrho}(t_0,t_0) - \frac{\mathrm{i}}{\hbar}\int_0^{t-t_0}\mathrm{d}\tau\,[\widetilde{H}_{\mathrm{coupl}}(t-\tau,t_0),\widetilde{\varrho}(t-\tau,t_0)]\ . \tag{3.19}$$

Upon re-insertion of this relation into the right-hand side of Eq. (3.18), we arrive at the integro-differential equation

$$\begin{aligned}\dot{\widetilde{\varrho}}(t,t_0) =& -\frac{\mathrm{i}}{\hbar}[\widetilde{H}_{\mathrm{coupl}}(t,t_0),\widetilde{\varrho}(t_0,t_0)]\\ &-\frac{1}{\hbar^2}\int_0^{t-t_0}\mathrm{d}\tau\,[\widetilde{H}_{\mathrm{coupl}}(t,t_0),[\widetilde{H}_{\mathrm{coupl}}(t-\tau,t_0),\widetilde{\varrho}(t-\tau,t_0)]]\ ,\end{aligned} \tag{3.20}$$

which still describes the exact dynamics of the total system $\varrho(t)$. At this point, we assume that the dynamics induced by transitions due to the weak coupling H_{coupl} is slow, so that we may approximate $\widetilde{\varrho}(t-\tau,t_0)$ by $\widetilde{\varrho}(t,t_0)$ in the integral. This so-called Born-Markov-approximation of course also requires $t \gg t_0$. After a back transformation into the Schrödinger picture, we therefore consider the asymptotic limit $t_0 \to -\infty$. Furthermore, we presume that the environment always stays in thermal equilibrium and neglect correlations between the wire and the environment, i.e., $\varrho(t) = \varrho_{\mathrm{wire}}(t)\otimes\varrho_{\mathrm{env,eq}}$ for all times t. Tracing out the environmental degrees of freedom, we finally arrive at the master equation

$$\begin{aligned}\dot{\varrho}_{\mathrm{wire}}(t) =& -\frac{\mathrm{i}}{\hbar}[H_{\mathrm{wire}}(t),\varrho_{\mathrm{wire}}(t)]\\ &-\frac{1}{\hbar^2}\int_0^{\infty}\mathrm{d}\tau\,\mathrm{Tr}_{\mathrm{env}}[H_{\mathrm{coupl}},[\widetilde{H}_{\mathrm{coupl}}(t-\tau,t),\varrho_{\mathrm{wire}}(t)\otimes\varrho_{\mathrm{env,eq}}]]\ .\end{aligned} \tag{3.21}$$

published by Shaker Verlag, Aachen, ISBN 3-8322-1979-X

Here, the first term describes the coherent dynamics of the isolated wire, while the second term corresponds to incoherent transitions between different wire states. Correspondingly, it cannot be cast into the commutator form of the first term.

Equation (3.21) determines the time-evolution of the expectation value $\langle O_{\rm wire}(t)\rangle_t = {\rm Tr}[\varrho(t) O_{\rm wire}(t)]$ of an arbitrary operator $O_{\rm wire}(t)$ in the Hilbert space of the wire. After some straightforward algebraic manipulations, we obtain the dynamical equation

$$\frac{\mathrm{d}}{\mathrm{d}t}\langle O_{\rm wire}(t)\rangle_t = \langle \mathring{O}_{\rm wire}(t)\rangle_t - \frac{1}{\hbar^2}\int_0^\infty \mathrm{d}\tau\, \langle [[O_{\rm wire}(t), H_{\rm coupl}], \widetilde{H}_{\rm coupl}(t-\tau,t)]\rangle_t \ , \tag{3.22}$$

where we have introduced the observable

$$\mathring{O}_{\rm wire}(t) := \frac{\mathrm{i}}{\hbar}[H_{\rm wire}(t), O_{\rm wire}(t)] + \frac{\mathrm{d}O_{\rm wire}(t)}{\mathrm{d}t} \ , \tag{3.23}$$

which describes the coherent time-variation of $O_{\rm wire}(t)$ [92].

3.2.1 Coherent dynamics

In principle, all one-electron wire expectation values at a time t can be expressed as linear combinations of the quantities $\langle c_n^\dagger c_{n'}\rangle_t$. However, as emphasised in Chapter 2, the coherent dynamics of a time-periodically driven system is most efficiently described by the Floquet modes $|\Phi_\alpha(t)\rangle$, i.e., the solutions of Eq. (2.3). This Floquet equation assumes in the present context, where $H(t) = H_{\rm wire}(t) = \sum_{nn'}|n\rangle H_{nn'}(t)\langle n'|$, the form

$$\Big(\sum_{n,n'}|n\rangle H_{nn'}(t)\langle n'| - \mathrm{i}\hbar\frac{\mathrm{d}}{\mathrm{d}t}\Big)|\Phi_\alpha(t)\rangle = \epsilon_\alpha|\Phi_\alpha(t)\rangle \ . \tag{3.24}$$

In terms of the fermionic creation and annihilation operators, the Floquet modes translate into a "Floquet picture", defined by the time-dependent transformation

$$c_\alpha(t) = \sum_n \langle\Phi_\alpha(t)|n\rangle\, c_n \ . \tag{3.25}$$

The inverse transformation

$$c_n = \sum_\alpha \langle n|\Phi_\alpha(t)\rangle\, c_\alpha(t) \tag{3.26}$$

follows from the mutual orthogonality (2.15) and the completeness of the Floquet states at equal times [26, 93]. Note that the right-hand side of Eq. (3.26) becomes t-independent after the summation. In the interaction picture, the operators $c_\alpha(t)$ obey

$$\tilde{c}_\alpha(t,t') = U_0^\dagger(t,t')\, c_\alpha(t)\, U_0(t,t') = e^{-\mathrm{i}\epsilon_\alpha(t-t')/\hbar}\, c_\alpha(t') \ . \tag{3.27}$$

published by Shaker Verlag, Aachen, ISBN 3-8322-1979-X

This is easily verified by differentiating the expression after the first equal sign with respect to t and by using that $|\Phi_\alpha(t)\rangle$ is a solution of the eigenvalue equation (3.24). The proof is completed by noting that Eq. (3.27) fulfils the initial condition $\tilde{c}_\alpha(t',t') = c_\alpha(t')$.

Using the operators $c^\dagger_\beta(t)c_\alpha(t)$ with $\alpha,\beta = 1,\ldots,N$, for $O_{\text{wire}}(t)$ in Eqs. (3.22) and (3.23), we obtain after a straightforward calculation that their coherent time-variation is very simple indeed, namely

$$(c^\dagger_\beta(t)\, c_\alpha(t))^\circ = -\frac{\mathrm{i}}{\hbar}(\epsilon_\alpha - \epsilon_\beta)\, c^\dagger_\beta(t)\, c_\alpha(t)\ . \tag{3.28}$$

In other words, the coherent part of Eq. (3.22) has been solved by the canonical transformation (3.25).

3.2.2 Incoherent dynamics

The discussion of the coherent time-evolution has yielded the adequate basis operators $O_{\text{wire}}(t) = c^\dagger_\beta(t)c_\alpha(t)$ with corresponding expectation values

$$P_{\alpha\beta}(t) := \langle c^\dagger_\beta(t)\, c_\alpha(t)\rangle_t\ . \tag{3.29}$$

As for the incoherent contributions, we now consider subsequently the terms resulting from the coupling to the electronic leads (3.5) and to the phonons (3.10). Note that each such contribution may be treated separately since the equilibrium distribution $\varrho_{\text{env,eq}}$ of the environmental degrees of freedom contained in the expectation value of the integrand of Eq. (3.22) contains no correlations between the different reservoirs. In the following, we will derive from the master equation (3.21) for the reduced, many-particle density matrix $\varrho_{\text{wire}}(t)$ within a mean-field approximation the non-linear kinetic equation

$$\begin{aligned}\frac{\mathrm{d}P_{\alpha\beta}(t)}{\mathrm{d}t} =& -\frac{\mathrm{i}}{\hbar}(\epsilon_\alpha - \epsilon_\beta)P_{\alpha\beta}(t)\\ &+\sum_{\alpha'\beta'}\left[\mathcal{R}^{\text{leads}}_{\alpha\beta\alpha'\beta'}(t) + \mathcal{R}^{\text{phonons}}_{\alpha\beta\alpha'\beta'}(t)\right]P_{\alpha'\beta'}(t)\\ &+\sum_{\alpha'\beta'\alpha''\beta''}\mathcal{Q}^{\text{phonons}}_{\alpha\beta\alpha'\beta'\alpha''\beta''}(t)\,P_{\alpha'\beta'}(t)\,P_{\alpha''\beta''}(t)\\ &+\mathcal{S}^{\text{leads}}_{\alpha\beta}(t)\ .\end{aligned} \tag{3.30}$$

for the one-particle expectation values $P_{\alpha\beta}(t)$. This equation presents one of the central formal results of the present work. Here, $\mathcal{R}^{\text{leads}}_{\alpha\beta\alpha'\beta'}(t)$ and $\mathcal{R}^{\text{phonons}}_{\alpha\beta\alpha'\beta'}(t)$ are Redfield tensors resulting from the wire-lead and electron-phonon coupling, respectively. In addition, within a mean-field approximation, the electron-phonon coupling contributes a

published by Shaker Verlag, Aachen, ISBN 3-8322-1979-X

quadratic term with coefficient tensor $\mathcal{Q}^{\text{phonons}}_{\alpha\beta\alpha'\beta'\alpha''\beta''}(t)$. Finally, the source term $S^{\text{leads}}_{\alpha\beta}(t)$ reflects the in- and outflux of electrons from and to the leads. The specific form of these contributions will be derived in the following sections.

Contribution from coupling to electronic leads

For a wire operator $O_{\text{wire}}(t)$ consisting of an even number of creation and/or destruction operators, the integral in Eq. (3.22) can be cast into the form

$$\begin{aligned}
&\frac{1}{\hbar^2}\int_0^\infty \mathrm{d}\tau\,\langle[[O_{\text{wire}}(t),H_{\text{wire-leads}}],\widetilde{H}_{\text{wire-leads}}(t-\tau,t)]\rangle_t \\
&=\sum_{\ell=1}^{L}\int_0^\infty\frac{\mathrm{d}\tau}{\hbar}\int\frac{\mathrm{d}\epsilon}{2\pi}\Gamma_\ell(\epsilon)\Big\{\mathrm{e}^{\mathrm{i}\epsilon\tau/\hbar}\Big[\langle[[O_{\text{wire}}(t),c_\ell],\tilde{c}^\dagger_\ell]_+\rangle_t f(\epsilon-\mu_\ell)-\langle\tilde{c}^\dagger_\ell[O_{\text{wire}}(t),c_\ell]\rangle_t\Big] \\
&\qquad\qquad -\mathrm{e}^{-\mathrm{i}\epsilon\tau/\hbar}\Big[\langle[[O_{\text{wire}}(t),c^\dagger_\ell],\tilde{c}_\ell]_+\rangle_t f(\epsilon-\mu_\ell)-\langle[O_{\text{wire}}(t),c^\dagger_\ell]\tilde{c}_\ell\rangle_t\Big]\Big\}\,.
\end{aligned} \tag{3.31}$$

Here, we have used for the lead operators the relation $\tilde{c}_{q\ell}(t-\tau,t)=\exp(\mathrm{i}\epsilon_{q\ell}\tau/\hbar)c_{q\ell}$ together with the equilibrium expectation values (3.4). For notational compactness, the time arguments of the interaction picture operators $\tilde{c}_\ell(t-\tau,t)$ have been suppressed.

In view of Eq. (3.29), we now have to consider the special case $O_{\text{wire}}(t)=c^\dagger_\beta(t)\,c_\alpha(t)$, for which the commutators in Eq. (3.31) are readily evaluated using Eq. (3.26) to read

$$[c^\dagger_\beta(t)\,c_\alpha(t),c_\ell]=-\langle\ell|\Phi_\beta(t)\rangle\,c_\alpha(t)\;,\quad [c^\dagger_\beta(t)\,c_\alpha(t),c^\dagger_\ell]=\langle\Phi_\alpha(t)|\ell\rangle\,c^\dagger_\beta(t)\;. \tag{3.32}$$

Moreover, the transformation (3.26) yields in conjunction with Eqs. (2.13), (2.14), (2.17), and (3.27) the spectral decomposition of the wire operators in the interaction picture,

$$\tilde{c}_\ell(t-\tau,t)=\sum_{\alpha' k}\mathrm{e}^{-\mathrm{i}k\Omega t}\,\mathrm{e}^{\mathrm{i}\epsilon_{\alpha',k}\tau/\hbar}\langle\ell|\Phi_{\alpha',k}\rangle\,c_{\alpha'}(t)\;. \tag{3.33}$$

With the aid of the last two equations, one may readily carry out the time and the energy integrations in Eq. (3.31). Inserting the resulting expressions into the dynamical equation (3.22) then yields the Redfield tensor

$$\begin{aligned}
\mathcal{R}^{\text{leads}}_{\alpha\beta\alpha'\beta'}(t)=-\frac{1}{2}\sum_{\ell=1}^{L}\sum_{kk'}\mathrm{e}^{\mathrm{i}(k'-k)\Omega t}\Big\{&\Gamma_\ell(\epsilon_{\alpha',k})\langle\Phi_{\alpha,k'}|\ell\rangle\langle\ell|\Phi_{\alpha',k}\rangle\,\delta_{\beta\beta'} \\
&+\Gamma_\ell(\epsilon_{\beta',k'})\langle\Phi_{\beta',k'}|\ell\rangle\langle\ell|\Phi_{\beta,k}\rangle\,\delta_{\alpha\alpha'}\Big\}
\end{aligned} \tag{3.34}$$

published by Shaker Verlag, Aachen, ISBN 3-8322-1979-X

and the source terms

$$\mathcal{S}^{\text{leads}}_{\alpha\beta}(t) = \frac{1}{2}\sum_{\ell=1}^{L}\sum_{kk'} \mathrm{e}^{\mathrm{i}(k'-k)\Omega t}\langle\Phi_{\alpha,k'}|\ell\rangle\langle\ell|\Phi_{\beta,k}\rangle\big\{\Gamma_\ell(\epsilon_{\alpha,k})f(\epsilon_{\alpha,k}-\mu_\ell) + \Gamma_\ell(\epsilon_{\beta,k})f(\epsilon_{\beta,k}-\mu_\ell)\big\}\ . \tag{3.35}$$

Note that principal value terms stemming from an energy renormalisation due to the coupling to the leads have been neglected in Eqs. (3.34) and (3.35). For later use, we note that in the wide-band limit (3.7) for the wire-lead coupling these expressions assume the more compact form

$$\mathcal{R}^{\text{leads}}_{\alpha\beta\alpha'\beta'}(t) = -\sum_{\ell=1}^{L}\frac{\Gamma_\ell}{2}\sum_{kk'} \mathrm{e}^{\mathrm{i}(k'-k)\Omega t}\left\{\langle\Phi_{\alpha,k'}|\ell\rangle\langle\ell|\Phi_{\alpha',k}\rangle\,\delta_{\beta\beta'} + \langle\Phi_{\beta',k'}|\ell\rangle\langle\ell|\Phi_{\beta,k}\rangle\,\delta_{\alpha\alpha'}\right\} \tag{3.36}$$

and

$$\mathcal{S}^{\text{leads}}_{\alpha\beta}(t) = \sum_{\ell=1}^{L}\frac{\Gamma_\ell}{2}\sum_{kk'} \mathrm{e}^{\mathrm{i}(k'-k)\Omega t}\langle\Phi_{\alpha,k'}|\ell\rangle\langle\ell|\Phi_{\beta,k}\rangle\left\{f(\epsilon_{\alpha,k}-\mu_\ell)+f(\epsilon_{\beta,k}-\mu_\ell)\right\}\ . \tag{3.37}$$

Contribution from coupling to phonons

For the derivation of the phononic contributions to the kinetic equation (3.30), we write the electron-phonon coupling Hamiltonian (3.10) as

$$H_{\text{wire-phonons}} = \sum_\nu X_\nu\, F_\nu \tag{3.38}$$

with the position and force operators

$$X_\nu := \sum_{n,n'} X_{nn'\nu}\, c_n^\dagger c_{n'}\ , \quad F_\nu := \sum_q M_{q\nu}(b_{q\nu}+b_{q\nu}^\dagger)\ . \tag{3.39}$$

Then, the integral in Eq. (3.21) can be expressed as

$$\begin{aligned}\frac{1}{\hbar^2}\int_0^\infty \mathrm{d}\tau\,\langle[[O_{\text{wire}}(t),H_{\text{wire-phonons}}],\widetilde{H}_{\text{wire-phonons}}(t-\tau,t)]\rangle_t \\ = \frac{1}{\hbar}\sum_\nu\int_0^\infty \mathrm{d}\tau\, S_\nu(\tau)\,\langle[[O_{\text{wire}}(t),X_\nu],\widetilde{X}_\nu(t-\tau,t)]\rangle_t \\ + \frac{\mathrm{i}}{\hbar}\sum_\nu\int_0^\infty \mathrm{d}\tau\, A_\nu(\tau)\,\langle[[O_{\text{wire}}(t),X_\nu],\widetilde{X}_\nu(t-\tau,t)]_+\rangle_t\ .\end{aligned} \tag{3.40}$$

published by Shaker Verlag, Aachen, ISBN 3-8322-1979-X

Here, we have introduced the symmetrised and antisymmetrised autocorrelation functions

$$S_\nu(\tau) := \frac{1}{2\hbar}\langle[\widetilde{F}_\nu(\tau), F_\nu]_+\rangle_{\mathrm{eq}} = \int_0^\infty \frac{\mathrm{d}\omega}{\pi} D_\nu(\omega)\coth(\hbar\omega/2k_\mathrm{B}T)\cos(\omega\tau) \ , \tag{3.41}$$

$$A_\nu(\tau) := \frac{1}{2\mathrm{i}\hbar}\langle[\widetilde{F}_\nu(\tau), F_\nu]\rangle_{\mathrm{eq}} = -\int_0^\infty \frac{\mathrm{d}\omega}{\pi} D_\nu(\omega)\sin(\omega\tau) \ , \tag{3.42}$$

which fully characterise the fluctuation properties of the environment. For the expression of the autocorrelation functions in terms of the spectral density (3.11) we have made use of the equilibrium expectation values (3.21) together with the relation $n_\mathrm{B}(\epsilon) = \frac{1}{2}[\coth(\epsilon/2k_\mathrm{B}T) - 1]$. Note that $\coth(x) = 1/x + \mathcal{O}(x)$ so that the existence of the low-frequency contributions to the integral (3.41) is well guaranteed by for the Ohmic and superohmic case (3.12).

Like for the wire-lead coupling, the next step consists in the evaluation of the dynamical equation (3.40) for $O_\mathrm{wire}(t) = c_\beta^\dagger(t)c_\alpha(t)$. Here, however, because of the different structure of the electron-phonon coupling Hamiltonian (3.38) compared with that of the wire-lead coupling (3.5), it is impossible to obtain a closed set of equations for the expectation values $P_{\alpha\beta}(t)$ like that in Eq. (3.34). Instead, the expectation values in the third line of Eq. (3.40), i.e., the terms proportional to the antisymmetrised autocorrelation functions $A_\nu(\tau)$, generate higher order terms of the structure $\langle c_\delta^\dagger(t)c_\gamma^\dagger(t)c_\beta(t)c_\alpha(t)\rangle_t$. This leads to a hierarchy of equations for all wire expectation values with up to N destruction and creation operators. To close this hierarchy already at the level of the $P_{\alpha\beta}(t)$, we adopt the mean-field approximation

$$\begin{aligned}\langle c_\delta^\dagger(t)c_\gamma^\dagger(t)c_\beta(t)c_\alpha(t)\rangle_t &\approx \langle c_\delta^\dagger(t)c_\alpha(t)\rangle_t\langle c_\gamma^\dagger(t)c_\beta(t)\rangle_t - \langle c_\delta^\dagger(t)c_\beta(t)\rangle_t\langle c_\gamma^\dagger(t)c_\alpha(t)\rangle_t \\ &= P_{\alpha\delta}(t)P_{\beta\gamma}(t) - P_{\beta\delta}(t)P_{\alpha\gamma}(t) \ .\end{aligned} \tag{3.43}$$

Though such a crude approximation does only cover the most basic properties of the many-particle problem (3.38), it enables an efficient treatment of the present problem. Moreover, in thermal equilibrium, i.e., in the absence of a time-dependent driving and without external bias, it gives a solution that guarantees that the current through the wire vanishes, as will be demonstrated in Sects. 3.4.1 and 5.3.1. In other words, the mean-field approximation (3.43) yields a description that is consistent with the second law of thermodynamics. We remark that in principle one could also include electron-electron interaction in the framework of the mean-field approximation (3.43), similar to the approach put forward in Refs. [94, 95]. However, in order to focus on the phonon-mediated interaction effects, we refrain from doing so in the present work.

We emphasise that if one considers only one particle, the mean-field approximation (3.43) fails completely, because then all two-particle expectation values at equal

published by Shaker Verlag, Aachen, ISBN 3-8322-1979-X

times vanish exactly. Consequently, non-linear terms of the type (3.43) do not appear. For the description of the transport problem, such a one-particle case is often assumed beforehand [74–79]. The same happens, if one considers a fixed number of wire electrons, say one, like in the case without a tunnelling coupling to external leads. Then, by omitting in the non-linear kinetic equation (3.30) all terms quadratic in $P_{\alpha\beta}(t)$, one arrives back at the linear master equation that has been used for the description of dissipative quantum systems, e.g., in Refs. [26, 96–102].

For the further evaluation of Eq. (3.40), we now express the operator X_ν and its interaction picture version $\tilde{X}_\nu(t-\tau,t)$ in terms of the Floquet picture operators at time t, yielding

$$X_\nu = \sum_{\alpha,\beta=1}^{N} \sum_{k} \mathrm{e}^{\mathrm{i}k\Omega t} \bar{X}^{\nu}_{\alpha\beta,k} c^\dagger_\alpha(t) c_\beta(t) \;, \tag{3.44}$$

$$\widetilde{X}_\nu(t-\tau,t) = \sum_{\alpha,\beta=1}^{N} \sum_{k} \mathrm{e}^{\mathrm{i}k\Omega t} \mathrm{e}^{\mathrm{i}(\epsilon_\beta-\epsilon_\alpha-k\hbar\Omega)\tau/\hbar} \bar{X}^{\nu}_{\alpha\beta,k} c^\dagger_\alpha(t) c_\beta(t) \;. \tag{3.45}$$

Here, we have abbreviated the time-averaged coupling matrix elements in the Floquet basis by

$$\bar{X}^{\nu}_{\alpha\beta,k} := \sum_{n,n'} \sum_{k'} \langle \Phi_{\alpha,k+k'}|n\rangle X_{nn'\nu} \langle n'|\Phi_{\beta,k'}\rangle \;. \tag{3.46}$$

Disregarding again the principal value integrals which correspond to an energy renormalisation due to the electron-phonon coupling, we arrive at the Redfield tensor of the electron-phonon coupling

$$\begin{aligned} \mathcal{R}^{\text{phonons}}_{\alpha\beta\alpha'\beta'}(t) = \sum_{\nu} \sum_{k,k'} \mathrm{e}^{\mathrm{i}(k'-k)\Omega t} \Big\{ & \left[N_\nu(\Delta_{\alpha\alpha',k'}) + N_\nu(\Delta_{\beta\beta',k}) \right] \bar{X}^{\nu}_{\alpha\alpha',k'} \bar{X}^{\nu}_{\beta'\beta,-k} \\ & - \delta_{\alpha\alpha'} \sum_{\alpha''} N_\nu(\Delta_{\alpha''\beta',k}) \bar{X}^{\nu}_{\alpha''\beta,k'} \bar{X}^{\nu}_{\beta'\alpha''-k} \\ & - \delta_{\beta\beta'} \sum_{\beta''} N_\nu(\Delta_{\beta''\alpha',k'}) \bar{X}^{\nu}_{\beta''\alpha',k'} \bar{X}^{\nu}_{\alpha\beta'',-k} \Big\} \;. \end{aligned} \tag{3.47}$$

Here, the functions $N_\nu(\epsilon)$ are defined for each phonon bath ν by

$$N_\nu(\epsilon) := \frac{1}{\hbar} D_\nu(\epsilon/\hbar)\, n_{\mathrm{B}}(\epsilon) \;. \tag{3.48}$$

Note that owing to the restriction (3.12), the $N_\nu(\epsilon)$ are well-defined in the limit $\epsilon \to 0$. Furthermore, we have abbreviated the quasienergy differences as

$$\Delta_{\alpha\beta,k} := \epsilon_\alpha - \epsilon_\beta + k\hbar\Omega \;. \tag{3.49}$$

published by Shaker Verlag, Aachen, ISBN 3-8322-1979-X

The coefficient tensor of the quadratic contributions reads

$$\begin{aligned}\mathcal{Q}^{\text{phonons}}_{\alpha\beta\alpha'\beta'\alpha''\beta''}(t) = \frac{1}{\hbar}\sum_{\nu}\sum_{k,k'} \mathrm{e}^{\mathrm{i}(k'-k)\Omega t}\Big\{ & D_\nu(\Delta_{\beta'\alpha'',k'}/\hbar)\bar{X}^{\nu}_{\beta'\alpha'',k'}\bar{X}^{\nu}_{\beta''\beta,-k}\delta_{\alpha\alpha'} \\ & + D_\nu(\Delta_{\beta'\alpha',k'}/\hbar)\bar{X}^{\nu}_{\beta'\alpha',k'}\bar{X}^{\nu}_{\alpha\alpha'',-k}\delta_{\beta\beta''} \\ & - D_\nu(\Delta_{\beta'\alpha',k'}/\hbar)\bar{X}^{\nu}_{\beta'\alpha',k'}\bar{X}^{\nu}_{\beta''\beta,-k}\delta_{\alpha\alpha''} \\ & - D_\nu(\Delta_{\beta''\alpha',k'}/\hbar)\bar{X}^{\nu}_{\beta''\alpha',k'}\bar{X}^{\nu}_{\alpha\alpha'',-k}\delta_{\beta\beta'}\Big\}\ .\end{aligned} \tag{3.50}$$

Obviously, these quadratic contributions do not depend on the temperature but only on the spectral densities $D_\nu(\omega)$ and the matrix elements $\bar{X}^{\nu}_{\alpha\beta,k}$ of the coupling to the phonon baths.

For later use, we remark that because of the particle number conserving coupling (3.10), the partial traces over the tensors $\mathcal{R}^{\text{phonons}}_{\alpha\beta\alpha'\beta'}(t)$ and $\mathcal{Q}^{\text{phonons}}_{\alpha\beta\alpha'\beta'\alpha''\beta''}(t)$ fulfil the identities

$$\sum_{\alpha}\mathcal{R}^{\text{phonons}}_{\alpha\alpha\alpha'\beta'}(t) = 0\ , \tag{3.51}$$

$$\sum_{\alpha}\mathcal{Q}^{\text{phonons}}_{\alpha\alpha\alpha'\beta'\alpha''\beta''}(t) = -\sum_{\alpha}\mathcal{Q}^{\text{phonons}}_{\alpha\alpha\alpha''\beta''\alpha'\beta'}(t)\ . \tag{3.52}$$

Their verification from the respective definitions (3.47) and (3.50) is straightforward.

3.3 Rotating-wave approximation

For a very weak coupling between the wire electrons and the environmental degrees of freedom, the coherent time-evolution (3.28) dominates the dynamics of the density matrix $P_{\alpha\beta}(t)$. Thus, it is convenient to define the interaction picture

$$\widetilde{P}_{\alpha\beta}(t) := \mathrm{e}^{\mathrm{i}(\epsilon_\alpha-\epsilon_\beta)t/\hbar}\,P_{\alpha\beta}(t) \tag{3.53}$$

with respect to the dynamics of the wire electrons including the oscillating driving-force. Inserting this definition into the kinetic equation (3.30), yields the new equations of motion

$$\frac{\mathrm{d}\widetilde{P}_{\alpha\beta}(t)}{\mathrm{d}t} = \sum_{\alpha'\beta'}\mathrm{e}^{\mathrm{i}(\epsilon_\alpha-\epsilon_\beta-\epsilon_{\alpha'}+\epsilon_{\beta'})t/\hbar}\,\mathcal{R}^{\text{leads}}_{\alpha\beta\alpha'\beta'}(t)\,\widetilde{P}_{\alpha'\beta'}(t) + \mathrm{e}^{\mathrm{i}(\epsilon_\alpha-\epsilon_\beta)t/\hbar}\,\mathcal{S}^{\text{leads}}_{\alpha\beta}(t)\ . \tag{3.54}$$

The contribution due to the coherent dynamics has moved to the exponential prefactors, which thereby have acquired an additional time-dependency. Since the rotating-wave approximation is most useful in a situation without electron-phonon coupling [cf. discussion after Eq. (3.59) below], we consider in Eq. (3.54) only the wire-lead coupling. The more tedious derivation of the RWA for the electron-phonon coupling

published by Shaker Verlag, Aachen, ISBN 3-8322-1979-X

is discussed in Appendix B.

The largest time-scale of the coherent evolution is determined by the smallest quasienergy difference $\Delta_{\alpha\beta,k}$, while the dissipative time-scale is of the order of the coupling rates $\Gamma_\ell(\epsilon)$. We now assume that both time-scales are well-separated, , i.e.,

$$|\epsilon_\alpha - \epsilon_\beta + k\hbar\Omega| \gg \hbar\Gamma_\ell(\epsilon) \quad \text{for all } \ell,\, k,\, \epsilon \text{ and } \alpha \neq \beta \; . \tag{3.55}$$

In particular, this requires that the quasienergy spectrum has no degeneracies. Then, it is possible to replace the time-dependent coefficients in Eq. (3.54) by their time-averages. This yields only contributions when either $\alpha = \alpha'$ and $\beta = \beta'$ or $\alpha = \beta$ and $\alpha' = \beta'$ (for details, see Appendix B). Thus, the dynamics of the diagonal and the off-diagonal density matrix elements separates

$$\dot{\widetilde{P}}_{\alpha\alpha}(t) = -w_\alpha^{\text{leads}}\, \widetilde{P}_{\alpha\alpha}(t) + s_\alpha^{\text{leads}} \; , \tag{3.56}$$

$$\dot{\widetilde{P}}_{\alpha\beta}(t) = -\frac{1}{2}\left(w_\alpha^{\text{leads}} + w_\beta^{\text{leads}}\right) \widetilde{P}_{\alpha\beta}(t) \; , \quad \alpha \neq \beta \; . \tag{3.57}$$

The rates of this RWA master equation are given by

$$w_\alpha^{\text{leads}} := \sum_{\ell=1}^{L} \sum_k |\langle \ell | \Phi_{\alpha,k} \rangle|^2 \, \Gamma_\ell(\epsilon_{\alpha,k}) \tag{3.58}$$

and

$$s_\alpha^{\text{leads}} := \sum_{\ell=1}^{L} \sum_k |\langle \ell | \Phi_{\alpha,k} \rangle|^2 \, \Gamma_\ell(\epsilon_{\alpha,k}) \, f(\epsilon_{\alpha,k} - \mu_\ell) \; . \tag{3.59}$$

We remark that a similar RWA approximation was used in Refs. [55, 56] for the description of driven transport in the presence of Coulomb interactions.

From the RWA master equation (3.56) follows that the off-diagonal elements decay on a time-scale determined by $(w_\alpha^{\text{leads}} + w_\beta^{\text{leads}})/2$, while the diagonal elements converge to a finite value. Therefore, the stationary solution is diagonal,

$$P_{\alpha\beta} = P_\alpha \, \delta_{\alpha\beta} \; , \tag{3.60}$$

with the populations P_α given by the weighted average

$$P_\alpha = \frac{s_\alpha^{\text{leads}}}{w_\alpha^{\text{leads}}} = \frac{\sum_{\ell=1}^{L} \sum_k |\langle \ell | \Phi_{\alpha,k} \rangle|^2 \; \Gamma_\ell(\epsilon_{\alpha,k}) f(\epsilon_{\alpha,k} - \mu_\ell)}{\sum_{\ell=1}^{L} \sum_k |\langle \ell | \Phi_{\alpha,k} \rangle|^2 \, \Gamma_\ell(\epsilon_{\alpha,k})} \; . \tag{3.61}$$

Thus, the one-particle density matrix becomes time-independent and diagonal in the Floquet basis.

published by Shaker Verlag, Aachen, ISBN 3-8322-1979-X

Finally, we note that in the presence of electron-phonon interaction, diagonal and off-diagonal dynamics no longer decouple [cf. Eqs. (B.6) and (B.9)]. Moreover, even if we conjecture that the reduced density matrix at asymptotic times is diagonal, we obtain from Eq. (B.6) a set of non-linear equations for the populations $P_{\alpha\alpha}(t)$, which, in general, cannot be solved analytically. This restricts the usefulness of the rotating-wave approximation in the presence of electron-phonon interaction.

3.4 Analytical solutions for two special cases

3.4.1 Thermal equilibrium

In thermal equilibrium, i.e., for a time-independent Hamiltonian ($H(t) =: H_0$) and in the absence of an external bias ($\mu_\ell = \text{const.} =: \mu$), the Fermi distribution

$$P_{\alpha\beta} = f(E_\alpha - \mu)\,\delta_{\alpha\beta} \tag{3.62}$$

solves the set (3.30) of *non-linear* equations.[2] Here, the indices α and β refer to the different eigenstates of H_0, and E_α is the corresponding eigenenergy. For details, we refer the reader to Appendix C. We only remark that the proof is based upon the identity (C.10) for Bose and Fermi functions. We will later see that the solution (3.62) guarantees the absence of a current through the molecule in thermal equilibrium.

3.4.2 Equal coupling to all leads in the wide-band limit without electron-phonon coupling

Let us consider the wide-band limit (3.7) with the additional restriction that each wire site is equally strong coupled to the adjacent lead, i.e.,

$$\Gamma_\ell = \Gamma \text{ and } L = N\ . \tag{3.63}$$

Note that a similar assumption was used in Refs. [50, 103]. However, for the typical situation of a contact to two leads ($L = 2$), it implies the restriction to a two-site wire ($N = 2$). From Eq. (3.36), we then obtain with the help of the completeness of the wire states $|\ell\rangle$ and the orthogonality of the Floquet modes $|\Phi_\alpha(t)\rangle$ at equal times the Redfield tensor

$$\mathcal{R}^{\text{leads}}_{\alpha\beta\alpha'\beta'}(t) = -\Gamma\,\delta_{\alpha\alpha'}\delta_{\beta\beta'}\ . \tag{3.64}$$

[2] Of course, thermal equilibrium requires all baths to be at a common temperature, as was put into our model from the very beginning.

published by Shaker Verlag, Aachen, ISBN 3-8322-1979-X

Without electron-phonon coupling, it is then possible to derive an explicit expression for the solution of the kinetic equation (3.30) at asymptotic times $t \to \infty$, namely

$$P_{\alpha\beta}(t) = \frac{\Gamma}{2} \sum_{kk'} \mathrm{e}^{\mathrm{i}(k-k')\Omega t} \frac{\sum_{\ell=1}^{L} \left[f(\epsilon_{\alpha,k} - \mu_\ell) + f(\epsilon_{\beta,k'} - \mu_\ell) \right] \langle \Phi_{\alpha,k} | \ell \rangle \langle \ell | \Phi_{\beta,k'} \rangle}{\mathrm{i}(\epsilon_{\alpha,k} - \epsilon_{\beta,k'})/\hbar + \Gamma} \ . \quad (3.65)$$

Granted that $\epsilon_{\alpha,k} \neq \epsilon_{\beta,k}$ for $\alpha \neq \beta$ and arbitrary k, k', the explicit solution (3.65) yields to first order in the coupling strength Γ a diagonal solution with the populations

$$P_\alpha = \sum_k \sum_{\ell=1}^{L} f(\epsilon_{\alpha,k} - \mu_\ell) |\langle \ell | \Phi_{\alpha,k} \rangle|^2 \quad (3.66)$$

of a state α, consistent with the RWA expression (3.61).

3.5 Numerical solution of the kinetic equation

In general, one has to resort to numerical methods for the solution of the master equation (3.30). Let us first discuss the situation without coupling to phonon baths, where the kinetic equation assumes a linear, dissipative, periodically time-dependent form. Hence, its solution $P_{\alpha\beta}(t)$ shares in the long-time limit the time-periodicity of the driving field, and can be decomposed in the Fourier series

$$P_{\alpha\beta}(t) = \sum_k \mathrm{e}^{-\mathrm{i}k\Omega t} P_{\alpha\beta,k} \ , \quad P_{\alpha\beta,k} := \int_0^T \mathrm{d}t \, \mathrm{e}^{\mathrm{i}k\Omega t} \, P_{\alpha\beta}(t) \ . \quad (3.67)$$

A spectral decomposition of the master equation (3.30) then yields an infinite set of linear equations for the $P_{\alpha\beta,k}$. In the wide-band limit (3.7), which we shall adopt in all numerical calculations below, they assume the form [90, 104]

$$\begin{aligned} \frac{\mathrm{i}}{\hbar}(\epsilon_\beta - \epsilon_\alpha + k\hbar\Omega) P_{\alpha\beta,k} = \sum_{\ell=1}^{L} \frac{\Gamma_\ell}{2} \sum_{k'} \Big\{ & \sum_{\alpha' k''} \langle \Phi_{\alpha,k'+k''} | \ell \rangle \langle \ell | \Phi_{\alpha',k+k''} \rangle P_{\alpha'\beta,k'} \\ & + \sum_{\beta' k''} \langle \Phi_{\beta',k'+k''} | \ell \rangle \langle \ell | \Phi_{\beta,k+k''} \rangle P_{\alpha\beta',k'} \\ & - \langle \Phi_{\alpha,k'} | \ell \rangle \langle \ell | \Phi_{\beta,k'+k} \rangle f(\epsilon_{\alpha,k'} - \mu_\ell) \\ & - \langle \Phi_{\alpha,k'-k} | \ell \rangle \langle \ell | \Phi_{\beta,k'} \rangle f(\epsilon_{\beta,k'} - \mu_\ell) \Big\} \ . \end{aligned} \quad (3.68)$$

Note that typically a large number of sidebands contributes significantly to the Fourier decomposition of the Floquet modes $|\Phi_\alpha(t)\rangle$. On the other hand, numerical convergence for the solution of the master equation (3.68) is already obtained by using a few sidebands for the decomposition of $P_{\alpha\beta}(t)$. This justifies *a posteriori* the use of the

published by Shaker Verlag, Aachen, ISBN 3-8322-1979-X

Floquet basis (3.26). In many cases it even suffices to only take into account the time-averages $P_{\alpha\beta,0}$, amounting to a moderate rotating-wave approximation [97, 98]. Thus, the numerical effort for the solution of Eq. (3.68) is rather small, and, in particular, not the limiting step of the entire numerical procedure.

In the presence of electron-phonon coupling, we use a numerical propagation scheme for the computation of the long-time limit of the solutions of the set of non-linear equations (3.30). From the resulting time-series one can first verify the T-periodicity of the solution and then compute the Fourier coefficients $P_{\alpha\beta,k}$ directly from their definition (3.67). In contrast to solving the set of linear equations (3.68), the propagation scheme is numerically rather time-consuming and, especially in the strongly driven regime, only applicable for not too large systems.

3.6 Summary

The topic of this chapter has been the description of a T-periodically driven molecular structure, being weakly coupled to several macroscopic electronic leads and to phonon baths of the surrounding. Starting from the exact dynamics (3.15) of the total system comprising molecule plus environment, we have derived the kinetic equation (3.30) for the reduced density matrix in the Floquet basis.

It turned out that the influence of an electronic lead ℓ is fully determined by the density of state of the coupling $\Gamma_\ell(\epsilon)$ defined in Eq. (3.6) together with the Fermi distribution function $f(\epsilon - \mu_\ell)$. In the sequel of this work, we will assume the wide-band limit (3.7), that is, spectral densities which do not depend on the energy ϵ. An important feature of the wire-lead coupling is that is does not conserve the electron number on the wire, resulting in source terms $\mathcal{S}^{\text{leads}}_{\alpha\beta}(t)$ in the kinetic equation (3.30).

The coupling to the phonon bath ν is specified by the coupling matrix elements $X_{nn'\nu}$ in conjunction with the spectral density $D_\nu(\omega)$ from Eqs. (3.11) and (3.13) as well as the Bose distribution $n_{\text{B}}(\hbar\omega)$. The form (3.10) of the electron-phonon coupling generates—even within the weak-coupling approach we have put forward—higher order expectation values, which do not occur within a single-particle theory. However, since the electron number on the wire is not fixed, we have to include them for a consistent theory. In the framework of our approach, this has been done within the mean-field approximation (3.43), leading to non-linear terms in the kinetic equation. Fortunately, this approximation yields the Fermi distribution as thermal equilibrium solution, thus preventing a non-zero current through the molecule.

Compared to the approaches mentioned in the introduction of this chapter [74–79], which use a one-particle picture, we put forward a description that takes into account the phonon-mediated interaction, albeit in a mean-field approximation. On the other hand, we have to require a weak-coupling of the wire-electrons to both the leads and the phonons, which is not necessary in a scattering approach like that of Refs. [74–76, 78, 79]. Yet, our approach goes beyond the rotating-wave approximation, which is

published by Shaker Verlag, Aachen, ISBN 3-8322-1979-X

frequently employed, e.g., in Refs. [55, 56]. Especially the latter point turns out to be crucial in certain parameter regimes (see, for instance, Sect. 5.4.1).

Apart from this equilibrium situation, an analytical solution has been found only in the special case of equal coupling between all sites and all leads in the wide-band limit without electron-phonon interaction. Otherwise, one has to resort to approximation schemes or numerical methods for the determination of the stationary solution of the master equation. Commonly employed is the rotating-wave approximation, which, in the absence of electron-phonon interaction, results in a decoupled set of equations that can be solved explicitly.

published by Shaker Verlag, Aachen, ISBN 3-8322-1979-X

4 Electrical current through the wire

The central quantity of interest in the present work is the electrical current through the molecular wire. We will derive here expressions for both the time-dependent and the time-averaged current across the different wire-lead contacts, which are based on the solution of the kinetic equation from the previous chapter.

4.1 Time-dependent electrical current

The net (incoming minus outgoing) current through contact ℓ is given by the negative time derivative of the electron number $N_\ell = \sum_q c^\dagger_{q\ell} c_{q\ell}$ in lead ℓ multiplied by the electron charge $-e$,

$$I_\ell(t) = e\frac{\mathrm{d}}{\mathrm{d}t}\langle N_\ell\rangle_t = \frac{\mathrm{i}e}{\hbar}\left\langle [H(t), N_\ell]\right\rangle_t \,. \tag{4.1}$$

For the Hamiltonian (3.1), the commutator in Eq. (4.1) is readily evaluated to read

$$I_\ell(t) = -\frac{2e}{\hbar}\,\mathrm{Im}\sum_q V_{q\ell}\langle c^\dagger_{q\ell} c_\ell\rangle_t \,. \tag{4.2}$$

It is now convenient to switch to the interaction picture with respect to the uncoupled dynamics, which is governed by the Liouville-von Neumann equation in its integrated form (3.18). Inserting into Eq. (4.2), we obtain for the current

$$\begin{aligned} I_\ell(t) = &-\frac{2e}{\hbar}\,\mathrm{Im}\sum_q V_{q\ell}\,\mathrm{Tr}\,[\tilde{c}^\dagger_{q\ell}(t-t_0)\tilde{c}_\ell(t,t_0)\,\widetilde{\varrho}(t_0,t_0)] \\ &+\frac{2e}{\hbar^2}\,\mathrm{Re}\sum_q V_{q\ell}\int_0^{t-t_0}\mathrm{d}\tau\,\mathrm{Tr}\left\{\tilde{c}^\dagger_{q\ell}(t-t_0)\tilde{c}_\ell(t,t_0)[\widetilde{H}_{\mathrm{coupl}}(t-\tau,t_0),\widetilde{\varrho}(t-\tau,t_0)]\right\} \,. \end{aligned} \tag{4.3}$$

Due to the factorising initial condition (3.16), the first line of the last equation vanishes. Using the identity $\mathrm{Tr}\,A[B,C] = \mathrm{Tr}[A,B]C$, we thus arrive at

$$I_\ell(t) = \frac{2e}{\hbar^2}\,\mathrm{Re}\sum_q V_{q\ell}\int_0^{t-t_0}\mathrm{d}\tau\,\mathrm{Tr}\left\{[\tilde{c}^\dagger_{q\ell}(t-t_0)\tilde{c}_\ell(t,t_0), \widetilde{H}_{\mathrm{coupl}}(t-\tau,t_0)]\;\tilde{\varrho}(t-\tau,t_0)\right\} \,. \tag{4.4}$$

published by Shaker Verlag, Aachen, ISBN 3-8322-1979-X

Evaluating the commutator appearing under the trace then yields after some algebra the stationary ($t_0 \to -\infty$), *time-dependent* net electrical current through the contact ℓ,

$$I_\ell(t) = \frac{e}{\pi\hbar}\,\mathrm{Re}\int_0^\infty \mathrm{d}\tau \int \mathrm{d}\epsilon\; \Gamma_\ell(\epsilon)\,\mathrm{e}^{\mathrm{i}\epsilon\tau/\hbar}\left\{\left\langle c_\ell^\dagger\,\tilde{c}_\ell(t,t-\tau)\right\rangle_{t-\tau} - [c_\ell^\dagger,\tilde{c}_\ell(t,t-\tau)]_+ f(\epsilon-\mu_\ell)\right\}. \tag{4.5}$$

Here, we have used that for a weak wire-lead coupling, expectation values of lead operators are at all times given by their equilibrium values (3.4). Note that the anti-commutator $[c_\ell^\dagger,\tilde{c}_\ell(t,t-\tau)]_+$ is in fact a c-number, which by means of the transformation (3.26) and the interaction picture dynamics (3.27) of the wire operators in the Floquet picture reads

$$[c_\ell^\dagger,\tilde{c}_\ell(t,t-\tau)]_+ = \sum_\alpha \mathrm{e}^{-\mathrm{i}\epsilon_\alpha\tau/\hbar}\,\langle\Phi_\alpha(t-\tau)|\ell\rangle\langle\ell|\Phi_\alpha(t)\rangle\;. \tag{4.6}$$

Similarly, the expectation value appearing in the current formula (4.5) can be expressed in terms of the density-matrix elements (3.29) as

$$\left\langle c_\ell^\dagger\,\tilde{c}_\ell(t,t-\tau)\right\rangle_{t-\tau} = \sum_{\alpha\beta} \mathrm{e}^{-\mathrm{i}\epsilon_\alpha\tau/\hbar}\,\langle\Phi_\beta(t-\tau)|\ell\rangle\langle\ell|\Phi_\alpha(t)\rangle\,P_{\alpha\beta}(t-\tau)\;. \tag{4.7}$$

Using the spectral decomposition (3.67) of the density matrix (see also discussion in last paragraph of Sect. 3.5), these relations together with the spectral decomposition (3.67) of the Floquet states allow to carry out the time and energy integrals in the expression (4.5) for the net current entering the wire from the lead ℓ. We shall only give the result in the wide-band limit (3.7)—its extension to the general case is straightforward. The first contribution of the ϵ-integral in Eq. (4.5) is then readily evaluated to yield an expression proportional to $\delta(\tau)$. Thus, we obtain for the current the spectral decomposition

$$I_\ell(t) = \sum_k \mathrm{e}^{-\mathrm{i}k\Omega t}\,I_\ell^k, \tag{4.8}$$

with the Fourier components

$$\begin{aligned} I_\ell^k = e\Gamma_\ell\Bigg[&\sum_{\alpha\beta k'k''} \langle\Phi_{\beta,k'+k''}|\ell\rangle\langle\ell|\Phi_{\alpha,k+k''}\rangle P_{\alpha\beta,k'} \\ &-\frac{1}{2}\sum_{\alpha k'}\Big(\langle\Phi_{\alpha,k'}|\ell\rangle\langle\ell|\Phi_{\alpha,k+k'}\rangle + \langle\Phi_{\alpha,k'-k}|\ell\rangle\langle\ell|\Phi_{\alpha,k'}\rangle\Big) f(\epsilon_{\alpha,k'}-\mu_\ell) \\ &-\frac{\mathrm{i}}{2}\sum_{\alpha k'}\Big(\langle\Phi_{\alpha,k'}|\ell\rangle\langle\ell|\Phi_{\alpha,k+k'}\rangle - \langle\Phi_{\alpha,k'-k}|\ell\rangle\langle\ell|\Phi_{\alpha,k'}\rangle\Big)\mathrm{P}\int\frac{\mathrm{d}\epsilon}{\pi}\frac{f(\epsilon-\mu_\ell)}{\epsilon-\epsilon_{\alpha,k'}}\Bigg]\;. \end{aligned} \tag{4.9}$$

published by Shaker Verlag, Aachen, ISBN 3-8322-1979-X

Here, P denotes the principal value of the integral; the corresponding term does not contribute to the time-averaged (dc) components I_ℓ^0.

4.2 Time-averaged current

Equation (4.8) implies that the current $I_\ell(t)$ obeys the time-periodicity of the driving field. Since we consider here excitations by a laser field, the corresponding frequency lies in the optical or infrared spectral range. The only experimentally relevant quantity is thus the time-average of the current. For the net current entering through contact ℓ it is in the wide-band limit given by

$$\bar{I}_\ell := I_\ell^0 = e\Gamma_\ell \sum_{\alpha k} \left[\sum_{\beta k'} \langle \Phi_{\beta,k'+k}|\ell\rangle\langle\ell|\Phi_{\alpha,k'}\rangle P_{\alpha\beta,k} - |\langle\ell|\Phi_{\alpha,k}\rangle|^2 f(\epsilon_{\alpha,k}-\mu_\ell) \right] . \quad (4.10)$$

The last equation represents one of the main formal results of this thesis. In conjunction with the master equation in Fourier decomposition (3.68) (without electron-phonon interaction) or the non-linear kinetic equation (3.30) (with electron-phonon interaction), it constitutes an efficient method for the computation of dc currents through a driven molecule.

Total charge conservation of the original system Hamiltonian (3.1) of course requires that the charge on the wire $Q_{\rm wire}(t)$ can only change by current flow, amounting to the continuity equation $\dot{Q}_{\rm wire}(t) = \sum_{\ell=1}^{L} I_\ell(t)$. Since asymptotically, the charge on the wire obeys at most the periodic time-dependence of the driving field, the time-average of $\dot{Q}_{\rm wire}(t)$ must vanish in the long-time limit. From the continuity equation one then finds

$$\sum_{\ell=1}^{L} \bar{I}_\ell = 0 \, . \quad (4.11)$$

For a wire connected to two leads $\ell = {\rm L,R}$, we can then introduce the time-averaged current

$$\bar{I} := \bar{I}_{\rm L} = -\bar{I}_{\rm R}. \quad (4.12)$$

For consistency, Eq. (4.11) must also follow from expression (4.10) for the average current in the wide-band limit. In fact, this can be shown by identifying $\sum_{\ell=1}^{L} \bar{I}_\ell$ as the sum over the right-hand side of the Fourier decomposed master equation (3.68) for $\alpha = \beta$ and $k = 0$,

$$\sum_{\ell=1}^{L} \bar{I}_\ell = \sum_{\alpha} \left[\frac{\rm i}{\hbar} (\epsilon_\beta - \epsilon_\alpha + k\hbar\Omega) P_{\alpha\beta,k} \right]_{\alpha=\beta,k=0} , \quad (4.13)$$

which vanishes as expected. In the presence of electron-phonon coupling, the proof requires additionally the identities (3.51) and (3.52), which reflect the electron-number

published by Shaker Verlag, Aachen, ISBN 3-8322-1979-X

conserving nature of the electron-phonon coupling.

4.2.1 Equal coupling to all leads

In the absence of electron-phonon interaction, where additionally all wire sites are equally strong coupled to the leads, the master equation can be solved explicitly (cf. Sect. 3.4.2). Then, the dc current (4.10) can in principle be expressed completely in terms of the Floquet states and quasienergies. However, since the corresponding result is rather lengthy, we focus on the limit of an infinite voltage bias, i.e., a situation where the electro-chemical potentials lie above or below all relevant wire energies. Then it is possible to obtain a compact analytical expression for the dc current. Consider for instance the situation with two leads (and hence two sites) and $\mu_{\mathrm{R}} = -\mu_{\mathrm{R}} = \infty$, where the explicit solution (3.65) of the master equation (3.30) reads

$$P_{\alpha\beta,k} = \frac{\Gamma \langle\!\langle \Phi_\alpha|\mathrm{R}\rangle\langle\mathrm{R}|\Phi_\beta^k\rangle\!\rangle}{\mathrm{i}(\epsilon_\alpha - \epsilon_\beta - k\hbar\Omega)/\hbar + \Gamma} \ . \tag{4.14}$$

Inserting this result into the current formula (4.10), we arrive at the dc current

$$\bar{I} = e\Gamma \sum_{\alpha\beta k} \frac{\Gamma \langle\!\langle \Phi_\beta^k|\mathrm{L}\rangle\langle\mathrm{L}|\Phi_\alpha\rangle\!\rangle\langle\!\langle \Phi_\alpha|\mathrm{R}\rangle\langle\mathrm{R}|\Phi_\beta^k\rangle\!\rangle}{\mathrm{i}(\epsilon_\alpha - \epsilon_\beta - k\hbar\Omega)/\hbar + \Gamma} \ . \tag{4.15}$$

4.2.2 Rotating-wave approximation

If we assume that within RWA, and this is only guaranteed for the case of a vanishing electron-phonon interaction (cf. Sect. 3.3), the stationary solution of the kinetic equation is time-independent and diagonal in the Floquet basis, i.e., of the form $P_{\alpha\beta}(t) = P_\alpha \delta_{\alpha\beta}$, we may simplify the expression (4.10) for the dc current to read

$$\bar{I}_\ell^{\mathrm{RWA}} = e\Gamma_\ell \sum_{\alpha k} |\langle\ell|\Phi_{\alpha,k}\rangle|^2 \left[P_\alpha - f(\epsilon_{\alpha,k} - \mu_\ell)\right] \ . \tag{4.16}$$

Without electron-phonon coupling, we can then employ formula (3.61) to obtain an explicit expression for the dc current across contact ℓ,

$$\bar{I}_\ell^{\mathrm{RWA}} = e \sum_\alpha \frac{\Gamma_\ell \sum_k |\langle\ell|\Phi_{\alpha,k}\rangle|^2 \sum_{\ell'=1}^L \Gamma_{\ell'} \sum_{k'} |\langle\ell'|\Phi_{\alpha,k'}\rangle|^2 \left[f(\epsilon_{\alpha,k'} - \mu_{\ell'}) - f(\epsilon_{\alpha,k} - \mu_\ell)\right]}{\sum_{\ell'=1}^L \Gamma_{\ell'} \sum_{k'} |\langle\ell'|\Phi_{\alpha,k'}\rangle|^2} \ . \tag{4.17}$$

Again, in a strongly biased system, that is in the limit where the electron-chemical potentials lie above or below all relevant wire energies, the last expression can be written in a more compact form. Suppose, as above, that there are $L = 2$ leads ($\ell = \mathrm{L}$ and $\ell = \mathrm{R}$) with $\mu_{\mathrm{L}} = -\infty$ and $\mu_{\mathrm{R}} = \infty$. Then, the Fermi functions assume a constant

published by Shaker Verlag, Aachen, ISBN 3-8322-1979-X

value, $f(\epsilon-\mu_{\mathrm{L}})=0$ and $f(\epsilon-\mu_{\mathrm{R}})=1$, and the scalar product in Sambe space, defined in Eq. (2.9), allows to write the RWA current as

$$\bar{I}_{\mathrm{L}}^{\mathrm{RWA}} = e\sum_{\alpha}\frac{\Gamma_{\mathrm{L}}\,\Gamma_{\mathrm{R}}\,\langle\!\langle\Phi_\alpha|\mathrm{L}\rangle\langle\mathrm{L}|\Phi_\alpha\rangle\!\rangle\,\langle\!\langle\Phi_\alpha|\mathrm{R}\rangle\langle\mathrm{R}|\Phi_\alpha\rangle\!\rangle}{\Gamma_{\mathrm{L}}\,\langle\!\langle\Phi_\alpha|\mathrm{L}\rangle\langle\mathrm{L}|\Phi_\alpha\rangle\!\rangle+\Gamma_{\mathrm{R}}\,\langle\!\langle\Phi_\alpha|\mathrm{R}\rangle\langle\mathrm{R}|\Phi_\alpha\rangle\!\rangle}\ . \tag{4.18}$$

Each Floquet mode thus contributes to the dc current proportionally to the product of its time-averaged overlaps with the terminal sites L and R. For equal coupling to both leads ($\Gamma_{\mathrm{L}}=\Gamma_{\mathrm{R}}=\Gamma$), this expression is in agreement with the result (4.15) evaluated in the RWA limit (3.55). Introducing the effective rates $\bar{\Gamma}_{\alpha\mathrm{L}}:=\Gamma_{\mathrm{L}}\,\langle\!\langle\Phi_\alpha|\mathrm{L}\rangle\langle\mathrm{L}|\Phi_\alpha\rangle\!\rangle$ for the transitions from the left lead to the Floquet mode $|\Phi_\alpha(t)\rangle$, and *mutatis mutandis* for the right lead, permits to write the RWA current in the more compact form

$$\bar{I}_{\mathrm{L}}^{\mathrm{RWA}} = e\sum_{\alpha}\frac{\bar{\Gamma}_{\alpha\mathrm{L}}\,\bar{\Gamma}_{\alpha\mathrm{R}}}{\bar{\Gamma}_{\alpha\mathrm{L}}+\bar{\Gamma}_{\alpha\mathrm{R}}}\ . \tag{4.19}$$

The current can thus be expressed as a sum over contributions which assume a form familiar from the description of resonant transport through a single site [47].

4.3 Summary

The derivation of the expressions for both the time-dependent and the time-averaged (dc) current through the different wire-lead contacts concludes the formal part of the present thesis. Due to the high-driving frequencies of a laser field, only the latter quantity is relevant for practical applications. Furthermore, we have shown that, consistent with charge conservation, the sum over the dc currents through the different contacts vanishes (see Eq. (4.11)). A compact expression for the dc current has been derived for the case of two sites which are equally strong coupled to the respective lead.

Within a rotating-wave approximation and in the absence of electron-phonon interaction, the current can be written in the explicit form (4.17). This result becomes even more intuitive, if one considers the limit of an infinite voltage bias, where one obtains the concise result (4.19).

published by Shaker Verlag, Aachen, ISBN 3-8322-1979-X

published by Shaker Verlag, Aachen, ISBN 3-8322-1979-X

5 Coherent current control

Having the necessary formalism at hand, we are now in the position to investigate the current through the molecule for several representative situations. However, before doing so, we need to specify some details of the model for the molecule. Since we deal with rather novel phenomena, we try to be as general as possible and employ rather generic models. To be close to a specific experiment, one could also use results from density functional calculations [105–109] as input to the present theory. A further, already in itself rather complicated problem, arises from the fact that transport through molecular wires is typically measured for finite voltage. Consequently, one has to self-consistently include the influence of the external voltage on the molecule [110–112]. Again, we restrict ourselves to a very generic model, where the molecule is viewed as a dielectric in between to parallel plates formed by the leads [11, 113].

Subsequently, we study three paradigmatic cases, each of which covers a specific aspect of the transport problem: (i) current amplification by means of a resonant laser field, (ii) generation of ratchet or pump currents, and (iii) optical switching of the current. The order of these examples has been chosen by increasing difficulty of an experimental realisation.

5.1 Tight-binding model for the wire

Except for the last subsection of this chapter, we will employ a one-dimensional tight-binding model (cf. Fig. 5.1), wherein the wire is described by a set of orthogonal states $|n\rangle$ with energy E_n, each of which is localised at a scaled position $x_n = (2n - N + 1)/2$. Two adjacent states are coupled by a hopping matrix element Δ, which, within our model, is assumed to be a constant throughout the wire. The laser field renders each level oscillating in time with a position dependent amplitude $a(t)x_n$, where the energy $a(t) = a(t+T)$ equals the electron charge e multiplied by the time-dependent electrical field of the laser and the distance between two neighbouring sites (cf. Sect. 2.4). Thus, the corresponding wire Hamiltonian reads

$$H_{nn'}(t) = -\Delta(\delta_{n,n'+1} + \delta_{n+1,n'}) + [E_n + a(t)x_n]\,\delta_{nn'} \ . \tag{5.1}$$

published by Shaker Verlag, Aachen, ISBN 3-8322-1979-X

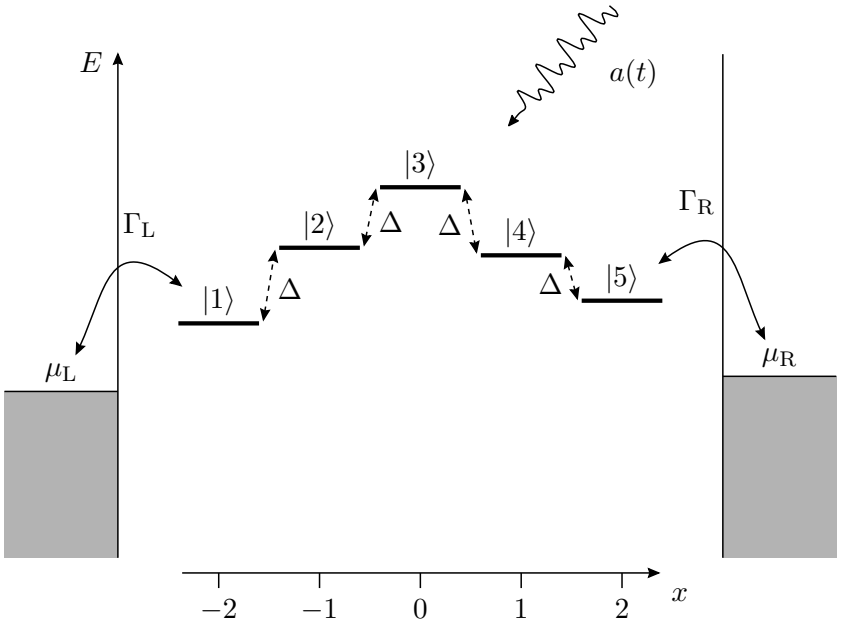

Figure 5.1: Schematic drawing of the molecule situated in between to metallic leads: Horizontal lines represent the sites with energies E_n for $n = 1,\ldots,5$. Arrows indicate the coupling between neighbouring sites via the hopping matrix element Δ. The terminal sites are connected to the adjacent leads with corresponding rates Γ_L and Γ_R. Additionally, a laser impinges on the molecule, leading to an additional time-dependent field $a(t)$.

We remark that for the sake of simplicity, intra-atomic dipole excitations are neglected within our model Hamiltonian. In an experiment, the site energies E_n can be controlled by attaching different chemical groups to an otherwise symmetric molecular wire [18, 114].

The two terminal sites $|1\rangle$ and $|N\rangle$, which we shall term donor and acceptor in the following, are connected to the corresponding leads via the tunnelling Hamiltonian (3.5) with the identification $\mathrm{L} \leftrightarrow 1$ and $\mathrm{R} \leftrightarrow N$. We will always consider the wide-band limit (3.7) and a symmetric coupling, $\Gamma_\mathrm{L} = \Gamma_\mathrm{R} = \text{const.} =: \Gamma$.

In all following numerical calculations, energy is expressed in units of the hopping matrix element Δ; we choose $\Delta = 0.1\,\mathrm{eV}$, which is a reasonable value for a realistic wire molecule. Furthermore, we assume that the effective couplings to the leads are by one order of magnitude smaller, $\hbar\Gamma = 0.1\Delta$, yielding typical currents $e\Gamma = 2.56 \times 10^{-5}\,\mathrm{A}$. This corresponds to a large contact resistance and ensures the applicability of a perturbational approach. A laser frequency $\Omega \approx 10\Delta/\hbar$ corresponds to a wavelength of about $1\,\mu\mathrm{m}$, which is in the near infrared spectral range. For a realistic distance of $1\,\text{Å}$ between two neighbouring sites, a laser amplitude $A = \Delta$ is equivalent to an electrical field strength of $10^7\,\mathrm{V/cm}$. Note that, as discussed in Sect. 3.1, the electrical

published by Shaker Verlag, Aachen, ISBN 3-8322-1979-X

field may be drastically enhanced due to the presence of the metallic tips.

Potential profile across the wire

An externally applied bias between the two leads results in an energy shift ΔE_n of the wire levels $|n\rangle$ according to the local electrostatic potential. Thereby, the potential profile across the wire, i.e., the local potential as a function of the position, depends crucially on the screening of electrical fields within the wire. Thus, in principle, its specification requires the solution of the coupled many-body Schrödinger and Poisson equation of the lead-molecule-lead system [110,111]. This in itself presents a formidable task we will not try to tackle. Instead, we shall use a simple model proposed in Refs. [11, 113], which views the two electrodes as parallel plates forming a capacitor with the molecule in between acting like a dielectric. This model has recently been recovered as a limiting case of a more detailed electrostatic model calculation, which also takes into account the screening length and the diameter of the molecule [112].

Within the capacitor picture one obtains a potential profile where the fractions $\eta_{\rm L}$ and $\eta_{\rm R}$ of the applied voltage V drop at the respective contact, while the fraction $\eta_{\rm M} = 1 - \eta_{\rm L} - \eta_{\rm R}$ establishes a linear potential profile

$$\Delta E_n = \eta_{\rm L} eV + \eta_{\rm M} \frac{n-1}{N-1} eV \tag{5.2}$$

along the wire. Figure 5.2 illustrates this for a situation where the energies of the wire levels in the absence of an applied voltage (dashed lines) are equal to the chemical potential in the leads, $E_n = \mu$. The actual levels (solid lines) are then shifted according to the voltage profile (5.2). Thereby, the electro-chemical potential $\mu_{\rm R} = \mu_{\rm L} + eV$ in the right electrode is assumed to lie higher in energy, thus favouring transport of electrons from right to left, corresponding to a positive electrical current from the left to the right electrode.

We note that within the electrostatic model of Ref. [112], for a "thick" molecule, i.e., for one whose diameter is much larger than the screening length, the electrostatic potential is constant along the molecule and, thus, the voltage drops entirely at the contacts, $\eta_{\rm L} = \eta_{\rm R} = 1$ and $\eta_{\rm M} = 0$. In the opposite limit of a "thin" molecule, the entire voltage drops linearly along the molecule, corresponding to our assumption (5.2) together with $\eta_{\rm L} = \eta_{\rm R} = 0$ and $\eta_{\rm M} = 1$.

5.2 Current spectroscopy

As a first example, we consider a molecule consisting of donor and acceptor, and $N-2$ bridge sites in between (cf. Fig. 5.3). The energies of the donor and the acceptor orbitals are assumed to be at the level of the chemical potentials of the attached leads, $E_1 = E_N = \mu_{\rm L} = \mu_{\rm R}$. The bridge levels E_n with $n = 2, \ldots, N-1$, lie $E_{\rm B} \gg \Delta$ above the

published by Shaker Verlag, Aachen, ISBN 3-8322-1979-X

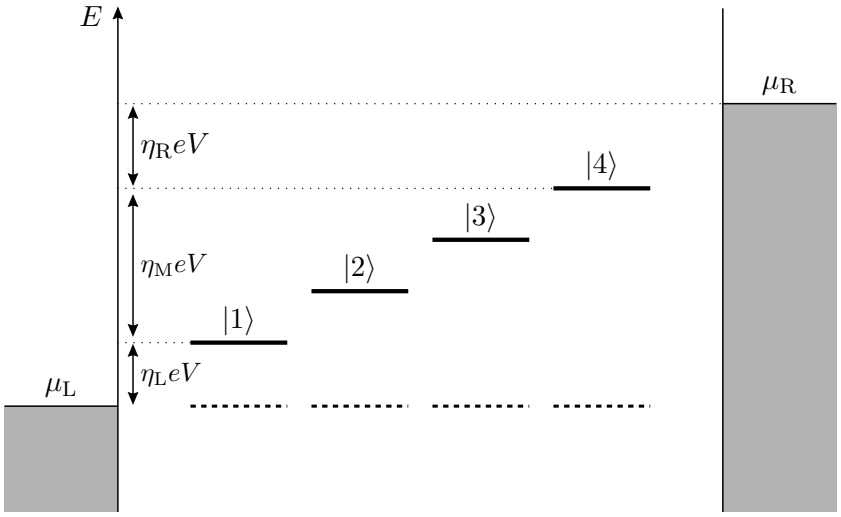

Figure 5.2: Shift of the wire levels due to a finite applied voltage for a situation where the energies of the states $|n\rangle$, $n = 1,\ldots,N = 4$ without external voltage (dashed lines) lie at the position of the chemical potential. The external voltage V shifts the levels to the positions marked by the full lines. η_L, η_M, and η_R denote the fractions of the total applied voltage which drop across the left contact, the wire, and the right contact, respectively.

chemical potential, as sketched in Figure 5.3. The applied voltage is always chosen so small that the bridge levels are located well above the chemical potentials of the leads, whereby, unless otherwise indicated, the voltage drop is presumed to occur at the contacts. Here, we will not take into account electron-phonon interaction.

5.2.1 Average current at resonant excitations

Let us first discuss the static problem in the absence of the field, i.e., for $A = 0$. In the present case where the coupling between two neighbouring sites is much weaker than the bridge energy, $\Delta \ll E_B$, one finds two types of eigenstates: One forms a doublet whose states are approximately given by $(|1\rangle \pm |N\rangle)/\sqrt{2}$. Its splitting can be estimated in a perturbational approach [115] and is approximately given by $2\Delta(\Delta/E_B)^{N-2}$. A second group of states is located on the bridge. It consists of $N-2$ levels with energies in the range $[E_B - 2\Delta, E_B + 2\Delta]$. In the absence of the driving field, these bridge states mediate the super-exchange between the donor and the acceptor. This yields an exponentially decaying length dependence of the conductance [9, 69].

This behaviour changes significantly when a driving field with a frequency $\Omega \approx E_B/\hbar$ is switched on. Then the resonant bridge levels merge with the donor and the acceptor state to form a Floquet state. This opens a direct channel for the transport resulting in an enhancement of the electrical current as depicted in Figure 5.4, which shows the current amplification, defined as the ratio $\bar{I}/I_0$ of the time-averaged current to the

published by Shaker Verlag, Aachen, ISBN 3-8322-1979-X

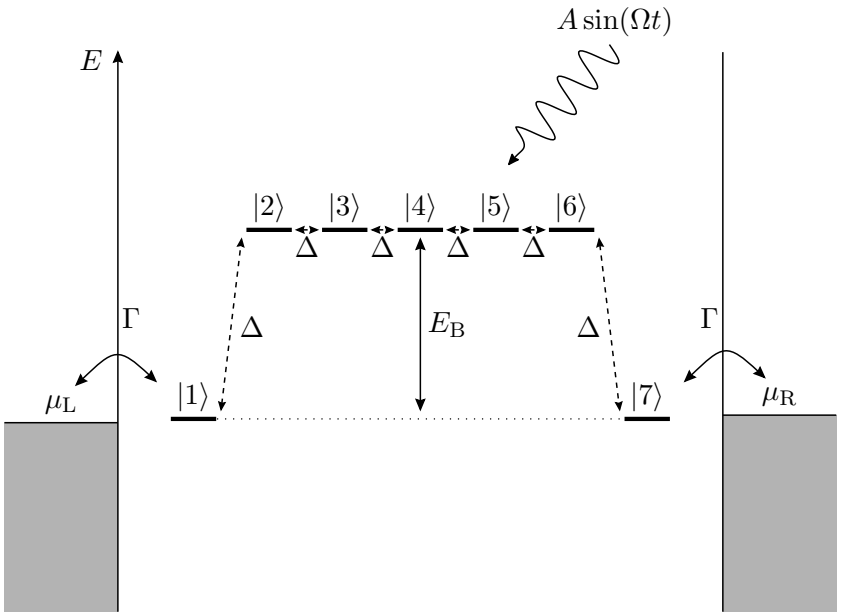

Figure 5.3: Level structure of a molecular wire with $N = 7$ atomic sites which are attached to two leads. The energies of $N - 2$ bridge levels in the middle lie $E_{\mathrm{B}} \gg \Delta$ above the chemical potential.

current in the absence of the laser. In a wire with $N = 8$ sites, one finds current peaks when the driving frequency matches the energy difference between the donor/acceptor doublet and one of the $N - 2 = 6$ bridge levels. The amplification can assume many orders of magnitude, cf. Fig. 5.4.

From an experimental point of view, such a "current spectroscopy" setup thus opens promising opportunities for a detailed investigation of the level structure of the contacted molecule. Note that if we take into account a voltage drop along the molecule, the site energies are shifted according to Eq. (5.2), resulting in a change of the eigenenergies of the molecular bridge. In particular, the external voltage may tune the system to resonance at a *fixed* laser frequency, as demonstrated in Fig. 5.5 for different values of the parameter η_{M} from Eq. (5.2) with equal voltage drop across both contacts ($\eta_{\mathrm{L}} = \eta_{\mathrm{R}}$).

The experimental realisation of such a measurement scheme for a quantum dot was reported, e.g., in Ref. [20]. We remark that, in turn, when the level structure of the molecule is known, it should be possible to extract information about the potential profile along the wire, which is otherwise a very difficultly accessible quantity.

Generally, the response of a system to a weak resonant driving scales with the damping and the driving amplitude. Figure 5.6 depicts this behaviour for the peaks of the electrical current. The peak heights at the maxima of the time-averaged current turn out to be proportional to A^2/Γ. A further scaling behaviour is found for the current peaks as a function of the wire length: The average current no longer exhibits

published by Shaker Verlag, Aachen, ISBN 3-8322-1979-X

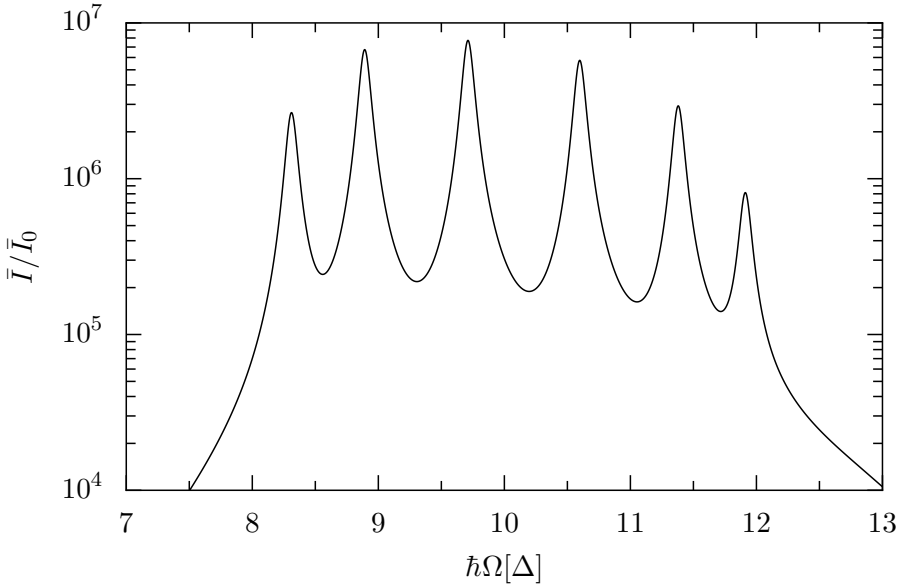

Figure 5.4: Amplification of the time-averaged current through the wire sketched in Figure 5.3 with $E_B = 10\Delta$. The scaled amplitude is $A = 0.1\Delta$; the applied voltage $\mu_L - \mu_R = 5\Delta/e$. The other parameters read $\Gamma = \Gamma_L = \Gamma_R = 0.1\Delta/\hbar$ and $k_B T = 0.25\Delta$.

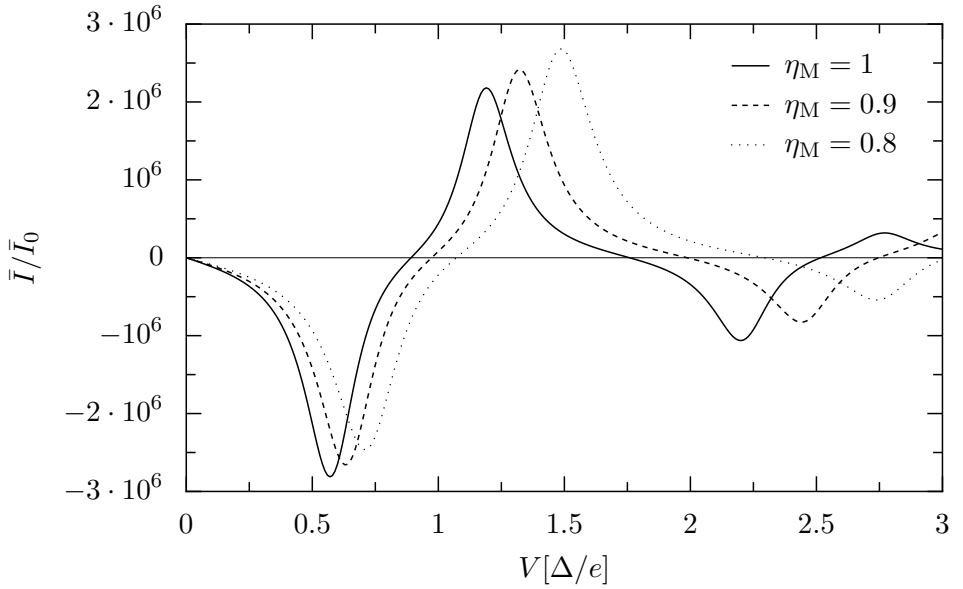

Figure 5.5: Amplification of the time-averaged current through the wire sketched in Figure 5.3 as a function of an external bias voltage V. The voltage drop is assumed to be of the form (5.2) with $\eta_L = \eta_R = (1 - \eta_M)/2$. A driving frequency $\Omega = 10\Delta/\hbar$ was chosen, while all other parameters are as in Fig. 5.4.

published by Shaker Verlag, Aachen, ISBN 3-8322-1979-X

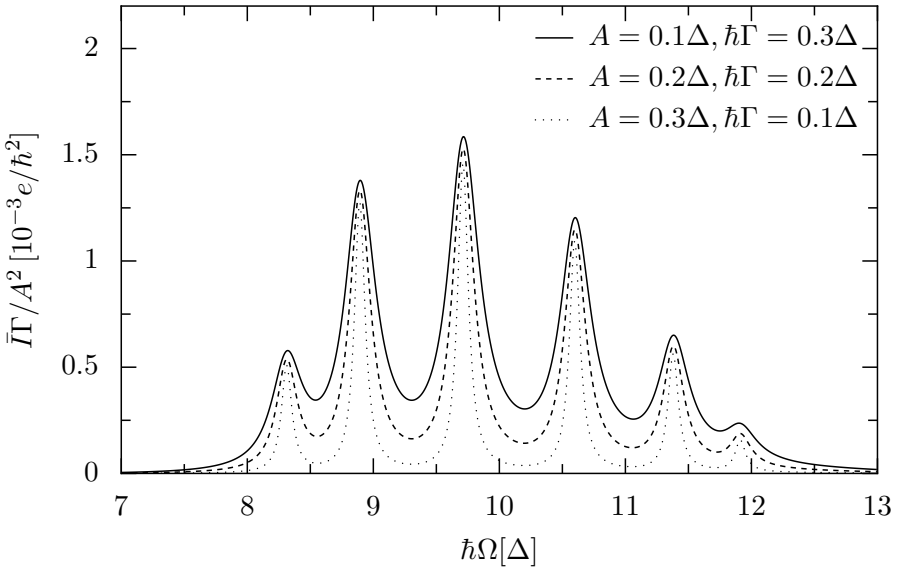

Figure 5.6: Average current $\bar{I}$ as a function of the driving frequency Ω for various driving amplitudes A and coupling strength $\Gamma = \Gamma_L = \Gamma_R$. All the other parameters are as in Fig. 5.4.

the exponentially decaying length dependence that has been found for bridged superexchange. By contrast, it emerges proportional to $1/(N-1)$. This can be appreciated in Fig. 5.7 where the scale of the abscissa is chosen proportional to $N-1$ such that it suggests a common envelope function. Put differently, the current is essentially inversely proportional to the length as in the case of Ohmic conductance.

In summary, we find current peaks whose height $\bar{I}_{\rm peak}$ scales according to

$$\bar{I}_{\rm peak} \propto \frac{A^2}{(N-1)\Gamma} \,. \tag{5.3}$$

Thus, the current is especially for long wires much larger than the corresponding current in the absence of the driving. Finally, we remark that a similar current enhancement was recently predicted using a scattering approach for the transport through the driven molecule [54].

5.3 Rectification of driving induced currents

In the previous section, we have demonstrated that a laser field can resonantly enhance a current which is already flowing across the molecule due to a *small external bias*. Let us now turn to the question whether the molecule can rectify the laser-induced oscillating electron motion, thereby establishing a non-zero dc current through the wire even in the *absence of an applied voltage*, i.e., for $\mu_L = \mu_R$. In this section, we

published by Shaker Verlag, Aachen, ISBN 3-8322-1979-X

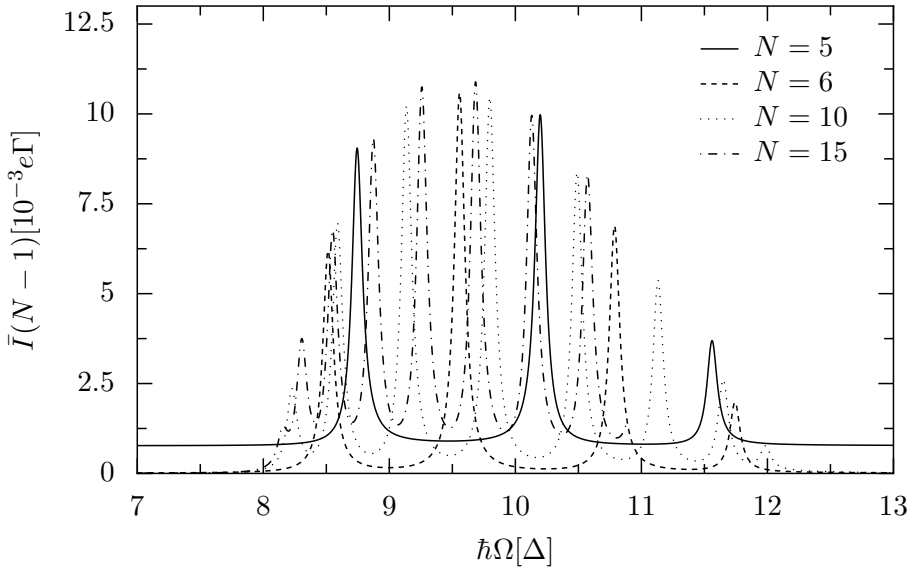

Figure 5.7: Average current $\bar{I}$ as a function of the the driving frequency Ω for various wire length N. All the other parameters are as in Fig. 5.4.

investigate the possibilities of such pump or ratchet currents in molecular wires.

Two basic types of phenomena have to be distinguished: (i) rectification of an external field with a harmonic time-dependence in a spatially asymmetric structure and (ii) rectification of an external laser field with a broken time symmetry in a spatially symmetric molecule. We relate our findings to the absence of the mentioned symmetries. Both situations will be discussed in the following for (A) a two-site wire and (B) a real wire consisting of N sites, namely, as before, $N-2$ bridge levels and two terminal sites, donor and acceptor, which establish the contact to the leads.

5.3.1 Symmetries

It is known from the study of deterministically rocked periodic potentials [116] and of overdamped classical Brownian motion [117] that the symmetry of the equations of motion may rule out any non-zero average current at asymptotic times. Thus, before starting to compute ratchet currents, let us first analyse what kind of symmetries may prevent a ratchet effect. Apart from the principle interest, such situations with vanishing average current are also of computational relevance since they allow to test the numerical implementations rather sensitively. Note that in the absence of all symmetries precluding a non-zero dc current, such a current does in general appear. In a more general context, this can be regarded as a consequence of Curie's principle, a heuristic fact which states that an effect always occurs unless it is ruled out by symmetries [31, 118].

published by Shaker Verlag, Aachen, ISBN 3-8322-1979-X

Detailed balance

The second law of thermodynamics states that it is impossible to extract useful work out of the microscopic fluctuations occurring in a system in thermal equilibrium. In other words, Maxwell's demon does not exist. The deeper reason for this behaviour lies in the so-called detailed-balance symmetry, a probabilistic symmetry which itself originates from the time-reversal symmetry of the total system, in our case, consisting of molecule plus environment.

A valid theory thus has to ensure that for an undriven molecule without external bias voltage and all baths at a common temperature, the current across the different molecule-lead contacts has to vanish—despite any possible asymmetry of the molecule itself or of its coupling to the environment. This is within our approach indeed the case, since in thermal equilibrium the solution of the kinetic equation is given by the Fermi distribution $P_{\alpha\beta} = f(E_\alpha - \mu)\delta_{\alpha\beta}$, as already emphasised in Sect. 3.4.1. Upon insertion into the current formula (4.10), we then immediately obtain that the current across an arbitrary contact ℓ vanishes as required:

$$\bar{I}_\ell = 0 \quad \text{(in thermal equilibrium)} \; . \tag{5.4}$$

Parity symmetry

We have already seen in Sect. 2.4 that it is possible to extend the concept of parity symmetry, i.e., the invariance of a system under the transformation $\mathsf{P} : x \mapsto -x$, in the presence of a periodically time-dependent force. For a Hamiltonian of the form (2.25), this has led us to the notion of a generalised parity and a time-reversal parity. The obvious question is now, what consequences arise from these symmetries for the dc current across a molecule.

Let us thus consider a molecule connected to two leads, whose static Hamiltonian is symmetric with respect to the centre of the wire. To simplify the discussion, we restrict ourselves to the situation without electron-phonon interaction, where the kinetic equation is linear. We observe that the current formula (4.9) and the Fourier decomposed master equation (3.68) contain, besides Fermi factors, the overlap of the Floquet states with the terminal sites at the left and right contact, $|1\rangle$ and $|N\rangle$, which therefore play a central role in the following discussion.

Generalised parity

As a first case, we investigate a driving field that obeys $a(t) = -a(t + \pi/\Omega)$. Then, as discussed in Sect. 2.4.1, the wire Hamiltonian (5.1) is invariant under the so-called generalized parity transformation [cf. Eq. (2.29)]

$$\mathsf{S}_{\mathrm{GP}} : (x, t) \to (-x, t + \pi/\Omega) \; . \tag{5.5}$$

published by Shaker Verlag, Aachen, ISBN 3-8322-1979-X

Consequently, the Floquet states are either even or odd under this transformation, i.e., they fulfil the relation (2.30), which reduces in the tight-binding limit to the following relation between the two terminal sites $|1\rangle$ and $|N\rangle$:

$$\langle 1|\Phi_{\alpha,k}\rangle = \sigma_\alpha\,(-1)^k\,\langle N|\Phi_{\alpha,k}\rangle\ . \tag{5.6}$$

Here, $\sigma_\alpha = \pm 1$ according to the generalised parity of the Floquet state $|\Phi_\alpha(t)\rangle$.

The average current $\bar{I}$ is defined in Eq. (4.12) by the current formula (4.10) in conjunction with the master equation (3.68). Applying the symmetry relation (5.6) to both interchanges donor state $|1\rangle$ and acceptor state $|N\rangle$. In addition, we substitute in both the master equation and the current formula $P_{\alpha\beta,k}$ by $\widetilde{P}_{\alpha\beta,k} = \sigma_\alpha\sigma_\beta(-1)^k P_{\alpha\beta,k}$. The result is that the new expressions for the current, including the master equation, are identical to the original ones except for the fact that $\bar{I}_{\mathrm{L}},\Gamma_{\mathrm{L}}$ and $\bar{I}_{\mathrm{R}},\Gamma_{\mathrm{R}}$ are now interchanged (recall that we consider the case $\mu_{\mathrm{L}} = \mu_{\mathrm{R}}$). Therefore, we can conclude that

$$\frac{\bar{I}_{\mathrm{L}}}{\Gamma_{\mathrm{L}}} = \frac{\bar{I}_{\mathrm{R}}}{\Gamma_{\mathrm{R}}}\ , \tag{5.7}$$

which yields together with the continuity relation (4.13) a vanishing average current $\bar{I} = 0$.

Time-reversal parity

We already know from Sect. 2.4.2 that a further symmetry is present if the driving is an odd function of time, $a(t) = -a(-t)$. Then, the Floquet eigenvalue equation (2.3) is invariant under the time-reversal parity [cf. Eq. (2.31)]

$$\mathsf{S}_{\mathrm{TP}} : (\Phi, x, t) \to (\Phi^*, -x, -t)\ , \tag{5.8}$$

i.e., the usual parity together with time-reversal and complex conjugation of the Floquet states Φ. The consequence for the Floquet states is the symmetry relation (2.32) which reads for a tight-binding system

$$\langle 1|\Phi_{\alpha,k}\rangle = \langle N|\Phi_{\alpha,k}\rangle^* = \langle \Phi_{\alpha,k}|N\rangle\ . \tag{5.9}$$

Inserting this into the current formula (4.10) would yield, if all $P_{\alpha\beta,k}$ were real, again the balance condition (5.7) and, thus, a vanishing average current. However, the $P_{\alpha\beta,k}$ are in general only real for $\Gamma_{\mathrm{L}} = \Gamma_{\mathrm{R}} = 0$, i.e., for very weak coupling such that the condition (3.55) for the applicability of the rotating-wave approximation holds. Under this condition, the solution of the master equation is dominated by the RWA solution (3.60), (3.61), which is real. In the general case, the solution of the master equation (3.68) is however complex and consequently the symmetry (5.9) does not inhibit a ratchet effect. Still we can conclude from the fact that within the RWA the average current vanishes, that $\bar{I}$ is of the order Γ^2 for $\Gamma \to 0$, while it is generally of

published by Shaker Verlag, Aachen, ISBN 3-8322-1979-X

the order Γ for broken time-reversal symmetry.

5.3.2 Rectification in two-level systems

The basic mechanisms behind the rectification of the laser induced currents can already be understood for a wire consisting of only two levels, where the Hamiltonian (5.1) specialises to

$$H_{\text{molecule}}(t) = \begin{pmatrix} E_{\text{L}} & -\Delta \\ -\Delta & E_{\text{R}} \end{pmatrix} + \frac{a(t)}{2} \begin{pmatrix} 1 & 0 \\ 0 & -1 \end{pmatrix} . \tag{5.10}$$

Apart from a trivial energy shift $(E_{\text{L}} + E_{\text{R}})/2$, this Hamiltonian is of the form (2.33) discussed in Sect. 2.5.1, if we identify $E_{\text{b}} = E_{\text{L}} - E_{\text{R}}$. In the following, we fix the chemical potentials in the leads at zero energy, $\mu_{\text{L}} = \mu_{\text{R}} = 0$, and set $\Gamma_{\text{L}} = \Gamma_{\text{R}} = \Gamma$, as throughout this chapter.

Rectification from spatial asymmetry

We first investigate a model (see Fig. 5.8) with a built-in spatial asymmetry, $E_{\text{L}} \neq E_{\text{R}}$, driven by a purely harmonic field

$$a(t) = A \sin(\Omega t) . \tag{5.11}$$

Figure 5.9 shows the resulting dc current as a function of the driving amplitude A for different angular frequencies Ω of the driving field. Consistent with detailed balance, for vanishing driving amplitude, i.e., in equilibrium, the current is always zero. In the presence of a driving, in general, a non-zero current is generated. As a function of the driving amplitude, it exhibits an oscillating behaviour with multiple current reversal. For a very strong driving, the amplitude of these oscillations decays. The driving-frequency dependency of the dc current (see Fig. 5.10) reveals that the observed effect occurs due to resonances between the external driving field and the energy differences of the two-site wire. In the weak driving regime, these resonances occur at a frequency matching the energy difference $\sqrt{(E_{\text{L}} - E_{\text{R}})^2 + 4\Delta^2}$ between the two eigenstates of the undriven system (which for the situation of Figs. 5.9 and 5.10 equals $\sqrt{5}\Delta/\hbar \approx 2.236\Delta/\hbar$). Larger driving amplitudes lead to a shift of the resonance frequency, the so called Bloch-Siegert shift [119, 120], and to the appearance of higher-order resonances around the subharmonic frequencies $\sqrt{5}\Delta/2\hbar$, $\sqrt{5}\Delta/3\hbar$, ...

The amplitude dependence of the dc current in the presence of electron-phonon interaction of the form (3.10) and (3.14), can be seen from Fig. 5.11. Panel 5.11a depicts the situation for a nearly resonant driving $\hbar\Omega = 2\Delta$. One observes that the dissipation damps out the oscillatory behaviour and decreases the overall amplitude of the pump current oscillations. However, for a very high driving frequency [cf. panel 5.11b], where the pumping effect without electron-phonon interaction is only moderately strong, one finds the opposite behaviour, namely an enhancement. Finally,

published by Shaker Verlag, Aachen, ISBN 3-8322-1979-X

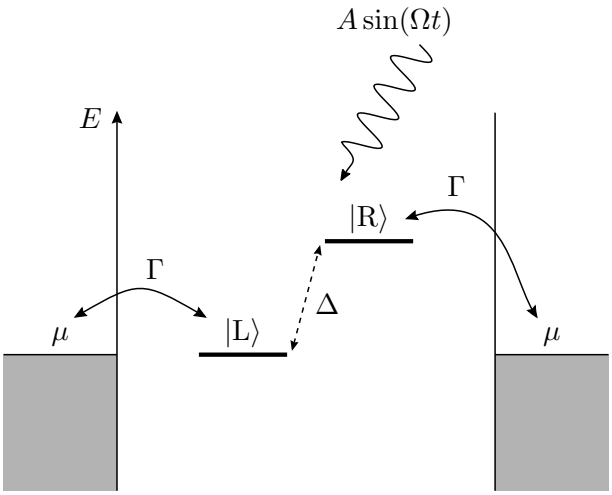

Figure 5.8: Two-site structure with internal bias ($E_\mathrm{L} \neq E_\mathrm{R}$) coupled to two leads acting as a rectifier for an externally applied harmonic laser field of the form $a(t) = A\sin(\Omega t)$.

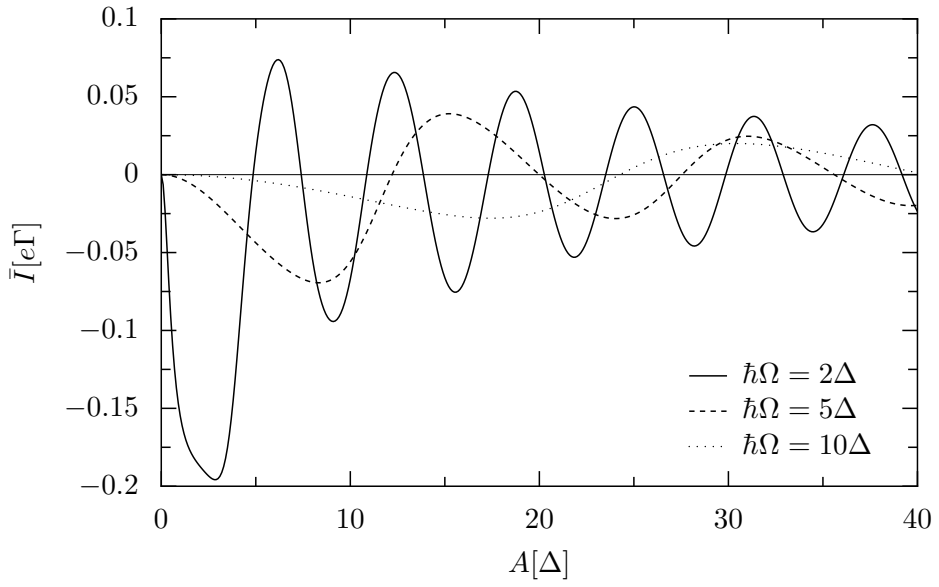

Figure 5.9: Average current through the spatially asymmetric, harmonically driven two-site molecule sketched in Fig. 5.8 as a function of the driving amplitude A for different angular frequencies Ω of the driving field. The wire-lead coupling strength is $\Gamma = 0.1\Delta$, the temperature $k_\mathrm{B}T = 0.25\Delta$, the energies of the two levels are $E_\mathrm{L} = 0$ and $E_\mathrm{R} = \Delta$, and no electron-phonon coupling is present ($\kappa = 0$).

published by Shaker Verlag, Aachen, ISBN 3-8322-1979-X

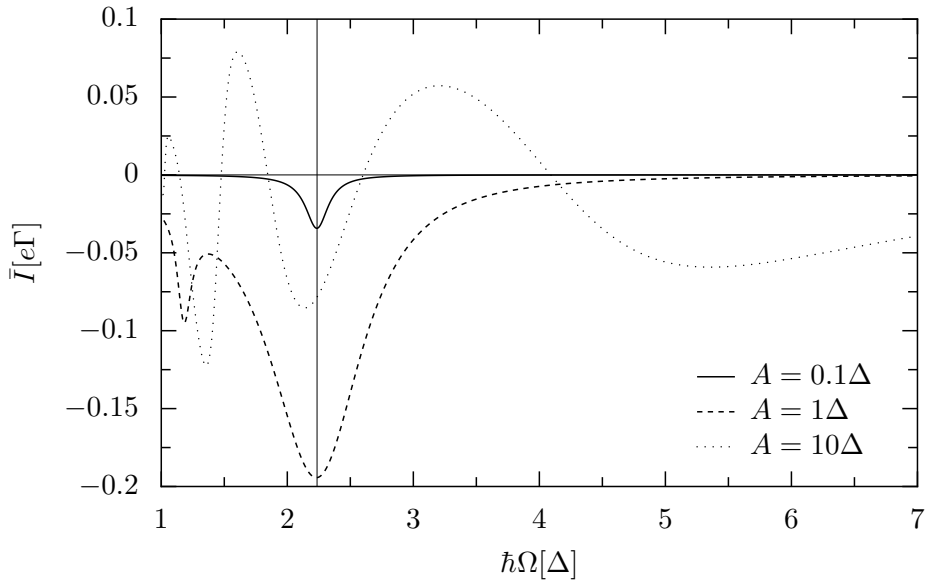

Figure 5.10: Time-averaged current through the spatially asymmetric, harmonically driven two-site molecule sketched in Fig. 5.8 as a function of the angular frequency Ω of the driving for different driving amplitudes A. All other parameters are as in Fig. 5.9. The linear resonance frequency $\Omega = \sqrt{5}\Delta/\hbar$ is indicated by a vertical line.

we remark that for suitably chosen driving parameters, one also observes a current reversal as a function of the electron-phonon coupling strength κ, which can be seen in the region around $A = 25\Delta$ in Fig. 5.11b.

Rectification from harmonic mixing

From the symmetry analysis in Sect. 5.3.1, we already know that a symmetric two-site wire (see Fig. 5.12), will not result in a non-zero driving amplitude, if the driving is purely harmonic, since then a non-zero value is forbidden by the generalised parity symmetry (5.5). A simple way to break this symmetry is to add a second harmonic to the driving field, i.e., a contribution with twice the fundamental frequency Ω, such that it is of the form

$$a(t) = A_1 \sin(\Omega t) + A_2 \sin(2\Omega t + \varphi), \tag{5.12}$$

as sketched in Fig. 5.13. While now shifting the time t by a half period π/Ω changes the sign of the fundamental frequency contribution, the second harmonic is left unchanged. The generalised parity is therefore broken and we find a non-vanishing average current. In general, by driving with the field (5.12), one also violates the time-reversal parity (5.8). Yet, for a phase shift $\varphi = 0$ (or equivalently any multiple of π) the time-reversal parity is still present. By tuning the phase shift, one can thus switch between

published by Shaker Verlag, Aachen, ISBN 3-8322-1979-X

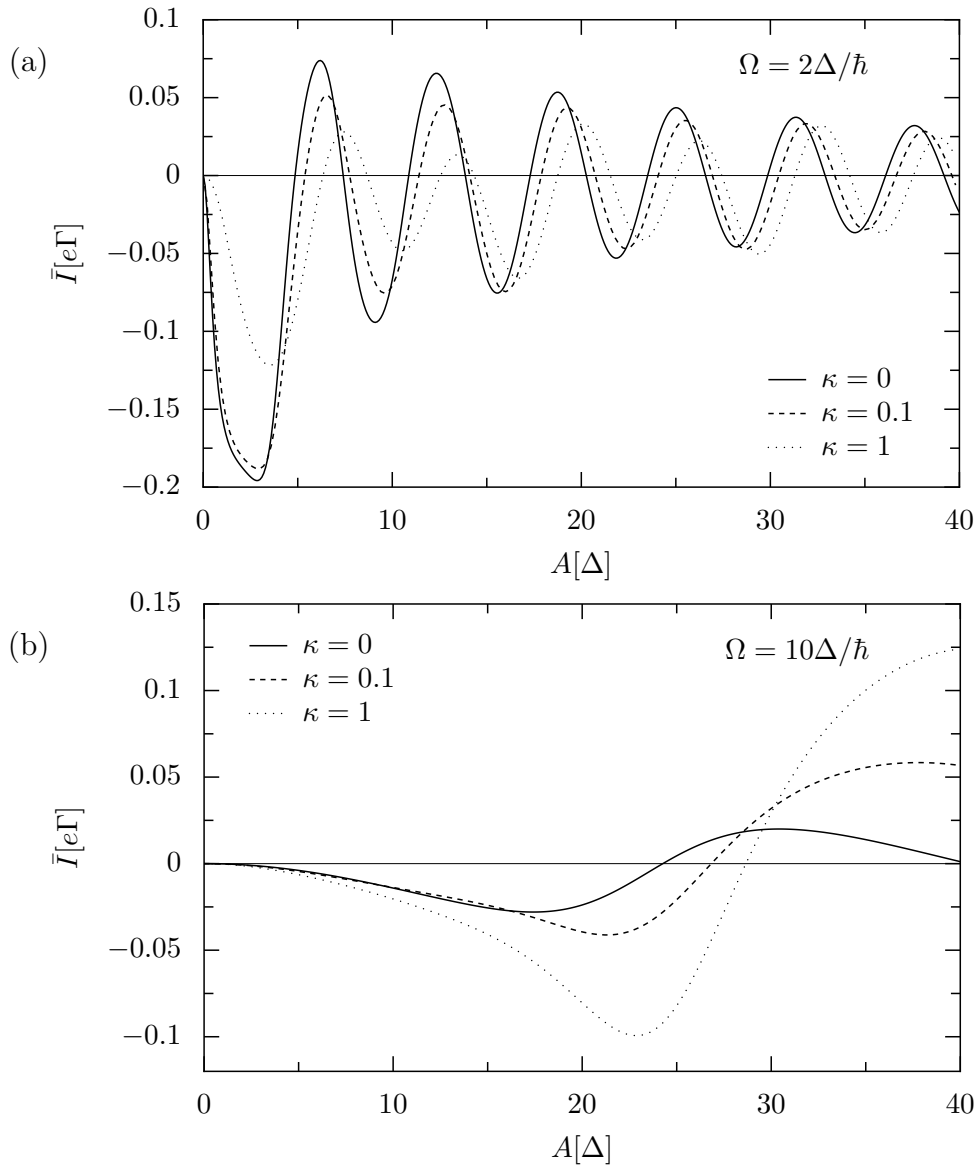

Figure 5.11: Time-averaged current through the spatially asymmetric, harmonically driven two-site molecule sketched in Fig. 5.8 as a function of the driving driving amplitudes A in the situation without (solid line) and with electron-phonon interaction of the form (3.10) and (3.14) (dashed and dotted lines). The angular frequency of the driving is $\Omega = 2\Delta/\hbar$ (upper panel) and $\Omega = 10\Delta/\hbar$ (lower panel). All other parameters are as in Fig. 5.9.

published by Shaker Verlag, Aachen, ISBN 3-8322-1979-X

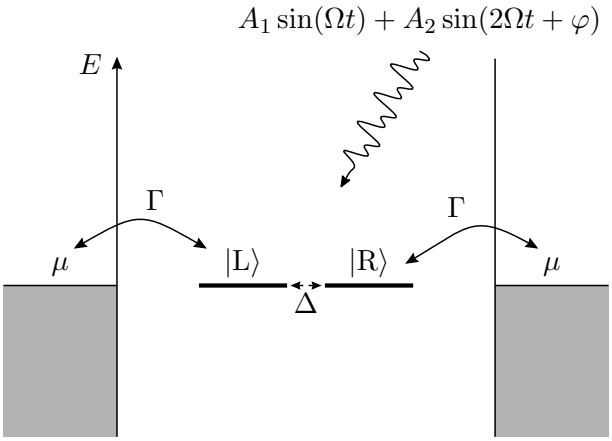

Figure 5.12: Symmetric two-site structure coupled to two leads which rectifies an externally applied laser field of the form $a(t) = A_1 \sin(\Omega t) + A_2 \sin(2\Omega t + \varphi)$.

these qualitatively different situations.

The harmonic mixing driving field (5.12) permits a sensitive control of the direction of the dc current as a function of the phase difference φ, as can be seen from Fig. 5.14 As mentioned above, for phase differences $\varphi = 0 \bmod \pi$, the time-reversal parity symmetry (5.8) is still present. Thus, according to the symmetry considerations above, the current vanishes within the rotating-wave approximation. However, we expect beyond RWA for small coupling a current $\bar{I} \propto \Gamma^2$ (cf. Sect. 5.3.1). Figure 5.15 confirms this prediction. Yet one observes that already a small deviation from $\varphi = 0$ is sufficient to restore the usual weak-coupling behaviour, namely a current proportional to the coupling strength Γ. We remark that a similar phase control of the current has been discussed previously in the limits of a purely coherent [38] and a fully incoherent, sequential transport [35] in infinite tight-binding systems.

The influence of an additional electron-phonon interaction of the form (3.10) and (3.14) is shown in Fig. 5.16 for a driving field with time-reversal parity ($\varphi = \pi/2$). For $\kappa \ll \hbar\Gamma/\Delta$, the dc current is proportional to Γ^2. In this regime, the main dissipation mechanism is due to the contacts with the leads and we obtain the same behaviour as before. However, for larger κ-values, the electron-phonon coupling on the wire starts to dominate and yields a strong enhancement of the current.

5.3.3 Rectification in long wires

Having discussed in detail the rectification properties in two-site system, we now move on to situations with more than two sites. Of particular interest is then the length dependence of the observed effects. Again, we discuss separately rectification effects resulting from a spatial asymmetry of the wire itself and those originating from harmonic mixing. Since we focus in the present section on the limiting case of long molecular wires, where the numerical solution of the non-linear kinetic equation (3.30)

published by Shaker Verlag, Aachen, ISBN 3-8322-1979-X

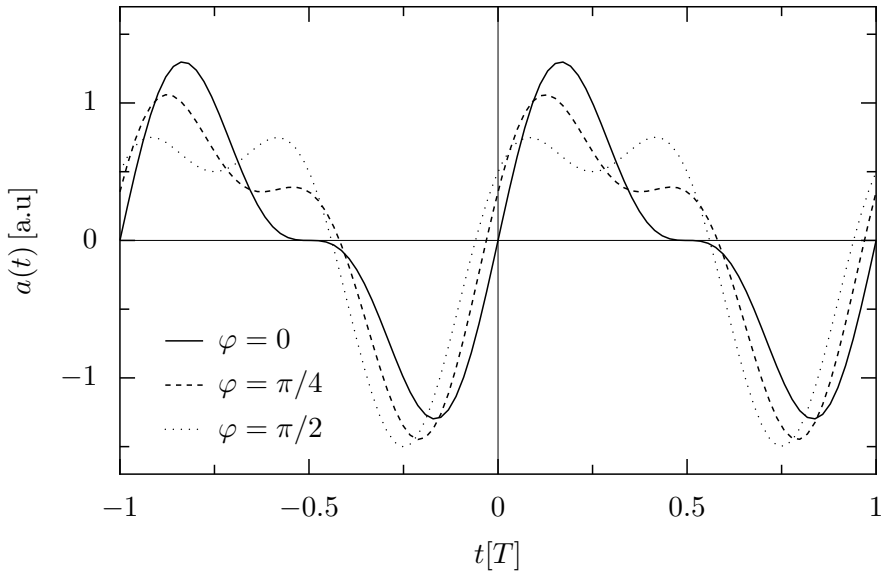

Figure 5.13: Shape of the harmonic mixing field $a(t)$ in Eq. (5.12) for $A_1 = 2A_2$ for different phase shifts φ. For $\varphi = 0$, the field changes its sign for $t \to -t$ which amounts to the time-reversal parity (5.8).

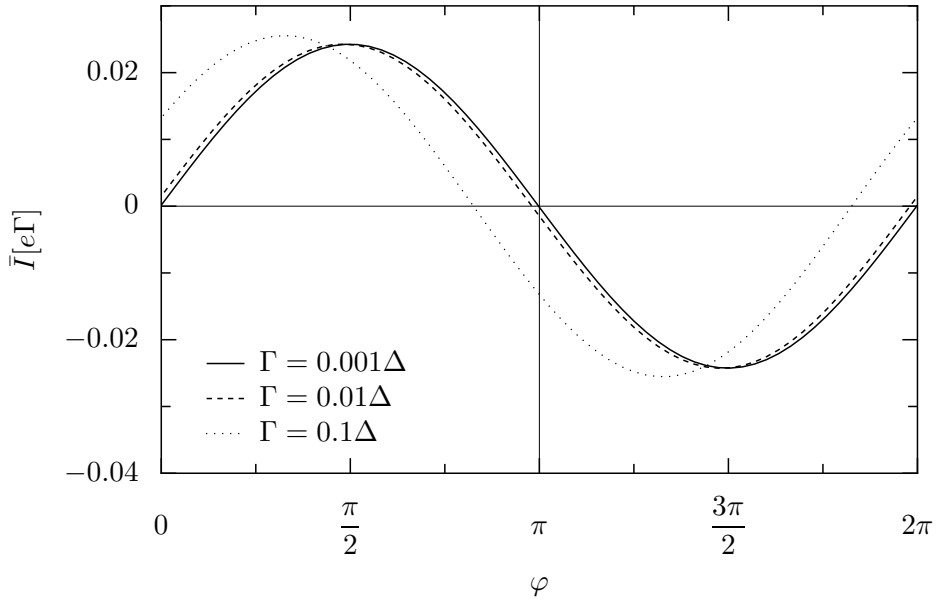

Figure 5.14: Average current through the two-site wire sketched in Fig. 5.12 driven by the harmonic mixing signal (5.12) as a function of the phase difference φ for different wire-lead coupling strengths Γ. The driving amplitudes are $A_1 = 2A_2 = \Delta$, the driving frequency is $\Omega = \Delta/\hbar$, and the temperature is $k_B T = 0.25\Delta$.

published by Shaker Verlag, Aachen, ISBN 3-8322-1979-X

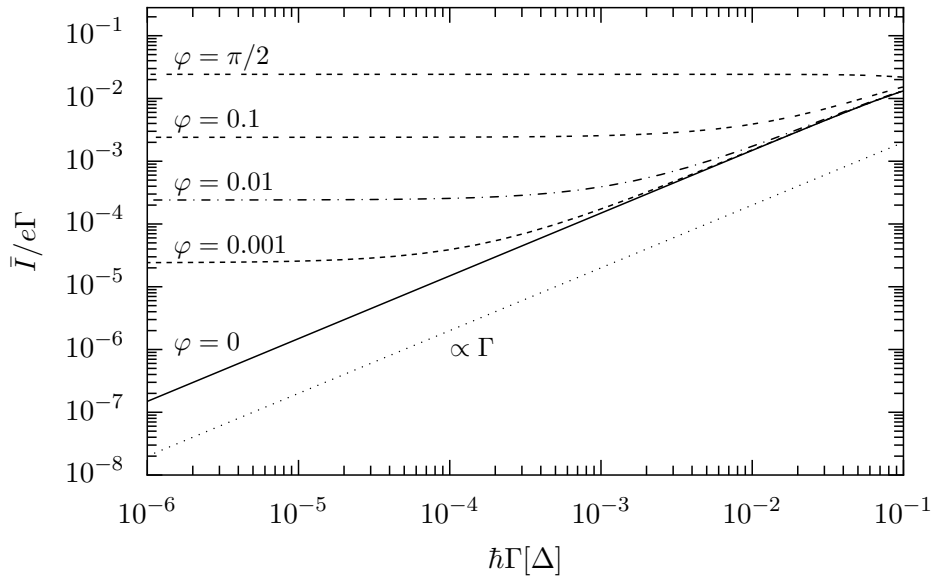

Figure 5.15: Average current through the two-site wire from Fig. 5.12 driven by the harmonic mixing signal (5.12) with amplitudes $A_1 = 2A_2 = \Delta$ as a function of the wire-lead coupling strength Γ for different values of the phase difference φ. All other parameters are as in Fig. 5.14. The dotted line is proportional to Γ, corresponding to a current that is proportional to Γ^2.

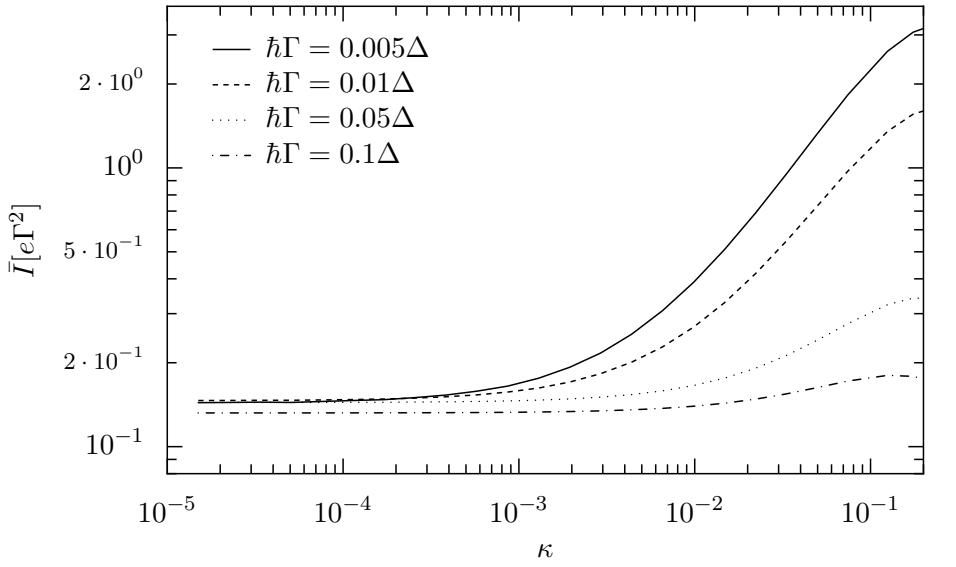

Figure 5.16: Average current (in units of $e\Gamma^2$) through the two-site wire sketched in Fig. 5.12 driven by the harmonic mixing signal (5.12) with amplitudes $A_1 = 2A_2 = \Delta$ and phase difference $\varphi = \pi/2$ as a function of the electron-phonon coupling strength κ in Eqs. (3.10) and (3.14). Different values of the wire-lead coupling strength Γ are shown.

published by Shaker Verlag, Aachen, ISBN 3-8322-1979-X

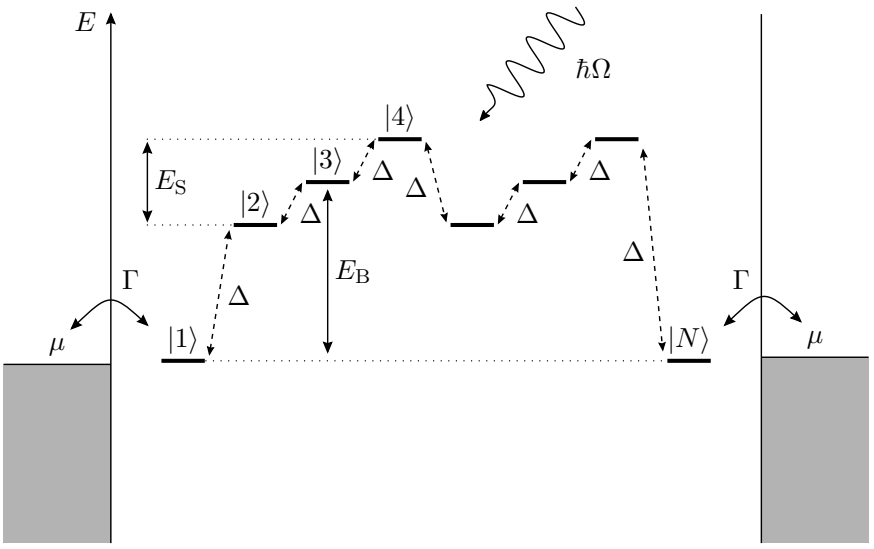

Figure 5.17: Level structure of the wire ratchet with $N = 8$ atomic sites, i.e., $N_g = 2$ asymmetric molecular groups. The bridge levels are E_B above the donor and acceptor levels and are shifted by $\pm E_S/2$.

becomes too time-consuming (cf. Sect. 3.5), we have to restrict ourselves to the situation without electron-phonon interaction.

Rectification in ratchet-like structures

Particularly interesting is the rectification behaviour of structures which are composed of repeated identical, inherently asymmetric molecular groups. An example for such a structure is sketched in Fig. 5.17, where the interior wire states $|2\rangle,\ldots,|N-1\rangle$ are arranged in N_g groups of three, i.e., $N-2=3N_g$. The energies of the donor $|1\rangle$ and the acceptor $|N\rangle$ orbitals are assumed to be at the level of the chemical potentials of the attached leads, $E_1 = E_N = \mu_L = \mu_R =: \mu$. The levels in each of the inner groups lie E_B above the chemical potential and are shifted by $\pm E_S/2$, forming an asymmetric sawtooth like structure [90, 121]. In the limit of a infinite number of groups one obtains a periodic but asymmetric arrangement, a discrete version of a so-called ratchet potential [122, 123]. For a concise overview over the transport properties of such systems, we refer the reader to the introductory articles Refs. [30, 32]. An exhaustive treatment can be found in the review article Ref. [31]. Asymmetry in molecular structures can be achieved in many ways, and was explored as a source of molecular rectifying since the seminal paper of Aviram and Ratner [6]. As noted after Eq. (5.1), it can be controlled by attaching different chemical groups to an otherwise symmetric molecule [18, 114].

The driving-amplitude dependency of the stationary time-averaged current $\bar{I}$ for the model (5.1) with the level structure depicted in Fig. 5.17 in conjunction with a harmonic driving (5.11) is shown in Fig. 5.18. In the limit of a very weak laser field,

published by Shaker Verlag, Aachen, ISBN 3-8322-1979-X

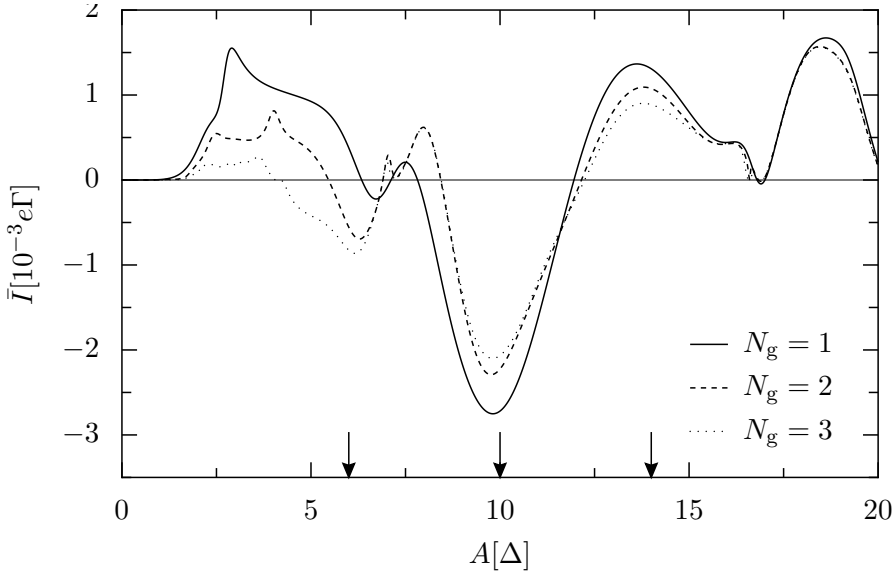

Figure 5.18: Time-averaged current through a molecular wire that consists of N_g bridge units as a function of the driving strength A. The bridge parameters are $E_B = 10\Delta$, $E_S = \Delta$; the driving frequency is $\Omega = 3\Delta/\hbar$, the coupling to the leads is chosen as $\Gamma_L = \Gamma_R = 0.1\Delta/\hbar$, and the temperature is $k_B T = 0.25\Delta$. The arrows indicate the driving amplitudes used in Fig. 5.20.

we find the scaling behaviour $\bar{I} \propto A^2 E_S$, as demonstrated in Fig. 5.19. This behaviour is expected from symmetry considerations: On the one hand, $\bar{I}$ vanishes for zero step size E_S since then both parity symmetries discussed in Sect. 5.3.1 are restored. On the other hand, the asymptotic current must be independent of any initial phase of the driving field and therefore is an even function of the field amplitude A. The latter A^2-dependence clearly indicates that the ratchet effect can only be obtained from a treatment *beyond linear response*. For strong laser fields, we find that $\bar{I}$ is almost independent of the wire length. If the driving is moderately strong, $\bar{I}$ depends in a short wire sensitively on the driving amplitude A and the number of asymmetric molecular groups N_g; even its sign may change with N_g, i.e., we find a current reversal as a function of the wire length. For long wires that comprise five or more wire units (corresponding to 17 or more sites), the average current becomes practically length-independent, as can be observed in Fig. 5.20. This stays in contrast to the situation with external bias (cf. Sect. 5.2) and identifies the current reversal as a finite size effect.

Figure 5.21 depicts the average current vs. the driving frequency Ω, exhibiting resonance peaks as a striking feature. Comparison with the quasienergy spectrum reveals that—like for the current amplification setup of Sect. 5.2—each peak corresponds to a non-linear resonance between the donor/acceptor and a bridge orbital. While the broader peaks at $\hbar\Omega \approx E_B = 10\Delta$ match the 1:1 resonance (i.e., the driving frequency equals the energy difference), one can identify the sharp peaks for $\hbar\Omega \lesssim 7\Delta$ as

published by Shaker Verlag, Aachen, ISBN 3-8322-1979-X

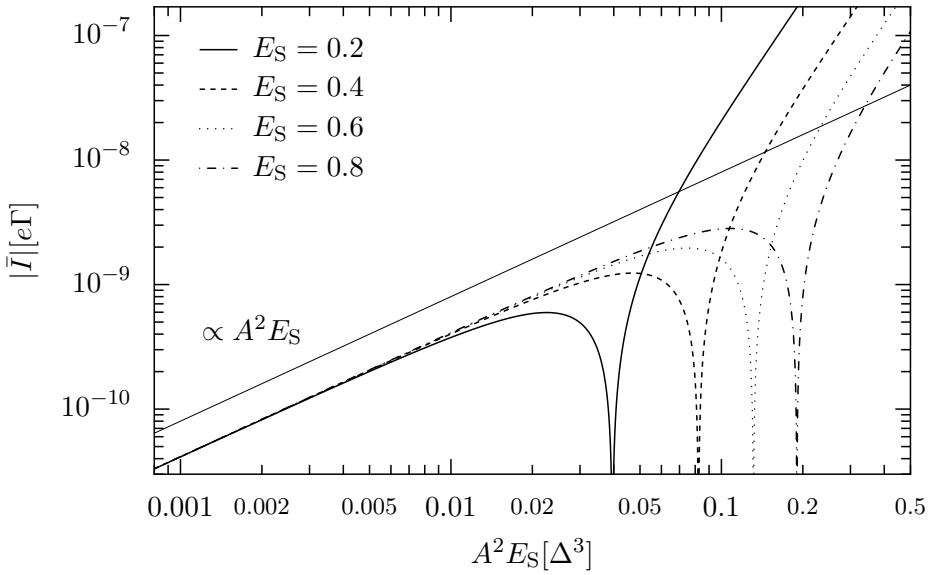

Figure 5.19: Absolute value of the time-averaged current in a ratchet-like structure with $N_g = 1$ as a function of $A^2 E_S$, demonstrating the proportionality to $A^2 E_S$ for small driving amplitudes. All other parameters are as in Fig. 5.18. At the dips on the right-hand side, the current $\bar{I}$ changes its sign.

multi-photon transitions. The current within a rotating-wave approximation (3.61) is plotted for comparison. While it reproduces the general features of the exact solution, its results are not reliable since it might even predict the wrong current direction.

Rectification from harmonic mixing

As in the two-site case (cf. Sect. 5.3.2), in a spatially symmetrical molecule like the wire bridge from Sect. 5.2, a non-vanishing dc response can be obtained by irradiating with the harmonic mixing field (5.12). Let us thus consider the situation of Fig. 5.22: The energies of the donor and the acceptor orbitals are, as always, assumed to be at the level of the chemical potentials of the attached leads, $E_1 = E_N = \mu_L = \mu_R =: \mu$. The bridge levels E_n, $n = 2,\ldots,N-1$, are located E_B above the chemical potential, and the form of the driving is given by (5.12).

The average current for such a harmonic mixing situation is depicted in Fig. 5.23. Like for the ratchet wire case, for large driving amplitudes, it becomes essentially independent of the wire length and, thus, a wire that consists of only a few orbitals, mimics the behaviour of an infinite tight-binding system. Figure 5.24 shows the length dependence of the average current for different driving strengths. The current saturates as a function of the length at a non-zero value. The convergence depends on the driving amplitude and is typically reached once the number of sites exceeds a value of $N \approx 10$. For low driving amplitudes the current response is more sensitive to the wire length.

The dependence of the dc current on the phase difference φ between the two har-

published by Shaker Verlag, Aachen, ISBN 3-8322-1979-X

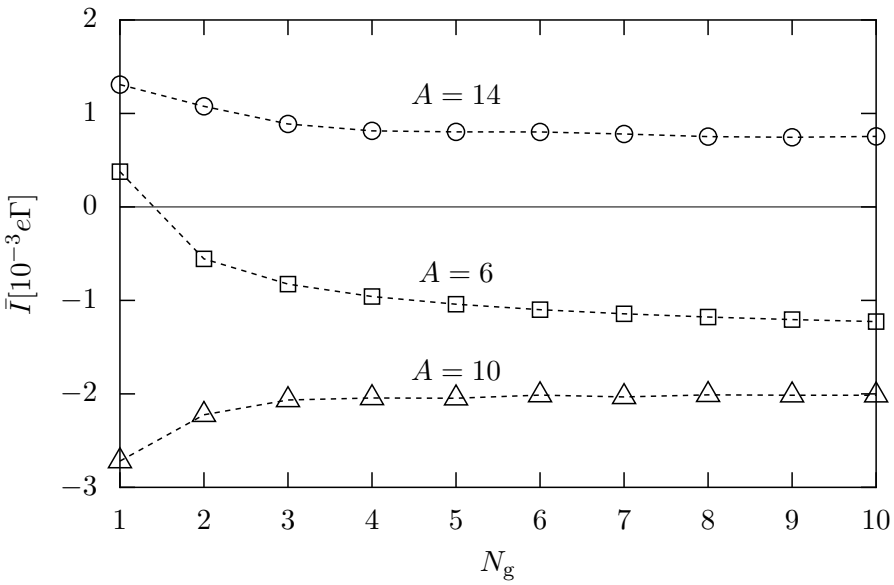

Figure 5.20: Time-averaged current as a function of the number of bridge units N_g, $N = 3N_g + 2$, for the laser amplitudes indicated in Fig. 5.18. All other parameters are as in Fig. 5.18. The connecting lines serve as a guide to the eye.

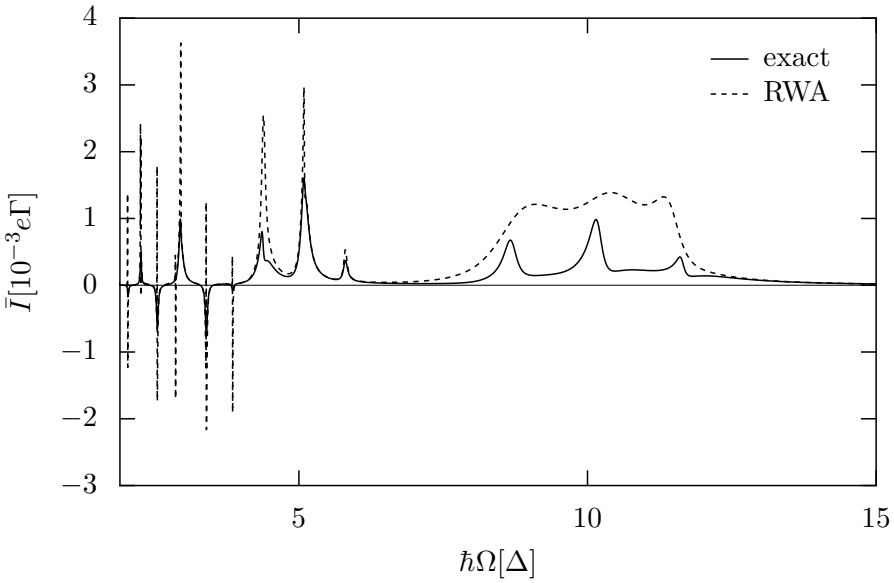

Figure 5.21: Time-averaged current as a function of the angular driving frequency Ω for $N_g = 1$. Solid: exact result. Dashed: RWA result (3.61). All other parameters are as in Fig. 5.18.

published by Shaker Verlag, Aachen, ISBN 3-8322-1979-X

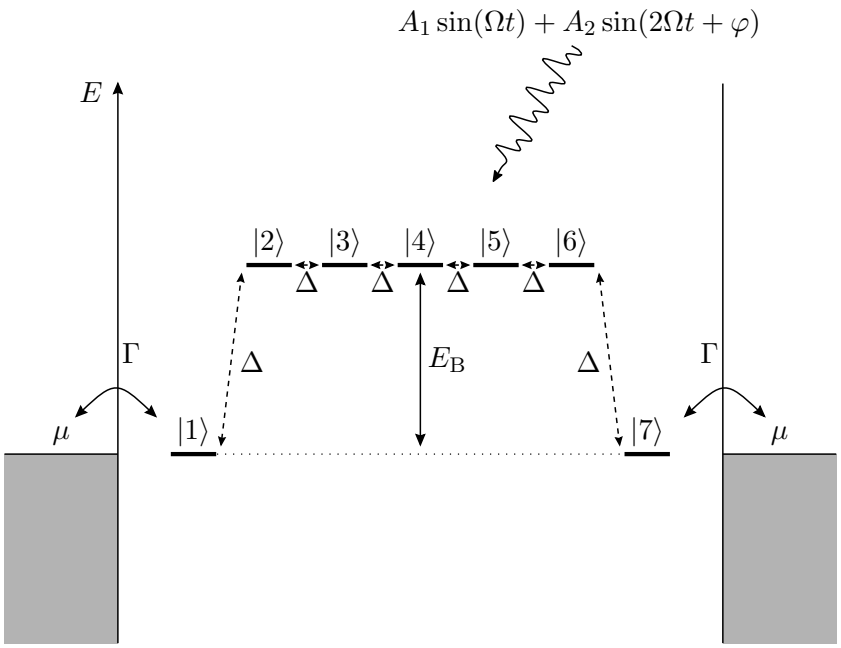

Figure 5.22: Level structure of the a wire bridge with $N = 7$ atomic sites. The bridge levels are E_B above the donor and acceptor levels, which lie at the level of the chemical potentials in the leads. The wire is irradiated by the harmonic mixing field (5.12).

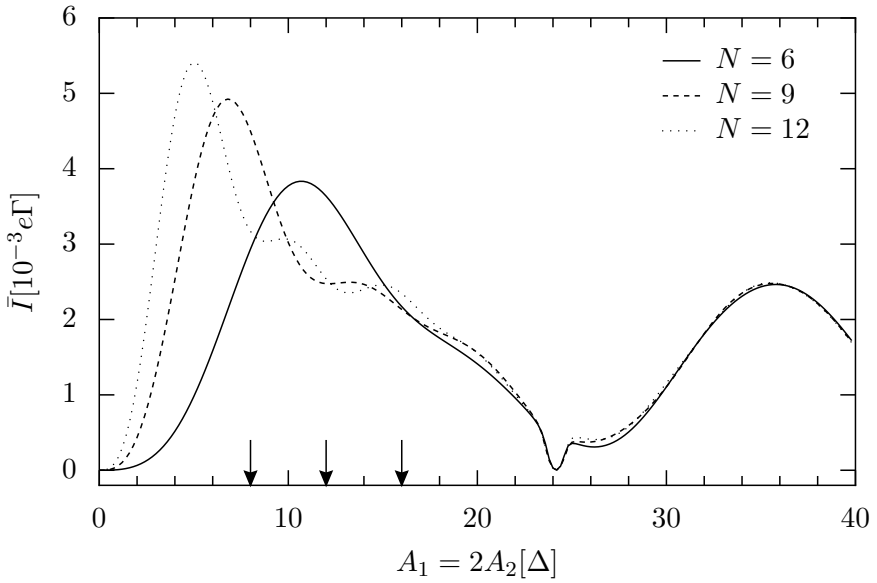

Figure 5.23: Average current response to the harmonic mixing signal (5.12) for $\Omega = 10\Delta/\hbar$ and phase $\varphi = \pi/2$. The wire-lead coupling strength is $\Gamma = 0.1\Delta$, the temperature $k_B T = 0.25\Delta$, and the bridge height $E_B = 5\Delta$. The arrows indicate the driving amplitudes used in Fig. 5.24.

published by Shaker Verlag, Aachen, ISBN 3-8322-1979-X

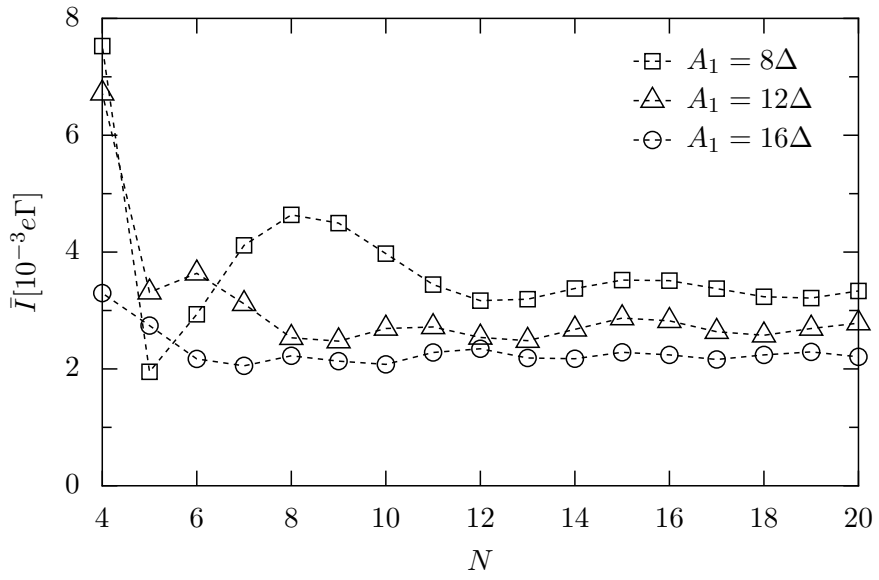

Figure 5.24: Length dependence of the average current for harmonic mixing with phase $\varphi = \pi/2$ for different driving amplitudes; the ratio of the driving amplitudes is fixed by $A_1 = 2A_2$. The other parameters are as in Fig. 5.23; the dotted lines serve as a guide to the eye.

monics of the signal (5.12) is depicted in Fig. 5.25. It exhibits again the same features as already discussed for the two-site situation (cf. Fig. 5.15): For $\varphi = 0$ or $\varphi = \pi$, i.e., in the presence of a time-reversal symmetry, the current vanishes with Γ^2 for $\Gamma \to 0$. For all other values of φ, one observes a proportionality to Γ.

5.4 Current switches

As a last application of our formalism, we investigate the possibilities for laser controlled switching of the electrical current through the wire. We hence consider a situation, where already in the absence of laser excitations a substantial current flows through the molecule due to an externally applied static voltage. The aim is then to control this current by means of suitable laser fields. As before, we first discuss the most simple setup, namely a two-site wire connected to two leads, which will yield an optical current gate. Subsequently, we shall consider a three-terminal device, in order to demonstrate the feasibility of an optical routing of electrical currents.

5.4.1 Current gate

Let us again consider the two-level Hamiltonian (5.10) in conjunction with a sinusoidal driving (5.11); a top view of the corresponding experimental setup is sketched in Fig. 5.26. Contrary to the situation in Sect. 5.3.2, we now take into account an

published by Shaker Verlag, Aachen, ISBN 3-8322-1979-X

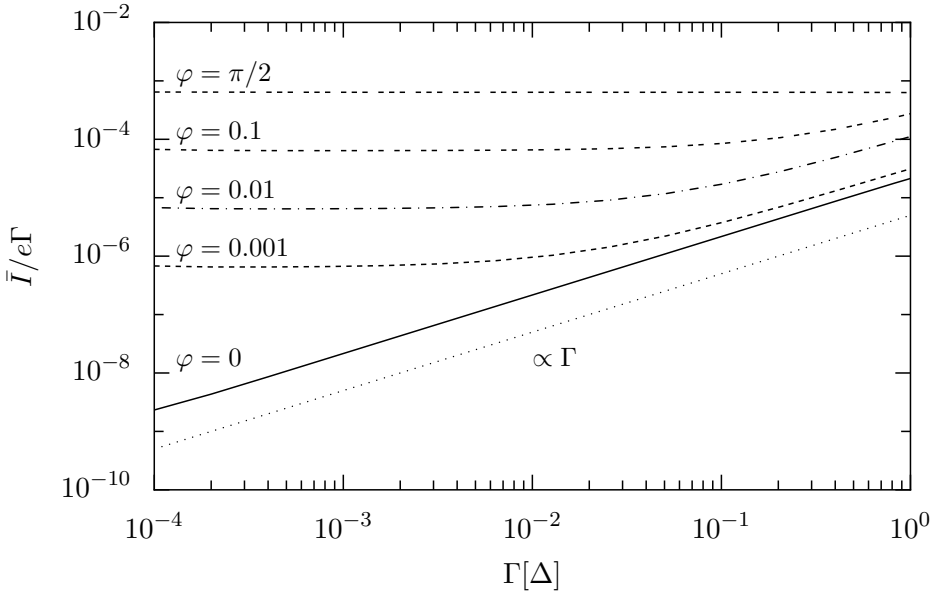

Figure 5.25: Average current response to the harmonic mixing signal with amplitudes $A_1 = 2A_2 = \Delta$, as a function of the coupling strength for different phase shifts φ. The remaining parameters are $\Omega = 10\Delta/\hbar$, $E_\mathrm{B} = 5\Delta$, $k_\mathrm{B}T = 0.25\Delta$, $N = 10$. The dotted line is proportional to Γ; it represents a current which is proportional to Γ^2.

external voltage V, i.e., a difference of the electro-chemical potentials, $\mu_\mathrm{L} - \mu_\mathrm{R} = -eV$. As discussed in Sect. 5.1, this may result in a voltage drop between the two sites, so that even for a symmetric molecule, for which initially $E_\mathrm{L} = E_\mathrm{R}$, the two site energies E_L and E_R may differ in the presence of the external voltage V. Again, the coupling to both leads is assumed to be equal, $\Gamma_\mathrm{L} = \Gamma_\mathrm{R} = \Gamma$.

In the limit of an infinitely strong voltage bias, an explicit expression for the dc current can be obtained from the analytical result (4.15) together with our earlier findings from a perturbation theory in the static Hamiltonian (cf. Sect. 2.5.1). It turns out that we only need the zeroth order expression (2.37) for the Floquet states together with the first order result (2.38) for the quasienergies. Inserting them into Eq. (4.15), we arrive at

$$\bar{I} = e\Gamma \frac{\sin^2\Theta}{2} \left[1 - \frac{\hbar^2\Gamma^2}{\left(\epsilon_{+,0} - \epsilon_{-,0}\right)^2 + \hbar^2\Gamma^2} \right] . \tag{5.13}$$

This equation, together with the expression (2.38) for the quasienergies $\epsilon_{\pm,0}$ and the definition (2.39) of the angle Θ, completely determines the dc current through the two-site wire in the presence of an infinite external bias voltage.

We can now immediately read off the main feature of the present setup, namely that the dc current breaks down whenever one of the conditions $\Theta = 0$ or $\epsilon_{+,0} = \epsilon_{-,0}$

published by Shaker Verlag, Aachen, ISBN 3-8322-1979-X

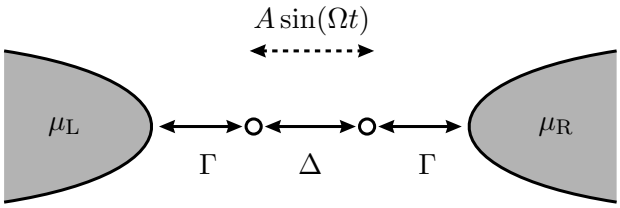

Figure 5.26: Schematic top view of a transport setup consisting of a two-site wire (coupled by a tunnel-matrix element Δ) equally connected to two leads at electrochemical potentials $\mu_{\rm L}$ and $\mu_{\rm R}$ by the rate Γ. A laser with angular frequency Ω and amplitude A permits the control of the dc current through the wire.

is satisfied. From the definitions of $\epsilon_{\pm,0}$ and Θ, we find that the former condition can only be fulfilled if $E_{\rm L} \neq E_{\rm R}$, i.e., for a system with biased on-site energies. By contrast, the latter equality requires an internally unbiased situation with $E_{\rm L} = E_{\rm R}$. However, in both cases $\Delta_0 = 0$ is the common requirement for the current suppression. By comparing with the discussion in Sect. 2.5.2, we thus identify the coherent destruction of tunneling (CDT) as the origin of the current break-downs. In other words: CDT should be observable in a transport measurement. We emphasise that since the RWA result (4.18) does not contain the second term of the sum in Eq. (5.13), the description of the predicted effect for a system without internal bias, requires a treatment beyond RWA.

These analytical predictions are in accordance with numerical results. Let us first consider the case $E_{\rm L} = E_{\rm R}$, where the time-averaged current $\bar{I}$ is depicted in Fig. 5.27. The numerically exact result (4.10) exhibits the sharp current break-downs. Comparing with the analytical result (5.13), which was derived for the case of an infinite external voltage, we observe for finite voltage a global decrease of the current with increasing laser field amplitude A. As discussed in the previous paragraph, within RWA, the suppressions do not occur. Figure 5.28 depicts the current $\bar{I}$ for $E_{\rm L} \neq E_{\rm R}$. Now, the RWA result and the exact solution agree reasonably well.

While the general features of the suppression effect are thus described by the analytical expression (5.13), closer inspection (cf. inset of Fig. 5.27) reveals that the dc current does not vanish exactly at the suppressions. Rather, a residual current of about 1% of its maximal value reached in the absence of the driving remains. This residual value of the current at the depression is proportional to the molecule-lead coupling Γ. Since the current in the undriven situation is proportional to Γ as well, we conclude that the maximal suppression ratio is Γ-independent.

An important question is, how robust the observed current suppression effect is in the presence of additional coupling of the electrons to phonon baths. Since in general, dissipation affects the CDT effect [97,98], the same has to be expected for the current suppression. And indeed, as demonstrated in Fig. 5.29, upon turning on an electron-phonon coupling of the form (3.10), (3.14), the depth of the suppression decreases with increasing coupling strength κ. However, we have not yet been able to reproduce the

published by Shaker Verlag, Aachen, ISBN 3-8322-1979-X

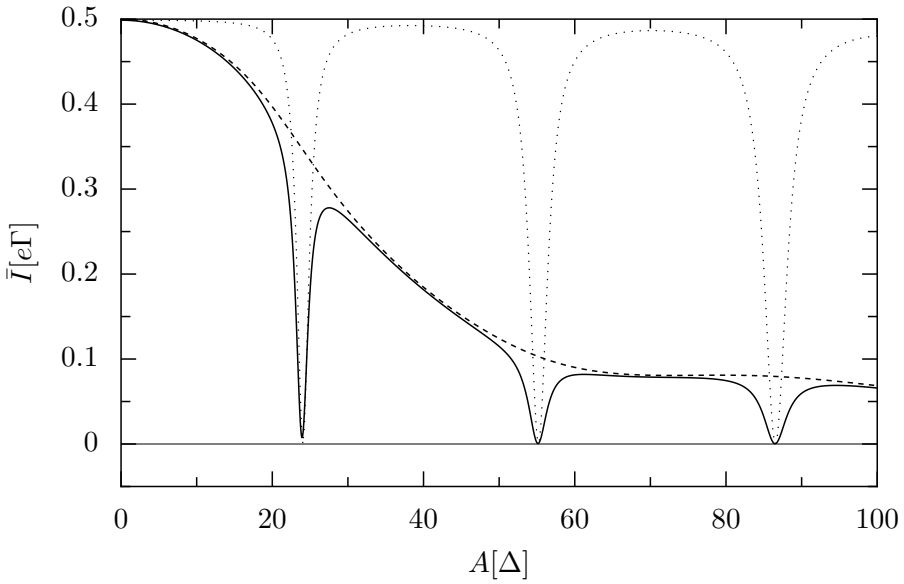

Figure 5.27: Average current vs. driving amplitude for a wire consisting of two sites between two electrodes for unbiased ($E_R = E_L = 0$) on-site energies. The leads' chemical potentials are $\mu_R = -\mu_L = 10\Delta$; the other parameters read $\hbar\Omega = 10\Delta$, $k_B T = 0.25\Delta$, $\hbar\Gamma = 0.1\Delta$. Solid: exact result (4.10). Dashed: result from rotating-wave approximation (4.17). Dotted: analytical result (5.13) valid for infinite bias $\mu_R = -\mu_R = \infty$.

counterintuitive effect of a stabilisation of CDT for a certain, optimal temperature, that has been reported in Refs. [97, 98].

5.4.2 Current router: molecular transistor

An experimentally more ambitious, three-terminal configuration consists in a planar molecule with $N = 4$ sites, three of which are coupled to a central site and are directly connected to the adjacent leads (see Fig. 5.30). We borrow from electrical engineering the designation E, C_1, and C_2 for the leads. Here, an external voltage is applied such that C_1 and C_2 have equal electro-chemical potential, i.e., $\mu_{C_1} = \mu_{C_2} \neq \mu_E$. In a perfectly symmetric molecule, where all on-site energies are equal, reflection symmetry at the horizontal axis ensures that any current which enters at E, is equally distributed among $C_{1,2}$, thus $I_{C_1} = I_{C_2} = -I_E/2$.

The fact that this structure is essentially two-dimensional brings about a new degree of freedom, the polarisation of the laser field. We assume it to be linear with an polarisation angle ϑ as sketched in Fig. 5.30. The effective driving amplitudes of the orbitals which are attached to the leads acquire now a geometric factor which is only the same for both orbitals C_1 and C_2 when $\vartheta = 0$. For any other polarisation angle, the mentioned reflection symmetry is broken and the outgoing currents may be different

published by Shaker Verlag, Aachen, ISBN 3-8322-1979-X

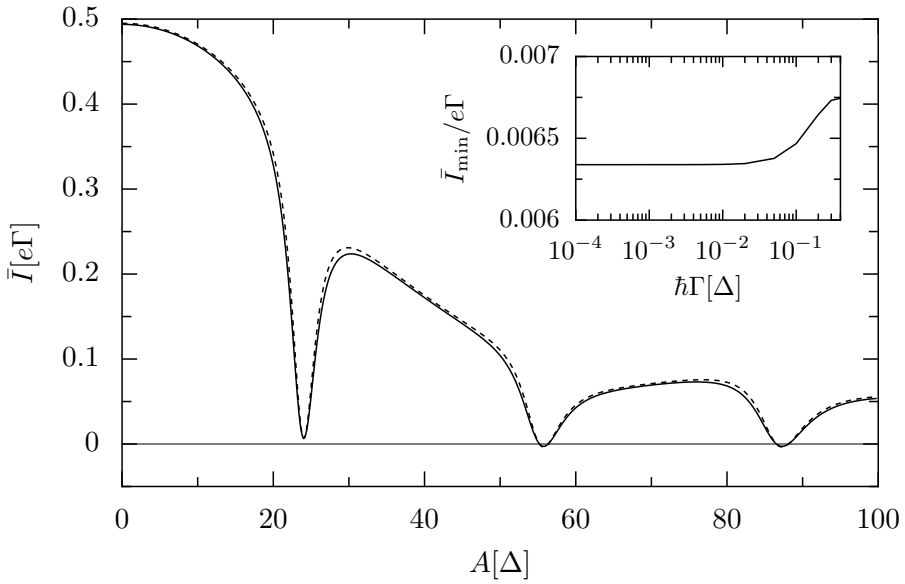

Figure 5.28: Average current vs. driving amplitude for a wire consisting of two sites between two electrodes for biased ($E_{\mathrm{L}} = -E_{\mathrm{R}} = 0.1\Delta$) on-site energies. All other parameters are as in Fig. 5.27. Solid: exact result (4.10). Dashed: result from rotating-wave approximation (4.17). Inset: Minimum value $\bar{I}_{\min}$ of the dc current at the first suppression as a function of the wire-lead coupling strength Γ. For small Γ, one obtains $\bar{I}_{\min} \propto \Gamma$.

from each other. The difference may be huge, as depicted in Fig. 5.31. Their ratio varies from unity for $\vartheta = 0$ up to the order of 100 for $\vartheta = 60°$. Thus, by changing the polarisation angle one is able to route the current towards the one or the other drain.

For the explanation of the mechanism behind this effect, it is instructive to look at the RWA expression (4.18) for the current in the strongly biased situation. Thereafter, each Floquet mode contributes to the current with an amount determined by the time-averaged matrix elements $\langle\langle \Phi_\alpha | n \rangle \langle n | \Phi_\alpha \rangle\rangle = \sum_k |\langle n | \Phi_{\alpha,k} \rangle|^2$ of the terminal sites $n = \mathrm{E}, \mathrm{C}_1, \mathrm{C}_2$. Figure 5.32 shows these quantities for three different polarisation angles ϑ. Consider, for instance, the current across contact C_1, which, in analogy to Eq. (4.18), can be written as

$$\bar{I}_{\mathrm{C}_1} = e\Gamma \sum_\alpha \frac{\langle\langle \Phi_\alpha | \mathrm{C}_1 \rangle \langle \mathrm{C}_1 | \Phi_\alpha \rangle\rangle \langle\langle \Phi_\alpha | \mathrm{E} \rangle \langle \mathrm{E} | \Phi_\alpha \rangle\rangle}{\sum_{\ell = \mathrm{C}_1, \mathrm{C}_2, \mathrm{E}} \langle\langle \Phi_\alpha | \ell \rangle \langle \ell | \Phi_\alpha \rangle\rangle} \,. \tag{5.14}$$

One observes that only Floquet modes which are both localised on the site C_1 and on the site E yield a non-vanishing contribution to the current. For a polarisation angle $\vartheta = -60°$, we can infer from Fig. 5.32 that this condition is fulfilled by the states with indices $\alpha = 1$, 3 and 4; a current flows from lead E into lead C_1. By contrast, for

published by Shaker Verlag, Aachen, ISBN 3-8322-1979-X

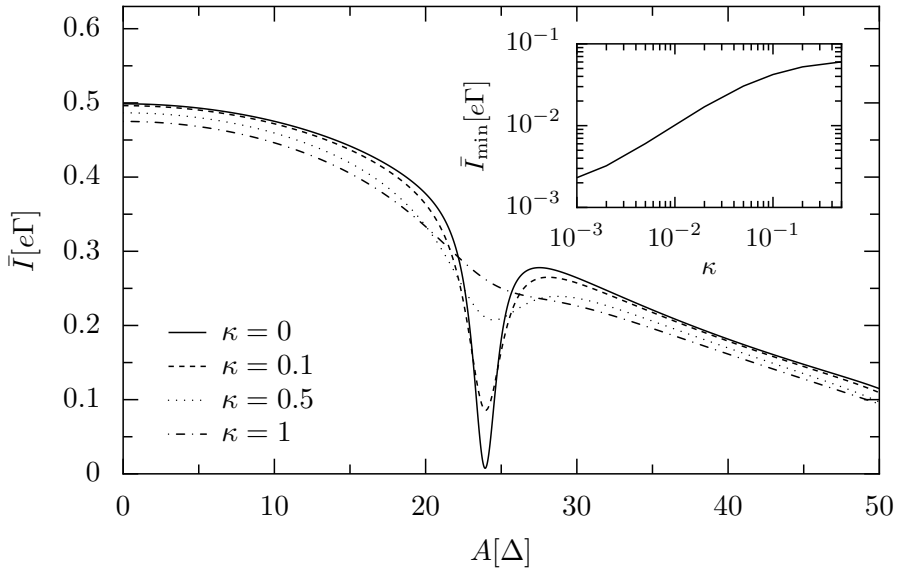

Figure 5.29: Average current vs. driving amplitude for a wire consisting of two sites between two electrodes for unbiased ($E_R = E_L = 0$) on-site energies for different strengths κ of an electron-phonon interaction of the form (3.10,3.14). All other parameters are as in Fig. 5.27. Inset: Minimum value $\bar{I}_{\min}$ of the dc current at the first suppression as a function of the electron-phonon coupling strength κ.

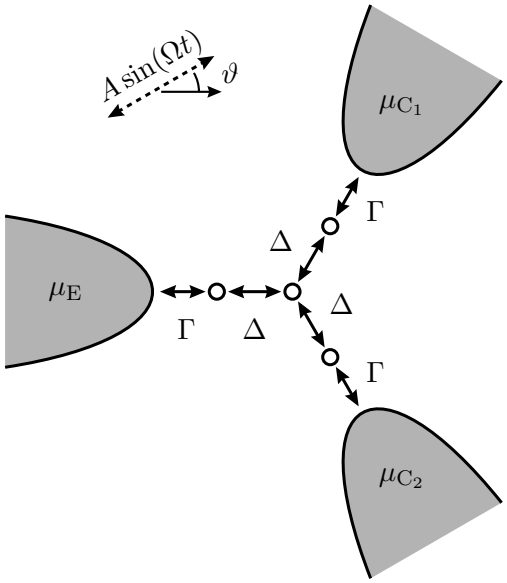

Figure 5.30: Schematic top view of a setup where a molecule connected to three leads allows to control the current flowing between the different leads (electro-chemical potentials μ_E, μ_{C_1}, and μ_{C_2}) as a function of the polarisation angle θ of a linearly polarised laser field.

published by Shaker Verlag, Aachen, ISBN 3-8322-1979-X

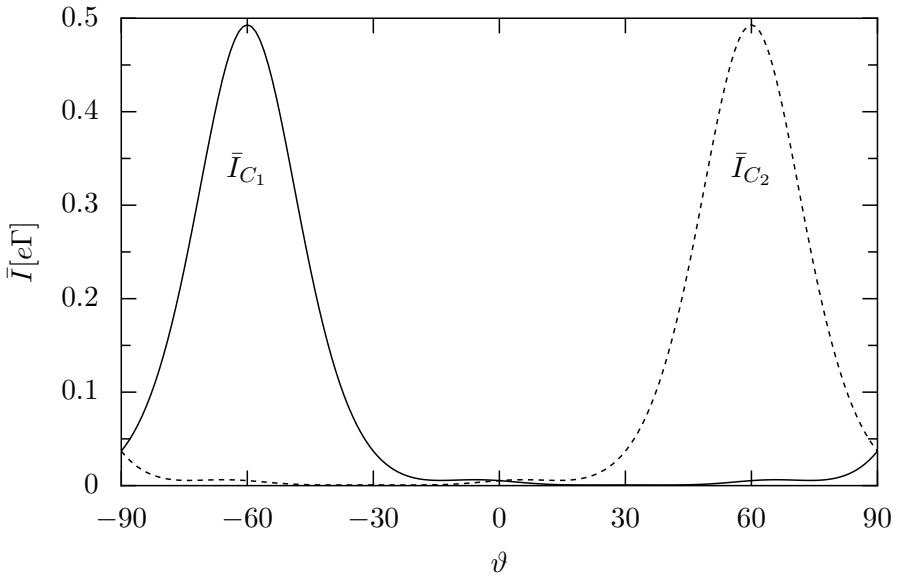

Figure 5.31: Average currents through contacts C_1 (solid) and C_2 (dashed) as a function of the polarisation angle ϑ for the three-terminal device depicted in the inset. The chemical potentials are $\mu_E = -\mu_{C_1} = -\mu_{C_2} = 50\Delta$; the on-site energies $E_n = 0$. The driving field is specified by the strength $A = 25\Delta$ and the angular frequency $\Omega = 10\Delta/\hbar$; the effective coupling is $\hbar\Gamma = 0.1\Delta$ and the temperature $k_B T = 0.25\Delta$. The maximal value of the current ratio $I_{C_1}/I_{C_2} \approx 100$ is assumed at $\vartheta = 60°$.

published by Shaker Verlag, Aachen, ISBN 3-8322-1979-X

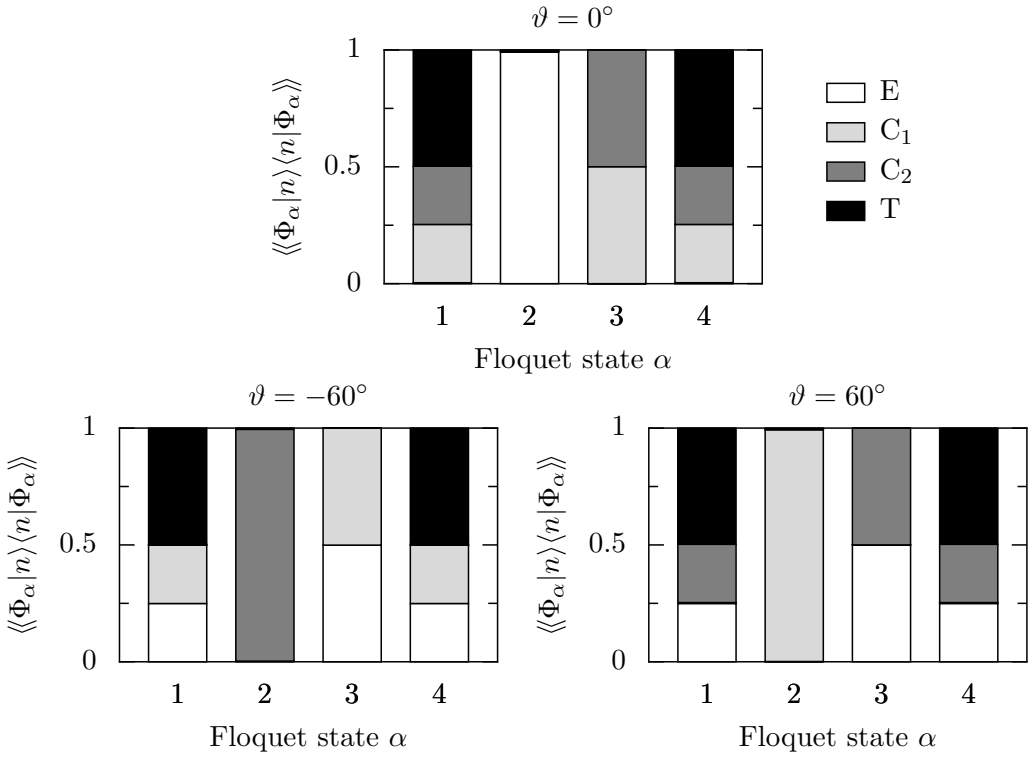

Figure 5.32: Contributions $\langle\langle\Phi_\alpha|n\rangle\langle n|\Phi_\alpha\rangle\rangle = \sum_k |\langle n|\Phi_{\alpha,k}\rangle|^2$ of the sites $n = \mathrm{E}, \mathrm{C}_1, \mathrm{C}_2$, and T (central site) to a Floquet state $|\Phi_\alpha(t)\rangle$ for three different polarisation angles ϑ. All parameters are as in Fig. 5.31. Note that for some states α not all contributions are resolved in this figure.

$\vartheta = 0$ and $\vartheta = 60°$, such current carrying states do not exist; the respective current is zero.

An alternative setup for an optically controllable router is sketched in Fig. 5.33. Now, the polarisation angle is fixed at $\vartheta = 0$ and the reflection symmetry is broken by using an intrinsically asymmetric molecule (see Fig. 5.33). This allows to control sensitively the ratio of the outgoing currents by the strength A of the external field, cf. Fig. 5.34. The switching range comprises up to four orders of magnitude with an exponential sensitivity.

published by Shaker Verlag, Aachen, ISBN 3-8322-1979-X

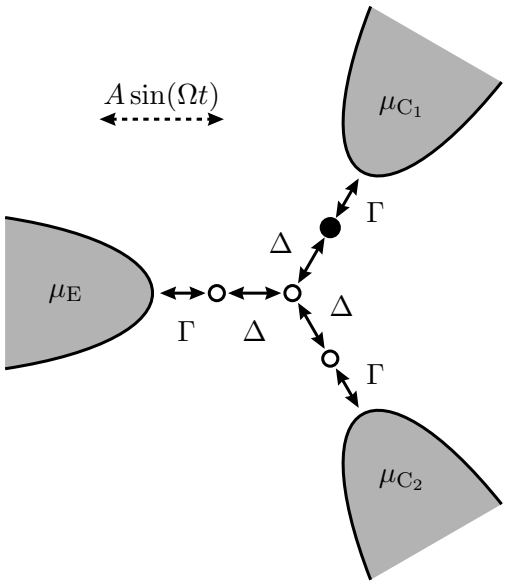

Figure 5.33: Schematic top view of a setup where a molecule connected to three leads allows to control the current flowing between the different leads (electro-chemical potentials μ_E, μ_{C_1}, and μ_{C_2}) as a function of the driving amplitude A of a linearly polarised laser field.

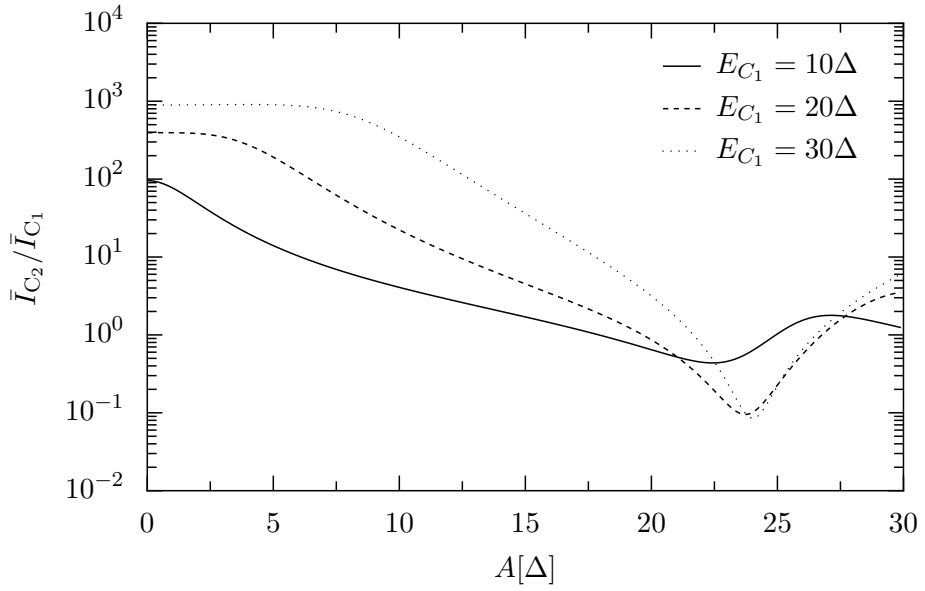

Figure 5.34: Ratio of the outgoing average currents vs. driving strength A for the three-terminal device at a polarisation angle $\vartheta = 0$. The filled circle in the inset depicts a site with an on-site energy E_{C_1} that differs from the others. All other on-site energies and parameters as in Fig. 5.31.

published by Shaker Verlag, Aachen, ISBN 3-8322-1979-X

published by Shaker Verlag, Aachen, ISBN 3-8322-1979-X

6 Summary and outlook

The present thesis deals with the description of electronic transport through driven nanosystems, where we usually have in mind molecular wires under the influence of laser fields. For the calculation of the electrical current across the different contacts between the nanosystem and the macroscopic leads, we put forward an efficient numerical procedure: In a first step, the quantum dynamics of the isolated system is solved using a Floquet approach. The resulting basis states then provide a vantage point for the inclusion of a weak coupling both to electronic leads and to phononic degrees of freedom in the framework of a kinetic equation approach. In conjunction with the Floquet states, we then have at our disposal the necessary input for the calculation of the electrical current.

As a first exemplary application of the developed formalism, we have discussed a current spectroscopy setup, which allows to gather information about the molecular levels by transport measurements. Thereby, a resonant laser field drastically enhances the current across the molecule. Since furthermore the length dependence of the current changes from an exponential decrease without driving to a $1/N$-behaviour, this effect is most pronounced for long wires.

Another phenomenon that has been studied is the generation of a non-zero dc current across the molecule in the absence of any voltage. Such quantum Brownian motor or ratchet currents require that the system is driven away from thermal equilibrium by a field that does not fulfil a generalised parity symmetry. This means that one has to either use a molecule with an asymmetric level structure or irradiate the molecule with a dynamically asymmetric laser field, for instance, one that contains higher harmonics of the fundamental driving frequency. The resulting current shows an intricate dependency on all model parameters, including multiple current reversals as a function of laser field amplitude and frequency or the phase difference between harmonic and second harmonic. These effects enable, e.g., a selective shuttling of electrons on the nanoscale.

Finally, possibilities of switching the electrical current by use of an external laser field have been explored. This has resulted in a setup for an optically controllable current gate, which allows to sensitively switch the current flowing between two leads on and off by means of a laser field with suitable frequency and amplitude. The extension to a three-terminal geometry yields an optical current router or molecular

published by Shaker Verlag, Aachen, ISBN 3-8322-1979-X

transistor that permits to steer the current to one or the other lead, as a function of either the polarisation angle of the laser field (cf. Fig. 5.31) or of the field strength (cf. Fig. 5.34).

The experimental realisation of the proposed setups, especially of the current switches, which require strong laser fields, is clearly a non-trivial task. One practical problem that immediately comes to mind is the illumination of the molecule, which might be hampered by the presence of the leads. However, by choosing a suitable geometry, for instance by irradiating from the bottom side—through the substrate—in a break-junction setup or by using an STM configuration, it should be possible to overcome this obstacle. Another question concerns the stability of the laser-irradiated molecule and of its bond to the metal surfaces. In particular, laser-induced desorption processes due to hot electrons originating from the electronic leads as well as the heating of the molecule could pose serious problems. On the positive side, our theoretical proposals are generic in the sense that they do not rely on a specific molecular structure, a fact which should facilitate their experimental realisation.

A completely different experimental implementation of our findings should be possible in semiconductor heterostructures, where instead of the molecule, quantum dots form the central system [20, 124]. Here, stability issues are less important, however one has to pay the price of a more difficult maintenance of quantum coherence.

So far, our formalism is restricted to continuously time-dependent laser fields. As a future extension of the present work, one should also include the equally important situation with pulsed laser fields. However, this requires a modification of the present Floquet method, since the convergence of the numerical scheme becomes slower with increasing period T of the driving: the width of the Brillouin zones decreases with $1/T$ and therefore the number of sidebands one has to take into account increases correspondingly. Thus, a modified numerical procedure has to be developed, which takes into account separately the fast dynamics within the pulse and the slow one due to the pulse shape.

Our numerical studies of the influence of electron-phonon interaction have been based on the simple on-site dissipation model in combination with an Ohmic spectral density of the phonon bath. While this already yields some insight into generic properties of the system, one should realistically also take into account different coupling forms and spectral densities. For instance, future work should examine the influence of a cut-off frequency as well as that of a peaked spectral density corresponding to vibrational modes of the molecule.

Two extensions of the present work have already been addressed. The first one concerns the limit of a weak wire-lead coupling, which we have been considering throughout this work. In a recent work [125], we have demonstrated that in fact the formalism can be generalised to the case of an arbitrarily strong wire-lead coupling, provided that no electron-phonon interaction is present. The Floquet equation then has to be modified to include a self-energy term due to the wire-lead coupling. The left and the

published by Shaker Verlag, Aachen, ISBN 3-8322-1979-X

right eigenvectors of the corresponding non-Hermitian eigenvalue problem then allow to express the current in a scattering form [45]. Unfortunately, the numerical effort for the solution of the complex eigenvalue problem limits this method to either smaller or not too strongly driven molecular systems.

As a second extension, we have investigated not only the mean value of the current but also its fluctuations, i.e., the current noise. In particular, the relative noise power at zero frequency, the so-called Fano factor, provides additional insight into the properties of the transport process [126]. An explicit expression for this quantity has been derived with the methods mentioned in the previous paragraph [125]. For the optical current gate presented in Sect. 5.4.1, we find that at the position of current suppression induced by CDT, the Fano factor assumes a maximum accompanied by two minima nearby. This opens perspectives of not only controlling the mean current but also its noise properties by means of tailored laser fields.

published by Shaker Verlag, Aachen, ISBN 3-8322-1979-X

published by Shaker Verlag, Aachen, ISBN 3-8322-1979-X

A Perturbation theory for the driven two-level system

A.1 General expression

One of the main benefits of the composite Hilbert space formalism described in Sect. 2.2 lies in the fact that it immediately allows to make use of the tools known from time-independent quantum mechanics. One example, which we will discuss in this appendix, is the stationary, degenerate perturbation theory. Suppose that the unperturbed Floquet Hamiltonian $\mathcal{H}_0$ possesses a d-fold degenerate eigenvalue $\epsilon_1^{(0)} = \epsilon_2^{(0)} = \ldots = \epsilon_d^{(0)}$ with a degenerate subspace spanned by the eigenstates $|\phi_1\rangle\rangle, |\phi_2\rangle\rangle, \ldots, |\phi_d\rangle\rangle$. As required by degenerate perturbation theory, we assume that this basis is already chosen in such a way that it diagonalises the perturbation operator $\mathcal{H}_1$ within the degenerate subspace. Then to first order in $\mathcal{H}_1$, the eigenvalues of the perturbed problem

$$(\mathcal{H}_0 + \mathcal{H}_1)|\Phi_\alpha\rangle\rangle = \epsilon_\alpha |\Phi_\alpha\rangle\rangle \tag{A.1}$$

are determined by

$$\epsilon_\alpha \approx \epsilon_\alpha^{(1)} := \epsilon_\alpha^{(0)} + \langle\langle \phi_\alpha | \mathcal{H}_1 | \phi_\alpha \rangle\rangle \ . \tag{A.2}$$

For $\alpha = 1,2,\ldots d$, the corresponding approximation for the eigenstates is given by[1]

$$|\Phi_\alpha\rangle\rangle \approx |\phi_\alpha\rangle\rangle + \sum_{\beta k}{}' |\phi_\beta^k\rangle\rangle \frac{\langle\langle \phi_\beta^k | \mathcal{H}_1 | \phi_\alpha \rangle\rangle}{\epsilon_\alpha^{(0)} - \epsilon_{\beta,k}^{(0)}} + \sum_{\beta}{}' \frac{|\phi_\beta\rangle\rangle}{\epsilon_\alpha^{(1)} - \epsilon_\beta^{(1)}} \sum_{\gamma,k}{}' \frac{\langle\langle \phi_\beta | \mathcal{H}_1 | \phi_\gamma^k \rangle\rangle \langle\langle \phi_\gamma^k | \mathcal{H}_1 | \phi_\alpha \rangle\rangle}{\epsilon_\alpha^{(0)} - \epsilon_{\gamma,k}^{(0)}} \ . \tag{A.3}$$

The first order eigenstates for $\alpha > d$ are determined by

$$|\Phi_\alpha\rangle\rangle \approx |\phi_\alpha\rangle\rangle + \sum_{\beta k}{}' |\phi_\beta^k\rangle\rangle \frac{\langle\langle \phi_\beta^k | \mathcal{H}_1 | \phi_\alpha \rangle\rangle}{\epsilon_\alpha^{(0)} - \epsilon_{\beta,k}^{(0)}} \ . \tag{A.4}$$

[1] The third term on the right-hand side of Eq. (A.3) is erroneously omitted in many standard text books on quantum mechanics [127], probably because it is seemingly of higher order in $\mathcal{H}_1$. Owing to Eq. (A.2), this is in fact not the case. We refer the reader to the classical treatise [128] by R. Courant and D. Hilbert for the correct expression.

published by Shaker Verlag, Aachen, ISBN 3-8322-1979-X

Here, where not restricted, the summation indices β,γ and k run over all states in the first Brillouin zone and all integers, respectively. Terms leading to a vanishing denominator are to be left out in the sum, which is indicated by the prime on the sum symbol. Note that, in particular, the first (second) sum in Eq. (A.3) contains only states which do (not) belong to the degenerate subspace corresponding to the eigenvalue $\epsilon_\alpha^{(0)}$.

A.2 Application to the two-level system

We now apply the general results (A.2)–(A.4) to the driven two-level dynamics (2.33) from Sect. 2.5. Thereby, the quasienergies to zeroth order are given by $\epsilon_1^{(0)} = \epsilon_2^{(0)} = 0$ and the first order correction (A.2) follows directly from Eq. (2.38):

$$\epsilon_\pm^{(1)} = \pm\frac{1}{2}\sqrt{E_\mathrm{b}^2 + 4|\Delta_0|^2}\ . \tag{A.5}$$

For the calculation of the first order correction (A.3) to the Floquet modes, one needs the matrix elements $\langle\langle\phi_\pm^k|\mathcal{H}_1|\phi_\pm\rangle\rangle$ for $k \neq 0$. Inserting

$$\langle\langle\Phi_n^k|\mathcal{H}_1|\Phi_{n'}^{k'}\rangle\rangle_{n,n'=1,2} = \begin{pmatrix} \delta_{kk'}E_\mathrm{b}/2 & -\Delta_{k'-k} \\ -\Delta_{k-k'}^* & -\delta_{kk'}E_\mathrm{b}/2 \end{pmatrix} \tag{A.6}$$

into the definition (2.37) of the zeroth order Floquet modes, one obtains

$$\begin{aligned} \langle\langle\phi_+^k|\mathcal{H}_1|\phi_+\rangle\rangle &= -\langle\langle\phi_-^k|\mathcal{H}_1|\phi_-\rangle\rangle = \frac{1}{2}\sin\Theta\left(\mathrm{e}^{\mathrm{i}\Xi}\Delta_k^* + \mathrm{e}^{-\mathrm{i}\Xi}\Delta_{-k}\right)\ , \\ \langle\langle\phi_+^k|\mathcal{H}_1|\phi_-\rangle\rangle &= \quad \langle\langle\phi_-^{-k}|\mathcal{H}_1|\phi_+\rangle\rangle^* = \sin^2(\Theta/2)\mathrm{e}^{\mathrm{i}\Xi}\Delta_k^* - \cos^2(\Theta/2)\mathrm{e}^{-\mathrm{i}\Xi}\Delta_{-k}\ . \end{aligned} \tag{A.7}$$

Here, the angles Θ and Ξ are defined in Eqs. (2.39) and (2.40), respectively. The products appearing in the second sum on the right-hand side of Eq. (A.3), are most easily expressed using the identity $\sum_{\alpha=\pm}|\phi_\alpha^k\rangle\rangle\langle\langle\phi_\alpha^k| = \sum_{n=1,2}|\phi_n^k\rangle\rangle\langle\langle\phi_n^k|$, valid for arbitrary k, together with the matrix elements

$$\begin{aligned} \langle\langle\phi_1^k|\mathcal{H}_1|\phi_+\rangle\rangle &= -\langle\langle\phi_2^{-k}|\mathcal{H}_1|\phi_-\rangle\rangle^* = \quad \sin(\Theta/2)\mathrm{e}^{-\mathrm{i}\Xi/2}\Delta_{-k}\ , \\ \langle\langle\phi_2^k|\mathcal{H}_1|\phi_+\rangle\rangle &= \quad \langle\langle\phi_1^{-k}|\mathcal{H}_1|\phi_-\rangle\rangle^* = -\cos(\Theta/2)\mathrm{e}^{\mathrm{i}\Xi/2}\Delta_k^*\ . \end{aligned} \tag{A.8}$$

Using the definition (2.43) of the asymmetry parameter λ, this yields

$$\begin{aligned} \sum_{\gamma=\pm}\langle\langle\phi_+|\mathcal{H}_1|\phi_\gamma^k\rangle\rangle\langle\langle\phi_\gamma^k|\mathcal{H}_1|\phi_-\rangle\rangle &= \sum_{\gamma=\pm}\langle\langle\phi_-|\mathcal{H}_1|\phi_\gamma^k\rangle\rangle\langle\langle\phi_\gamma^k|\mathcal{H}_1|\phi_+\rangle\rangle \\ &= \lambda\sqrt{E_\mathrm{b}^2 + 4|\Delta_0|^2}\ . \end{aligned} \tag{A.9}$$

published by Shaker Verlag, Aachen, ISBN 3-8322-1979-X

Collecting all terms, we arrive at the following expression for the first order Floquet modes:

$$
\begin{aligned}
|\Phi_+\rangle\rangle \approx |\phi_+\rangle\rangle - \lambda|\phi_-\rangle\rangle - \frac{\sin\Theta}{2}\sum_{k\neq 0}\frac{\mathrm{e}^{\mathrm{i}\Xi}\Delta_k^* + \mathrm{e}^{-\mathrm{i}\Xi}\Delta_{-k}}{k\hbar\Omega}|\phi_+^k\rangle\rangle \\
- \sum_{k\neq 0}\frac{\sin^2(\Theta/2)\mathrm{e}^{-\mathrm{i}\Xi}\Delta_{-k} - \cos^2(\Theta/2)\mathrm{e}^{\mathrm{i}\Xi}\Delta_k^*}{k\hbar\Omega}|\phi_-^k\rangle\rangle \ , \\
|\Phi_-\rangle\rangle \approx |\phi_-\rangle\rangle + \lambda|\phi_+\rangle\rangle + \frac{\sin\Theta}{2}\sum_{k\neq 0}\frac{\mathrm{e}^{\mathrm{i}\Xi}\Delta_k^* + \mathrm{e}^{-\mathrm{i}\Xi}\Delta_{-k}}{k\hbar\Omega}|\phi_-^k\rangle\rangle \\
- \sum_{k\neq 0}\frac{\sin^2(\Theta/2)\mathrm{e}^{\mathrm{i}\Xi}\Delta_k^* - \cos^2(\Theta/2)\mathrm{e}^{-\mathrm{i}\Xi}\Delta_{-k}}{k\hbar\Omega}|\phi_+^k\rangle\rangle \ .
\end{aligned}
\tag{A.10}
$$

published by Shaker Verlag, Aachen, ISBN 3-8322-1979-X

published by Shaker Verlag, Aachen, ISBN 3-8322-1979-X

B Rotating-wave approximation

We have seen in Sect. 3.3 for the special case without electron-phonon interaction, that for very weak wire-environment coupling, the dynamics is often well described by a master equation in the so-called rotating-wave approximation. We now discuss the derivation of such an approximative equation in the general situation with electron-phonon coupling. To this end, as discussed in Sect. 3.3, we first switch to the kinetic equation (3.30) in the interaction picture (3.53),

$$\begin{aligned}\frac{\mathrm{d}\widetilde{P}_{\alpha\beta}(t)}{\mathrm{d}t} =& \sum_{\alpha'\beta'} \mathrm{e}^{\mathrm{i}(\epsilon_\alpha-\epsilon_\beta-\epsilon_{\alpha'}+\epsilon_{\beta'})t/\hbar}\left[\mathcal{R}^{\text{leads}}_{\alpha\beta\alpha'\beta'}(t)+\mathcal{R}^{\text{phonons}}_{\alpha\beta\alpha'\beta'}(t)\right]\widetilde{P}_{\alpha'\beta'}(t) \\ &+ \sum_{\alpha'\beta'\alpha''\beta''} \mathrm{e}^{\mathrm{i}(\epsilon_\alpha-\epsilon_\beta-\epsilon_{\alpha'}+\epsilon_{\beta'}-\epsilon_{\alpha''}+\epsilon_{\beta''})t/\hbar}\mathcal{Q}^{\text{phonons}}_{\alpha\beta\alpha'\beta'\alpha''\beta''}(t)\,\widetilde{P}_{\alpha'\beta'}(t)\,\widetilde{P}_{\alpha''\beta''}(t) \\ &+ \mathrm{e}^{\mathrm{i}(\epsilon_\alpha-\epsilon_\beta)t/\hbar}\mathcal{S}^{\text{leads}}_{\alpha\beta}(t)\ .\end{aligned} \tag{B.1}$$

Assuming that the typical time-scales of the deterministic and dissipative dynamics are well separated, we are allowed to replace the time-dependent coefficients on the right-hand side of Eq. (B.1) by their respective time-averages. In a first step, we replace the *exponential prefactors* by their respective time-averages over one driving period T. For the contributions from the wire-lead coupling this yields with Eq. (3.35) the source terms

$$\mathcal{S}^{\text{leads}}_{\alpha\beta} = \frac{1}{2}\sum_{\ell=1}^{L}\sum_{k}\langle\Phi_{\alpha,k}|\ell\rangle\langle\ell|\Phi_{\beta,k}\rangle\left\{\,\Gamma_\ell(\epsilon_{\alpha,k})f(\epsilon_{\alpha,k}-\mu_\ell)+\Gamma_\ell(\epsilon_{\beta,k})f(\epsilon_{\beta,k}-\mu_\ell)\right\} \tag{B.2}$$

and with Eq. (3.34) the Redfield tensor

$$\begin{aligned}\mathcal{R}^{\text{leads}}_{\alpha\beta\alpha'\beta'} = -\frac{1}{2}\sum_{\ell=1}^{L}\sum_{k}\Big\{&\Gamma_\ell(\epsilon_{\alpha',k})\langle\Phi_{\alpha,k}|\ell\rangle\langle\ell|\Phi_{\alpha',k}\rangle\,\delta_{\beta\beta'} \\ &+\Gamma_\ell(\epsilon_{\beta',k})\langle\Phi_{\beta',k}|\ell\rangle\langle\ell|\Phi_{\beta,k}\rangle\,\delta_{\alpha\alpha'}\Big\}\ .\end{aligned} \tag{B.3}$$

published by Shaker Verlag, Aachen, ISBN 3-8322-1979-X

The coefficients of the linear terms stemming from the electron-phonon coupling assume the form [cf. Eq. (3.47)]

$$\begin{aligned}\mathcal{R}^{\text{phonons}}_{\alpha\beta\alpha'\beta'} = \sum_\nu \sum_k \Big\{ & \left[N_\nu(\Delta_{\alpha\alpha',k}) + N_\nu(\Delta_{\beta\beta',k})\right] \bar{X}^\nu_{\alpha\alpha',k} \bar{X}^\nu_{\beta'\beta,-k} \\ & - \delta_{\alpha\alpha'} \sum_{\alpha''} N_\nu(\Delta_{\alpha''\beta',k}) \bar{X}^\nu_{\alpha''\beta,k} \bar{X}^\nu_{\beta'\alpha'',-k} \\ & - \delta_{\beta\beta'} \sum_{\beta''} N_\nu(\Delta_{\beta''\alpha',k}) \bar{X}^\nu_{\beta''\alpha',k} \bar{X}^\nu_{\alpha\beta'',-k} \Big\} ,\end{aligned} \tag{B.4}$$

and the quadratic part (3.50) reads

$$\begin{aligned}\mathcal{Q}^{\text{phonons}}_{\alpha\beta\alpha'\beta'\alpha''\beta''} = \frac{1}{\hbar} \sum_\nu \sum_k \Big\{ & D_\nu(\Delta_{\beta'\alpha'',k}/\hbar) \bar{X}^\nu_{\beta'\alpha'',k} \bar{X}^\nu_{\beta''\beta,-k} \delta_{\alpha\alpha'} \\ & + D_\nu(\Delta_{\beta'\alpha',k}/\hbar) \bar{X}^\nu_{\beta'\alpha',k} \bar{X}^\nu_{\alpha\alpha'',-k} \delta_{\beta\beta''} \\ & - D_\nu(\Delta_{\beta'\alpha',k}/\hbar) \bar{X}^\nu_{\beta'\alpha',k} \bar{X}^\nu_{\beta''\beta,-k} \delta_{\alpha\alpha''} \\ & - D_\nu(\Delta_{\beta''\alpha',k}/\hbar) \bar{X}^\nu_{\beta''\alpha',k} \bar{X}^\nu_{\alpha\alpha'',-k} \delta_{\beta\beta'} \Big\} .\end{aligned} \tag{B.5}$$

Next, we observe that only terms with zero phase in the *exponentials* contribute to the time-average of Eq. (B.1). This yields the kinetic equation in RWA, which we first give here and will derive subsequently. The dynamics of the diagonal density matrix elements is determined by

$$\begin{aligned}\dot{\widetilde{P}}_{\alpha\alpha}(t) = & - w^{\text{leads}}_\alpha P_{\alpha\alpha}(t) + \sum_{\alpha'} \left(w^{\text{phonons}}_{\alpha\alpha'} \widetilde{P}_{\alpha'\alpha'}(t) - w^{\text{phonons}}_{\alpha'\alpha} \widetilde{P}_{\alpha\alpha}(t) \right) \\ & + 2 \sum_{\alpha'} q^{\text{phonons}}_{\alpha\alpha'} \widetilde{P}_{\alpha\alpha}(t) \widetilde{P}_{\alpha'\alpha'}(t) + \sum_{\alpha' \neq \alpha} \left(q^{\text{phonons}}_{\alpha'\alpha} - q^{\text{phonons}}_{\alpha\alpha'} \right) \widetilde{P}_{\alpha\alpha'}(t) \widetilde{P}_{\alpha'\alpha}(t) \\ & + s^{\text{leads}}_\alpha ,\end{aligned} \tag{B.6}$$

where the coefficients of the linear and quadratic terms are defined by the rates w^{leads}_α from Eq. (3.58) and

$$w^{\text{phonons}}_{\alpha\alpha'} = 2 \sum_\nu \sum_k N_\nu(\Delta_{\alpha\alpha',k}) \left| \bar{X}^\nu_{\alpha\alpha',k} \right|^2 , \tag{B.7}$$

$$q^{\text{phonons}}_{\alpha\alpha'} = \frac{1}{\hbar} \sum_\nu \sum_k D_\nu(\Delta_{\alpha\alpha',k}/\hbar) \left| \bar{X}^\nu_{\alpha\alpha',k} \right|^2 . \tag{B.8}$$

The contribution of the source term $s^{\text{leads}}_\alpha = \mathcal{S}^{\text{leads}}_{\alpha\alpha}$ has already been defined in Eq. (3.59). The off-diagonal matrix dynamics is governed by the differential equa-

published by Shaker Verlag, Aachen, ISBN 3-8322-1979-X

tions

$$\begin{aligned}\dot{\widetilde{P}}_{\alpha\beta}(t) = &-\frac{1}{2}\left(w_\alpha^{\text{leads}} + w_\beta^{\text{leads}}\right)\widetilde{P}_{\alpha\beta}(t) - \bar{w}_{\alpha\beta}^{\text{phonons}}\,\widetilde{P}_{\alpha\beta}(t) \\ &+ \sum_{\alpha'\neq\alpha} q_{\beta\alpha'}^{\text{phonons}}\,\widetilde{P}_{\alpha\beta}(t)\widetilde{P}_{\alpha'\alpha'}(t) + \sum_{\beta'\neq\beta} q_{\alpha\beta'}^{\text{phonons}}\,\widetilde{P}_{\alpha\beta}(t)\widetilde{P}_{\beta'\beta'}(t) \\ &+ \sum_{\alpha'\neq\alpha} q_{\alpha'\beta}^{\text{phonons}}\,\widetilde{P}_{\alpha\alpha'}(t)\widetilde{P}_{\alpha'\beta}(t) + \sum_{\beta'\neq\beta} q_{\beta'\alpha}^{\text{phonons}}\,\widetilde{P}_{\alpha\beta'}(t)\widetilde{P}_{\beta'\beta}(t)\ ,\end{aligned} \tag{B.9}$$

where we have introduced the quantities

$$\begin{aligned}\bar{w}_{\alpha\beta}^{\text{phonons}} = -\sum_\nu \sum_k \Big\{ &2N_\nu(k\hbar\Omega)\bar{X}^\nu_{\alpha\alpha,k}\bar{X}^\nu_{\beta\beta,-k} \\ &- \sum_{\alpha'} N_\nu(\Delta_{\alpha'\alpha,k})|\bar{X}^\nu_{\alpha'\alpha,k}|^2 - \sum_{\beta'} N_\nu(\Delta_{\beta'\beta,k})|\bar{X}^\nu_{\beta'\beta,k}|^2\Big\}\ .\end{aligned} \tag{B.10}$$

Let us now discuss the origin of the different contributions to Eqs. (B.6) and (B.9).

RWA contribution from the source term $\mathcal{S}_{\alpha\beta}^{\text{leads}}(t)$

The condition $\epsilon_\alpha - \epsilon_\beta = 0$ requires $\alpha = \beta$. Equation (3.59) then follows immediately from Eq. (B.2).

RWA contribution from the linear terms $\mathcal{R}_{\alpha\beta\alpha'\beta'}^{\text{leads/phonons}}(t)$

Here, the condition $\epsilon_\alpha - \epsilon_\beta - \epsilon_{\alpha'} + \epsilon_{\beta'} = 0$ requires the distinction between diagonal ($\alpha = \beta$) and off-diagonal ($\alpha \neq \beta$) terms. For $\alpha = \beta$, we can conclude that $\alpha' = \beta'$ has to be fulfilled. Thus, we obtain the first line of Eq. (B.6) together with the rates w_α^{leads} from Eq. (3.58) and $w_{\alpha\alpha'}^{\text{phonons}}$ from Eq. (B.7).

For the off-diagonal matrix elements $P_{\alpha\beta}$, $\alpha \neq \beta$, only terms with $\alpha = \alpha'$ and $\beta = \beta'$ contribute. The corresponding rate coefficients $(w_\alpha^{\text{leads}} + w_\beta^{\text{leads}})/2$ [cf. Eq. (3.58)] and $\bar{w}_{\alpha\beta}^{\text{phonons}}$ from Eq. (B.10) follow immediately from Eqs. (B.3) and (B.4), respectively.

RWA contribution from the quadratic terms $\mathcal{Q}_{\alpha\beta\alpha'\beta'\alpha''\beta''}^{\text{phonons}}(t)$

The RWA condition for the quadratic terms in the second line of Eq. (B.1) requires to distinguish even more cases. Starting with

$$\epsilon_\alpha - \epsilon_\beta - \epsilon_{\alpha'} + \epsilon_{\beta'} - \epsilon_{\alpha''} + \epsilon_{\beta''} = 0\ , \tag{B.11}$$

we again treat the diagonal ($\alpha = \beta$) and the off-diagonal ($\alpha \neq \beta$) terms separately. For $\alpha = \beta$, we again consider two cases, namely:

published by Shaker Verlag, Aachen, ISBN 3-8322-1979-X

I. $\alpha' = \beta'$: From Eq. (B.11), we obtain that only terms with $\alpha'' = \beta''$ contribute to the sum in Eq. (B.1). The corresponding coefficients are:

$$\mathcal{Q}^{\text{phonons}}_{\alpha\alpha\alpha'\alpha'\alpha''\alpha''}\,\delta_{\alpha'\beta'}\,\delta_{\alpha''\beta''}\ . \tag{B.12}$$

II. $\alpha' \neq \beta'$: Non-vanishing contributions to Eq. (B.1) require $\alpha' = \beta''$ and $\alpha'' = \beta'$:

$$\mathcal{Q}^{\text{phonons}}_{\alpha\alpha\alpha'\beta'\beta'\alpha'}\ (1-\delta_{\alpha'\beta'})\,\delta_{\alpha'\beta''}\,\delta_{\alpha''\beta'}\ . \tag{B.13}$$

Altogether, we obtain the contribution

$$\sum_{\alpha'\alpha''} \mathcal{Q}^{\text{phonons}}_{\alpha\alpha\alpha'\alpha'\alpha''\alpha''}\,\widetilde{P}_{\alpha'\alpha'}(t)\widetilde{P}_{\alpha''\alpha''}(t) + \sum_{\beta'}\sum_{\alpha'\neq\beta'} \mathcal{Q}^{\text{phonons}}_{\alpha\alpha\alpha'\beta'\beta'\alpha'}\,\widetilde{P}_{\alpha'\beta'}(t)\widetilde{P}_{\beta'\alpha'}(t)\ . \tag{B.14}$$

Making use of the relations

$$\mathcal{Q}^{\text{phonons}}_{\alpha\alpha\alpha'\alpha'\alpha''\alpha''} = 2q^{\text{phonons}}_{\alpha\alpha''}\delta_{\alpha\alpha'}\ , \tag{B.15}$$

$$\mathcal{Q}^{\text{phonons}}_{\alpha\alpha\alpha'\beta'\beta'\alpha'} = q^{\text{phonons}}_{\beta'\alpha}\delta_{\alpha\alpha'} - q^{\text{phonons}}_{\alpha\alpha'}\delta_{\alpha\beta'}\ , \tag{B.16}$$

which follow directly from Eqs. (3.12), (3.13), (B.5) and (B.8), we arrive at the second line of Eq. (B.6).

For the off-diagonal ($\alpha \neq \beta$) elements, we have to distinguish between the following cases:

I. $\alpha = \alpha'$: The condition (B.11) then assumes the form

$$\epsilon_{\beta'} - \epsilon_{\beta} + \epsilon_{\beta''} - \epsilon_{\alpha''} = 0 \tag{B.17}$$

and we have to treat the following subcases separately:

A. $\beta = \beta'$: Then necessarily $\alpha'' = \beta''$, and hence the only contributions are

$$\mathcal{Q}^{\text{phonons}}_{\alpha\beta\alpha\beta\alpha''\alpha''}\,\delta_{\alpha\alpha'}\,\delta_{\beta\beta'}\,\delta_{\alpha''\beta''}\ . \tag{B.18}$$

B. $\beta \neq \beta'$: This case requires $\alpha'' = \beta'$ and $\beta = \beta''$, yielding

$$\mathcal{Q}^{\text{phonons}}_{\alpha\beta\alpha\beta'\beta'\beta}\,\delta_{\alpha\alpha'}\,(1-\delta_{\beta\beta'})\,\delta_{\alpha''\beta'}\,\delta_{\beta\beta''}\ . \tag{B.19}$$

II. $\alpha \neq \alpha'$: This immediately leads to $\alpha = \alpha''$ (remember that we are considering the off-diagonal case $\alpha \neq \beta$) and hence Eq. (B.11) reduces to

$$\epsilon_{\beta'} - \epsilon_{\beta} + \epsilon_{\beta''} - \epsilon_{\alpha'} = 0\ . \tag{B.20}$$

We now have to distinguish between two cases:

published by Shaker Verlag, Aachen, ISBN 3-8322-1979-X

A. $\beta = \beta'$: Then we find $\alpha' = \beta''$ and hence contributions of the form

$$\mathcal{Q}^{\text{phonons}}_{\alpha\beta\alpha'\beta\alpha\alpha'} \, (1 - \delta_{\alpha\alpha'}) \, \delta_{\alpha\alpha''} \, \delta_{\beta\beta'} \, \delta_{\alpha'\beta''} \ . \tag{B.21}$$

B. $\beta \neq \beta'$: This case leads to $\alpha' = \beta'$ and $\beta = \beta''$ and thus contributes with terms

$$\mathcal{Q}^{\text{phonons}}_{\alpha\beta\alpha'\alpha'\alpha\beta} \, (1 - \delta_{\alpha\alpha'}) \, \delta_{\alpha\alpha''} \, (1 - \delta_{\beta\beta'}) \, \delta_{\alpha'\beta'} \, \delta_{\beta\beta''} \ . \tag{B.22}$$

Gathering all terms, we arrive at

$$\begin{aligned} &\sum_{\alpha''} \mathcal{Q}^{\text{phonons}}_{\alpha\beta\alpha\beta\alpha''\alpha''} \widetilde{P}_{\alpha\beta}(t) \widetilde{P}_{\alpha''\alpha''}(t) + \sum_{\beta' \neq \beta} \mathcal{Q}^{\text{phonons}}_{\alpha\beta\alpha\beta'\beta'\beta} \widetilde{P}_{\alpha\beta'}(t) \widetilde{P}_{\beta'\beta}(t) \\ &+ \sum_{\alpha' \neq \alpha} \mathcal{Q}^{\text{phonons}}_{\alpha\beta\alpha'\beta\alpha\alpha'} \widetilde{P}_{\alpha'\beta}(t) \widetilde{P}_{\alpha\alpha'}(t) + \sum_{\alpha' \neq \alpha, \beta} \mathcal{Q}^{\text{phonons}}_{\alpha\beta\alpha'\alpha'\alpha\beta} \widetilde{P}_{\alpha'\alpha'}(t) \widetilde{P}_{\alpha\beta}(t) \end{aligned} \ , \tag{B.23}$$

which in conjunction with

$$\mathcal{Q}^{\text{phonons}}_{\alpha\beta\alpha\beta\alpha''\alpha''} = (1 - \delta_{\alpha\alpha''}) \, q^{\text{phonons}}_{\beta\alpha''} + (1 - \delta_{\beta\alpha''}) \, q^{\text{phonons}}_{\alpha\alpha''} \ , \tag{B.24}$$

$$\mathcal{Q}^{\text{phonons}}_{\alpha\beta\alpha\beta'\beta'\beta} = (1 - \delta_{\alpha\beta} - \delta_{\beta\beta'}) \, q^{\text{phonons}}_{\beta'\alpha} \ , \tag{B.25}$$

$$\mathcal{Q}^{\text{phonons}}_{\alpha\beta\alpha'\beta\alpha\alpha'} = (1 - \delta_{\alpha\alpha'}) \, q^{\text{phonons}}_{\alpha'\beta} \ , \tag{B.26}$$

$$\mathcal{Q}^{\text{phonons}}_{\alpha\beta\alpha'\alpha'\alpha\beta} = 0 \tag{B.27}$$

yields the second and third line of Eq. (B.9).

Having the RWA kinetic equation (B.6) and (B.9) at hand, let us for completeness discuss a case, where the coupling to the leads is not present [cf. discussion after Eq. (3.50)]. Then, of course, the number of electrons on the wire is fixed. If we consider, for instance, the one-electron case, the mean-field approximation (3.43) fails completely, since all two-particle expectation values at equal times are zero. Yet the correct dynamics can directly be read from Eqs. (B.6) and (B.9) by omitting all terms that are quadratic in $\widetilde{P}_{\alpha\beta}(t)$. Since in the subspace of a single electron $P_{\alpha\beta}$ reduces to the density matrix in the basis of the Floquet states, we arrive at the master equation which has been used to describe dissipative driven quantum systems in Refs. [26, 96–102]. In rotating wave approximation, like for the case with coupling to the leads only (see Sect. 3.3), diagonal and off-diagonal dynamics then decouple and the off-diagonal elements converge to zero in the long-time limit. Thus, the stationary solution is of the diagonal form $P_{\alpha\beta} = P_\alpha \delta_{\alpha\beta}$. The only difference to the previous case of a pure coupling to electronic leads is that this time the populations $P_{\alpha\alpha}(t)$ are not only determined by Eq. (B.6) but also by the normalisation condition $\sum_\alpha P_{\alpha\alpha}(t) = 1$. Finally, in equilibrium, the detailed-balance relation

$$\frac{w^{\text{phonons}}_{\alpha\alpha'}}{w^{\text{phonons}}_{\alpha'\alpha}} = \mathrm{e}^{(\epsilon_{\alpha'} - \epsilon_\alpha)/k_\mathrm{B}T} \tag{B.28}$$

published by Shaker Verlag, Aachen, ISBN 3-8322-1979-X

holds, which corresponds to the canonical distribution $P_\alpha = \exp(-\epsilon_\alpha/k_\mathrm{B}T)/Z$ with the partition function $Z = \sum_\alpha \exp(-\epsilon_\alpha/k_\mathrm{B}T)$.

published by Shaker Verlag, Aachen, ISBN 3-8322-1979-X

C Equilibrium solution of the kinetic equation

An important consistency check for the present theory is that in thermal equilibrium, i.e., for a time-independent Hamiltonian ($H(t) =: H_0$) and in the absence of an external bias ($\mu_\ell = \text{const.} =: \mu$), the current through the different molecule-lead contacts has to vanish; otherwise the second-law of thermodynamics would be violated. The discussion in Sect. 5.3.1 shows that a sufficient condition for a zero current is that the equilibrium solution of the kinetic equation Eq. (3.30) is given by the Fermi distribution (3.62). In this appendix, we show that this is indeed the case. To this end, we insert the solution (3.62) as an ansatz into Eq. (3.30), yielding

$$\sum_{\alpha'} \left[\mathcal{R}^{\text{leads}}_{\alpha\beta\alpha'\alpha'} + \mathcal{R}^{\text{phonons}}_{\alpha\beta\alpha'\alpha'}\right] f(\epsilon_{\alpha'}) + \sum_{\alpha'\alpha''} \mathcal{Q}^{\text{phonons}}_{\alpha\beta\alpha'\alpha'\alpha''\alpha''} f(\epsilon_{\alpha'})\, f(\epsilon_{\alpha''}) + \mathcal{S}^{\text{leads}}_{\alpha\beta} = 0\ . \quad \text{(C.1)}$$

Note that we have set, without loss of generality, the common chemical potential μ to zero. Let us now treat separately the contributions stemming from the coupling to the leads and to the phonons, respectively. Concerning the lead's contribution, we note that for arbitrary α and β the identity

$$\sum_{\alpha'} \mathcal{R}^{\text{leads}}_{\alpha\beta\alpha'\alpha'} f(E_{\alpha'}) + \mathcal{S}^{\text{leads}}_{\alpha\beta} = 0 \quad \text{(C.2)}$$

holds true. This can readily inferred from the equilibrium form

$$\mathcal{R}^{\text{leads}}_{\alpha\beta\alpha'\alpha'} = -\frac{1}{2}\sum_{\ell=1}^{L} \Gamma_\ell(E_{\alpha'}) \langle\Phi_\alpha|\ell\rangle\langle\ell|\Phi_\beta\rangle\, (\delta_{\beta\alpha'} + \delta_{\alpha\alpha'}) \quad \text{(C.3)}$$

of the Redfield tensor (3.34) and the source term (3.35), which reads

$$\mathcal{S}^{\text{leads}}_{\alpha\beta} = \frac{1}{2}\sum_{\ell=1}^{L} \langle\Phi_\alpha|\ell\rangle\langle\ell|\Phi_\beta\rangle \big\{\Gamma_\ell(E_\alpha) f(E_\alpha) + \Gamma_\ell(E_\beta) f(E_\beta)\big\}\ . \quad \text{(C.4)}$$

published by Shaker Verlag, Aachen, ISBN 3-8322-1979-X

Here, $|\Phi_\alpha\rangle$ and E_α are the eigenstates and the eigenenergies, respectively, of H_0. The proof of Eq. (C.1) is completed by demonstrating that the phononic contributions to the left-hand side of Eq. (C.1) vanish for arbitrary α and β, i.e.,

$$\sum_{\alpha'} \mathcal{R}^{\text{phonons}}_{\alpha\beta\alpha'\alpha'} f(E_{\alpha'}) + \sum_{\alpha'\alpha''} \mathcal{Q}^{\text{phonons}}_{\alpha\beta\alpha'\alpha'\alpha''\alpha''} f(E_{\alpha'})\, f(E_{\alpha''}) = 0 \ . \tag{C.5}$$

Therefore, we write the Redfield tensor for the equilibrium case as [cf. Eq. (3.47)]

$$\begin{aligned} \mathcal{R}^{\text{phonons}}_{\alpha\beta\alpha'\alpha'} = \sum_\nu \Big\{ & [N_\nu(E_\alpha - E_{\alpha'}) + N_\nu(E_\beta - E_{\alpha'})]\, \bar{X}^\nu_{\alpha\alpha'} \bar{X}^\nu_{\alpha'\beta} \\ & -(\delta_{\alpha\alpha'} + \delta_{\beta\alpha'}) \sum_{\alpha''} N_\nu(E_{\alpha''} - E_{\alpha'}) \bar{X}^\nu_{\alpha\alpha''} \bar{X}^\nu_{\alpha''\beta} \Big\} \ , \end{aligned} \tag{C.6}$$

with the matrix elements

$$\bar{X}^\nu_{\alpha\beta} := \sum_{n,n'} \langle \Phi_\alpha | n \rangle X_{nn'\nu} \langle n' | \Phi_\beta \rangle \ . \tag{C.7}$$

The coefficient tensor (3.50) of the quadratic terms now reads

$$\mathcal{Q}^{\text{phonons}}_{\alpha\beta\alpha'\alpha'\alpha''\alpha''} = \frac{1}{\hbar}(\delta_{\alpha\alpha'} + \delta_{\beta\alpha'}) \sum_\nu D_\nu((E_{\alpha'} - E_{\alpha''})/\hbar) \bar{X}^\nu_{\alpha\alpha''}\, \bar{X}^\nu_{\alpha''\beta} \ . \tag{C.8}$$

Upon insertion of Eqs. (C.6) and (C.8) into Eq. (C.5), we obtain

$$\begin{aligned} & \sum_{\alpha'} \mathcal{R}^{\text{phonons}}_{\alpha\beta\alpha'\alpha'} f(E_{\alpha'}) + \sum_{\alpha'\alpha''} \mathcal{Q}^{\text{phonons}}_{\alpha\beta\alpha'\alpha'\alpha''\alpha''} f(E_{\alpha'}) f(E_{\alpha''}) = \frac{1}{\hbar} \sum_\nu \sum_{\alpha'} \bar{X}^\nu_{\alpha\alpha'} \bar{X}^\nu_{\alpha'\beta} \\ & \times \Big\{ D_\nu(E_\alpha - E_{\alpha'}) \big[n_{\mathrm{B}}(E_\alpha - E_{\alpha'}) f(E_{\alpha'}) + n_{\mathrm{B}}(E'_\alpha - E_\alpha) f(E_\alpha) + f(E_\alpha) f(E_{\alpha'}) \big] \\ & \quad + D_\nu(E_\beta - E_{\alpha'}) \big[n_{\mathrm{B}}(E_\beta - E_{\alpha'}) f(E_{\alpha'}) + n_{\mathrm{B}}(E'_\alpha - E_\beta) f(E_\beta) + f(E_\beta) f(E_{\alpha'}) \big] \Big\} \ . \end{aligned} \tag{C.9}$$

Using the remarkable identity between Bose and Fermi functions,

$$n_{\mathrm{B}}(E - E') f(E') + n_{\mathrm{B}}(E' - E) f(E) + f(E) f(E') = 0 \ , \tag{C.10}$$

which can directly be verified by insertion of the definitions of $n_{\mathrm{B}}(E)$ and $f(E)$, we can conclude that the right-hand side of Eq. (C.9) vanishes, thereby establishing the validity of Eq. (C.5) and therefore that of the condition (C.1) for the validity of the Fermi distribution as equilibrium solution.

published by Shaker Verlag, Aachen, ISBN 3-8322-1979-X

References

[1] G. E. Moore, *Cramming More Components Onto Integrated Circuits*, Electronics **38**, 114 (1965).

[2] See the current International Technology Roadmap for Semiconductors, available online from `http://public.itrs.net/`.

[3] R. Feynman, *There is Plenty of Room at the Bottom*, lecture given at the APS meeting 1959. For a transcript, see `http://www.its.caltech.edu/~feynman/plenty.html`.

[4] G. Binnig and H. Rohrer, *Scanning Tunneling Microscopy*, Physica B & C **127**, 37 (1984).

[5] D. M. Eigler and E. K. Schweizer, *Positioning single atoms with a scanning tunnelling microscope*, Nature **344**, 524 (1990).

[6] A. Aviram and M. A. Ratner, *Molecular Rectifiers*, Chem. Phys. Lett. **29**, 277 (1974).

[7] Special Issue: *Processes in Molecular Wires*, edited by P. Hänggi, M. Ratner, and S. Yaliraki, Chem. Phys. **281**, pages 111–502 (2002).

[8] J. C. Ellenbogen and J. C. Love, *Architectures for Molecular Electronic Computers*, Proc. IEEE **88**, 386 (2000).

[9] A. Nitzan, *Electron transmission through molecules and molecular interfaces*, Annu. Rev. Phys. Chem. **52**, 681 (2001).

[10] M. Dorogi, J. Gomez, R. Osifchin, R. P. Andres, and R. Reifenberger, *Room-temperature Coulomb blockade from a self-assembled molecular nanostructure*, Phys. Rev. B **52**, 9071 (1995).

[11] S. Datta, W. Tian, S. Hong, R. Reifenberger, J. I. Henderson, and C. P. Kubiak, *Current-Voltage Characteristics of Self-Assembled Monolayers by Scanning Tunneling Microscopy*, Phys. Rev. Lett **79**, 2530 (1997).

published by Shaker Verlag, Aachen, ISBN 3-8322-1979-X

[12] M. A. Reed, C. Zhou, C. J. Muller, T. P. Burgin, and J. M. Tour, *Conductance of a Molecular Junction*, Science **278**, 252 (1997).

[13] C. J. Muller, J. M. van Ruitenbeek, and L. J. de Jongh, *Conductance and supercurrent discontinuities in atomic scale metallic constrictions of variable width*, Phys. Rev. Lett. **69**, 140 (1992).

[14] J. M. Krans, J. M. van Ruitenbeek, V. V. Fisun, I. K. Janson, and L. J. de Jongh, *The signature of conductance quantization in metallic point contacts*, Nature **375**, 767 (1995).

[15] E. Scheer, P. Joyez, D. Esteve, C. Urbina, and M. H. Devoret, *Conduction Channel Transmissions of Atomic-Size Aluminum Contacts*, Phys. Rev. Lett. **78**, 3535 (1997).

[16] C. Zhou, M. R. Deshpande, M. A. Reed, L. Jones II, and J. M. Tour, *Nanoscale metal/self-assembled monolayer/metal heterostructures*, Appl. Phys. Lett. **71**, 611 (1997).

[17] H. B. Weber, J. Reichert, F. Weigend, R. Ochs, D. Beckmann, M. Mayor, R. Ahlrichs, and H. von Löhneysen, *Electronic transport through single conjugated molecules*, Chem. Phys. **281**, 113 (2002).

[18] J. Reichert, R. Ochs, D. Beckmann, H. B. Weber, M. Mayor, and H. von Löhneysen, *Driving current through single organic molecules*, Phys. Rev. Lett. **88**, 176804 (2002).

[19] X. D. Cui, A. Primak, X. Zarate, J. Tomfohr, O. F. Sankey, A. L. Moore, T. A. Moore, D. Gust, G. Harris, and S. M. Lindsay, *Reproducible Measurement of Single-Molecule Conductivity*, Science **294**, 571 (2001).

[20] A. Zrenner, E. Beham, S. Stufler, F. Findeis, M. Bichler, and G. Abstreiter, *Coherent properties of a two-level system based on a quantum-dot photodiode*, Nature **418**, 612 (2002).

[21] F. Grossmann, T. Dittrich, P. Jung, and P. Hänggi, *Coherent Destruction of Tunneling*, Phys. Rev. Lett. **67**, 516 (1991).

[22] F. Grossmann, P. Jung, T. Dittrich, and P. Hänggi, *Tunneling in a periodically driven bistable system*, Z. Phys. B **84**, 315 (1991).

[23] F. Großmann and P. Hänggi, *Localization in a Driven Two-Level Dynamics*, Europhys. Lett. **18**, 571 (1992).

[24] M. Morillo and R. I. Cukier, *Control of proton-transfer reactions with external fields*, J. Chem. Phys. **98**, 4548 (1993).

published by Shaker Verlag, Aachen, ISBN 3-8322-1979-X

[25] I. A. Goychuk, E. G. Petrov, and V. May, *Control of the dynamics of a dissipative two-level system by a strong periodic field*, Chem. Phys. Lett. **253**, 428 (1996).

[26] M. Grifoni and P. Hänggi, *Driven Quantum Tunneling*, Phys. Rep. **304**, 229 (1998).

[27] P. Hänggi and R. Bartussek, *Brownian Rectifiers: How to Convert Brownian Motion into Directed Transport*, in *Nonlinear Physics of Complex Systems—Current Status and Future Trends*, edited by J. Parisi, S. C. Müller, and W. W. Zimmermann (Springer, Berlin, 1996), Vol. 476 of Lecture Notes in Physics, pages 294–308.

[28] R. D. Astumian, *Thermodynamics and Kinetics of a Brownian Motor*, Science **276**, 917 (1997).

[29] F. Jülicher, A. Adjari, and J. Prost, *Modeling Molecular Motors*, Rev. Mod. Phys. **69**, 1269 (1997).

[30] P. Reimann and P. Hänggi, *Introduction to the physics of Brownian motors*, Appl. Phys. A **75**, 169 (2002).

[31] P. Reimann, *Brownian Motors: Noisy Transport far from Equilibrium*, Phys. Rep. **361**, 57 (2002).

[32] R. D. Astumian and P. Hänggi, *Brownian Motors*, Physics Today **55**(11), 33 (2002).

[33] P. Reimann, M. Grifoni, and P. Hänggi, *Quantum Ratchets*, Phys. Rev. Lett. **79**, 10 (1997).

[34] I. Goychuk, M. Grifoni, and P. Hänggi, *Nonadiabatic Quantum Brownian Rectifiers*, Phys. Rev. Lett. **81**, 649 (1998), erratum: ibid. **81**, 2837 (1998).

[35] I. Goychuk and P. Hänggi, *Quantum rectifiers from harmonic mixing*, Europhys. Lett. **43**, 503 (1998).

[36] I. Goychuk and P. Hänggi, *Minimal Quantum Brownian Rectifiers*, J. Phys. Chem. B **105**, 6642 (2001).

[37] H. Linke, T. E. Humphrey, A. Löfgren, A. O. Shuskov, R. Newbury, R. P. Taylor, and P. Omling, *Experimental tunneling ratchets*, Science **286**, 2314 (1999).

[38] I. Goychuk and P. Hänggi, *Directed Current Without Dissipation: Reincarnation of a Maxwell-Loschmidt Demon*, in *Stochastic Processes in Physics, Chemistry, and Biology*, edited by J. Freund and T. Pöschel (Springer, Berlin, 2000), Vol. 557 of Lecture Notes in Physics, pages 7–20.

published by Shaker Verlag, Aachen, ISBN 3-8322-1979-X

[39] T. Dittrich, R. Ketzmerick, M.-F. Otto, and H. Schanz, *Classical and quantum transport in deterministic Hamiltonian ratchets*, Ann. Phys. (Berlin) **9**, 755 (2000).

[40] H. Schanz, M.-F. Otto, R. Ketzmerick, and T. Dittrich, *Classical and Quantum Hamiltonian Ratchets*, Phys. Rev. Lett. **87**, 070601 (2001).

[41] D. J. Thouless, *Quantization of particle transport*, Phys. Rev. B **27**, 6083 (1983).

[42] P. W. Brouwer, *Scattering approach to parametric pumping*, Phys. Rev. B **58**, 10135 (1998).

[43] B. L. Altshuler and L. I. Glazman, *Pumping Electrons*, Science **283**, 1864 (1999).

[44] M. Switkes, C. M. Marcus, K. Campman, and A. C. Gossard, *An Adiabatic Quantum Electron Pump*, Science **283**, 1905 (1999).

[45] R. Landauer, *Spatial Variation of Currents and Fields Due to Localized Scatterers in Metallic Conduction*, IBM J. Res. Dev. **1**, 223 (1957).

[46] Y. Imry and R. Landauer, *Conductance viewed as transmission*, Rev. Mod. Phys. **71**, S306 (1999).

[47] S. Datta, *Electronic Transport in Mesoscopic Systems* (Cambridge University Press, Cambridge, 1995).

[48] H. U. Baranger and A. D. Stone, *Electrical linear-response theory in an arbitrary magnetic field: A new Fermi-surface formation*, Phys. Rev. B **40**, 8169 (1989).

[49] S. Datta and M. P. Anantram, *Steady-state transport in mesoscopic systems illuminated by alternating fields*, Phys. Rev. B **45**, 13761 (1992).

[50] A.-P. Jauho, N. S. Wingreen, and Y. Meir, *Time-dependent transport in interacting and noninteracting resonant-tunneling systems*, Phys. Rev. B **50**, 5528 (1994).

[51] H. Haug and A.-P. Jauho, *Quantum kinetics in transport and optics of semiconductors*, Vol. 123 of Springer series in solid-state sciences (Springer, Berlin, 1996).

[52] A. Tikhonov, R. D. Coalson, and Y. Dahnovsky, *Calculating electron current in a tight-binding model of a field-driven molecular wire: Floquet theory approach*, J. Chem. Phys. **116**, 10909 (2002).

[53] A. Tikhonov, R. D. Coalson, and Y. Dahnovsky, *Calculating electron current in a tight-binding model of a field-driven molecular wire: Application to xylyl-dithiol*, J. Chem. Phys. **117**, 567 (2002).

published by Shaker Verlag, Aachen, ISBN 3-8322-1979-X

[54] A. Keller, O. Atabek, M. Ratner, and V. Mujica, *Laser-assisted conductance of molecular wires*, J. Phys. B **35**, 4981 (2002).

[55] C. Bruder and H. Schoeller, *Charging Effects in Ultrasmall Quantum Dots in the Presence of Time-Varying Fields*, Phys. Rev. Lett. **72**, 1076 (1994).

[56] P. Brune, C. Bruder, and H. Schoeller, *Photon-assisted transport through ultrasmall quantum dots: Influence of intradot transitions*, Phys. Rev. B **56**, 4730 (1997).

[57] C. Cohen-Tannoudji, J. Dupont-Roc, and G. Grynberg, *Atom-Photon Interaction: Basic Processes and Applications* (John Wiley & Sons, New York, 1992).

[58] N. W. Ashcroft and N. D. Mermin, *Solid State Physics* (Saunders College, Philadelphia, 1976).

[59] H. Sambe, *Steady States and Quasienergies of a Quantum-Mechanical System in an Oscillating Field*, Phys. Rev. A **7**, 2203 (1973).

[60] H. Risken, *The Fokker-Planck Equation*, Vol. 18 of Springer Series in Synergetics (Springer, Berlin, 1989), 2nd ed.

[61] I. M. Gradshteyn and I. S. Ryzhik, *Table of Integrals, Series, and Products* (Academic Press, San Diego, 1994), 5th ed.

[62] G. Yao and S.-I. Chu, *Complex-scaling Fourier-grid Hamiltonian method. III. Oscillatory behavior of complex quasienergies and the stability of negative ions in very intense laser fields*, Phys. Rev. A **45**, 6735 (1992).

[63] A. Peres, *Dynamical quasidegeneracies and quantum tunneling*, Phys. Rev. Lett. **67**, 158 (1991).

[64] M. Holthaus, *The quantum theoy of an ideal superlattice responding to far-infrared laser radiation*, Z. Phys. B **89**, 251 (1992).

[65] J. H. Shirley, *Solution of the Schrödinger Equation with a Hamiltonian Periodic in Time*, Phys. Rev. **138**, B979 (1965).

[66] Y. Kayanuma, *Role of phase coherence in the transition dynamics of a periodically driven two-level system*, Phys. Rev. A **50**, 843 (1994).

[67] J. von Neumann and E. Wigner, *Über merkwürdige diskrete Eigenwerte*, Physik. Z. **30**, 467 (1929).

[68] H. Wang and X.-G. Zhao, *Dynamics of two-level systems driven by dc-ac fields*, Phys. Lett. A **217**, 225 (1996).

published by Shaker Verlag, Aachen, ISBN 3-8322-1979-X

[69] V. Mujica, M. Kemp, and M. A. Ratner, *Electron conduction in molecular wires. I. A scattering formalism*, J. Chem. Phys. **101**, 6849 (1994).

[70] V. Mujica, M. Kemp, and M. A. Ratner, *Electron conduction in molecular wires. II. Application to scanning tunneling microscopy*, J. Chem. Phys. **101**, 6856 (1994).

[71] E. G. Petrov and P. Hänggi, *Nonlinear Electron Current through a Short Molecular Wire*, Phys. Rev. Lett. **86**, 2862 (2001).

[72] E. G. Petrov, V. May, and P. Hänggi, *Controlling electron transfer processes through short molecular wires*, Chem. Phys. **281**, 211 (2002).

[73] J. Lehmann, G.-L. Ingold, and P. Hänggi, *Incoherent charge transport through molecular wires: interplay of Coulomb interaction and wire population*, Chem. Phys. **281**, 199 (2002).

[74] J. Bonča and S. A. Trugman, *Effect of Inelastic Processes on Tunneling*, Phys. Rev. Lett. **75**, 2566 (1995).

[75] H. Ness and A. J. Fisher, *Quantum inelastic conductance through molecular wires*, Phys. Rev. Lett. **83**, 452 (1999).

[76] E. G. Emberly and G. Kirczenow, *Landauer theory, inelastic scattering, and electron transport in molecular wires*, Phys. Rev. B **61**, 5740 (2000).

[77] V. May, *Electron transfer through a molecular wire: Consideration of electron-vibrational coupling within the Liouville space pathway technique*, Phys. Rev. B **66**, 245411 (2002).

[78] D. Segal, A. Nitzan, W. B. Davis, M. R. Wasielewski, and M. A. Ratner, *Electron Transfer Rates in Bridged Molecular Systems 2: A Steady-State Analysis of Coherent Tunneling and Thermal Relaxation*, J. Phys. Chem. **104**, 3817 (2000).

[79] D. Segal and A. Nitzan, *Steady state quantum mechanics of thermally relaxing systems*, Chem. Phys. **268**, 315 (2001).

[80] C. Kittel, *Introduction to Solid State Physics* (John Wiley & Sons, New York, 1996), 7th ed.

[81] F. Demming, J. Jersch, K. Dickmann, and P. I. Geshev, *Calculation of the field enhancement on laser-illuminated scanning probe tips by the boundary element method*, Appl. Phys. B **66**, 593 (1998).

[82] M. Fleischmann, P. J. Hendra, and A. J. McQuillan, *Raman spectra of pyridine adsorbed at a silver electrode*, Chem. Phys. Lett. **26**, 163 (1974).

published by Shaker Verlag, Aachen, ISBN 3-8322-1979-X

[83] D. L. Jeanmaire and R. P. V. Duyne, *Surface Raman spectroelectrochemistry Part I. Heterocyclic, aromatic, and aliphatic amines adsorbed on the anodized silver electrode*, J. Electroanal. Chem. **84**, 1 (1977).

[84] D. M. Newns, *Self-Consistent Model of Hydrogen Chemisorption*, Phys. Rev. **178**, 1123 (1969).

[85] S. N. Yaliraki and M. A. Ratner, *Molecule-interface coupling effects on electronic transport in molecular wires*, J. Chem. Phys. **109**, 5036 (1998).

[86] G. D. Mahan, *Many-Particle Physics* (Plenum Press, New York, 1990), 2nd ed.

[87] T. Holstein, *Polaron motion. I. Molecular-crystal model*, Ann. Phys. (N.Y.) **8**, 325 (1959).

[88] S. Nakajima, *On Quantum Theory of Transport Phenomena*, Prog. Theor. Phys. **20**, 948 (1958).

[89] R. Zwanzig, *Ensemble methods in the theory of irreversibility*, J. Chem. Phys. **33**, 1338 (1960).

[90] J. Lehmann, S. Kohler, P. Hänggi, and A. Nitzan, *Molecular Wires Acting as Coherent Quantum Ratchets*, Phys. Rev. Lett. **88**, 228305 (2002).

[91] J. Lehmann, S. Kohler, P. Hänggi, and A. Nitzan, *Rectification of laser-induced electronic transport through molecules*, J. Chem. Phys. **118**, 3283 (2003).

[92] E. Fick, *Einführung in die Grundlagen der Quantentheorie* (Aula-Verlag, Wiesbaden, 1988).

[93] P. Hänggi, *Driven Quantum Systems*, in *Quantum Transport and Dissipation* (Wiley-VCH, Weinheim, 1998), Chap. 5, pages 249–286.

[94] V. May, *A New Switching Mechanism for the Charge Transfer Through a Molecular Chain*, J. Mol. Electron. **6**, 187 (1990).

[95] V. May, *Excess electron motion in a molecular chaing and nonlinear rate equations*, Phys. Lett. A **161**, 118 (1991).

[96] R. Blümel, A. Buchleitner, R. Graham, L. Sirko, U. Smilansky, and H. Walter, *Dynamical localisation in the microwave interaction of Rydberg atoms: The influence of noise*, Phys. Rev. A **44**, 4521 (1991).

[97] T. Dittrich, B. Oelschlägel, and P. Hänggi, *Driven Dissipative Tunneling*, Europhys. Lett. **22**, 5 (1993).

[98] B. Oelschlägel, T. Dittrich, and P. Hänggi, *Damped Periodically Driven Quantum Transport in Bistable Systems*, Acta Physica Polonica B **24**, 845 (1993).

published by Shaker Verlag, Aachen, ISBN 3-8322-1979-X

[99] S. Kohler, T. Dittrich, and P. Hänggi, *Floquet-Markovian description of the parametrically driven, dissipative harmonic quantum oscillator*, Phys. Rev. E **55**, 300 (1997).

[100] S. Kohler, R. Utermann, P. Hänggi, and T. Dittrich, *Coherent and incoherent chaotic tunneling near singlet-doublet crossings*, Phys. Rev. E **58**, 7219 (1998).

[101] P. Hänggi, S. Kohler, and T. Dittrich, *Driven Tunneling: Chaos and Decoherence*, in *Statistical and Dynamical Aspects of Mesoscopic Systems*, edited by D. Reguera, G. Platero, L. L. Bonilla, and J. M. Rubí (Springer, Berlin, 2000), Vol. 547 of Lecture Notes in Physics, pages 125–157.

[102] S. Kohler and P. Hänggi, *Decoherence in resonantly driven bistable systems*, in *Quantum Information Processing* (Wiley-VCH, Weinheim, 2003), Chap. 12, pages 145–156.

[103] C. A. Stafford and N. S. Wingreen, *Resonant Photon-Assisted Tunneling through a Double Quantum Dot: An Electron Pump from Spatial Rabi Oscillations*, Phys. Rev. Lett. **76**, 1916 (1996).

[104] J. Lehmann, S. Camalet, S. Kohler, and P. Hänggi, *Laser controlled molecular switches and transistors*, Chem. Phys. Lett. **368**, 282 (2003).

[105] M. Di Ventra, S. T. Pantelides, and N. D. Lang, *First Principles Calculation of Transport Properties of a Molecular Device*, Phys. Rev. Lett. **84**, 979 (2000).

[106] M. Di Ventra and N. D. Lang, *Transport in nanoscale conductors from first principles*, Phys. Rev. B **65**, 045402 (2002).

[107] Y. Xue, S. Datta, and M. A. Ratner, *First-principles based matrix Green's function approach to molecular electronic devices: general formalism*, Chem. Phys. **281**, 151 (2002).

[108] P. Damle, A. W. Ghosh, and S. Datta, *First-principles analysis of molecular conduction using quantum chemistry software*, Chem. Phys. **281**, 171 (2002).

[109] J. Heurich, J. C. Cuevas, W. Wenzel, and G. Schön, *Electrical Transport through Single-Molecule Junctions: From Molecular Orbitals to Conduction Channels*, Phys. Rev. Lett. **88**, 256803 (2002).

[110] V. Mujica, A. E. Roitberg, and M. Ratner, *Molecular wire conductance: Electrostatic potential spatial profile*, J. Chem. Phys. **112**, 6834 (2000).

[111] S. Pleutin, H. Grabert, G.-L. Ingold, and A. Nitzan, *The electrostatic potential profile along a biased molecular wire: A model quantum-mechanical calculation*, J. Chem. Phys. **118**, 3756 (2003).

published by Shaker Verlag, Aachen, ISBN 3-8322-1979-X

[112] A. Nitzan, M. Galperin, G.-L. Ingold, and H. Grabert, *On the electrostatic potential profile in biased molecular wires*, J. Chem. Phys. **117**, 10837 (2002).

[113] W. Tian, S. Datta, S. Hong, R. Reifenberger, J. I. Henderson, and C. P. Kubiak, *Conductance spectra of molecular wires*, J. Chem. Phys. **109**, 2874 (1998).

[114] J. Chen, M. A. Reed, A. M. Rawlett, and J. M. Tour, *Large On-Off Ratios and Negative Differential Resistance in a Molecular Electronic Device*, Science **286**, 1550 (1999).

[115] M. A. Ratner, *Bridge-Assisted Electron Transfer: Effective Electronic Coupling*, J. Phys. Chem. **94**, 4877 (1990).

[116] S. Flach, O. Yevtushenko, and Y. Zolotaryuk, *Directed Current due to Broken Time-Space Symmetry*, Phys. Rev. Lett. **84**, 2358 (2000).

[117] P. Reimann, *Supersymmetric Ratchets*, Phys. Rev. Lett. **86**, 4992 (2001).

[118] P. Curie, *Sur la symétrie dans les phénomenes physiques, symétrie d'un champ électrique et d'un champ magnétique*, J. Phys. (Paris) 3. Série (théorique et appliqué) **3**, 393 (1894).

[119] F. Bloch and A. Siegert, *Magnetic Resonance for Nonrotating Fields*, Phys. Rev. **57**, 522 (1940).

[120] P. Aravind and J. Hirschfelder, *Two-state systems in semiclassical and quantized fields*, J. Phys. Chem. **88**, 4788 (1984).

[121] Note that in all figures and captions of Ref. [90], the driving amplitude A should read $A/2$.

[122] M. von Smoluchowski, *Experimentell nachweisbare, der üblichen Thermodynamik widersprechende Molekularphänomene*, Physik. Z. **13**, 1069 (1912).

[123] R. P. Feynman, R. B. Leighton, and M. Sands, *The Feynman Lectures on Physics*, Vol. 1 (Addison Wesley, Reading MA, 1963).

[124] R. H. Blick, R. J. Haug, J. Weis, D. Pfannkuche, K. von Klitzing, and K. Eberl, *Single-electron tunneling through a double quantum dot: The artificial molecule*, Phys. Rev. B **53**, 7899 (1996).

[125] S. Camalet, J. Lehmann, S. Kohler, and P. Hänggi, *Current noise in ac-driven nanoscale conductors*, Phys. Rev. Lett. (2003), in press; preprint: `arXiv:cond-mat/0212247`.

[126] Y. M. Blanter and M. Büttiker, *Shot noise in mesoscopic conductors*, Phys. Rep. **336**, 1 (2000).

published by Shaker Verlag, Aachen, ISBN 3-8322-1979-X

[127] D. H. Lyons, *Degeneracy in perturbation*, Physics Today **38**(1), 124 (1985).

[128] R. Courant and D. Hilbert, *Methoden der mathematischen Physik* (Springer-Verlag, Berlin, Heidelberg, 1968).

published by Shaker Verlag, Aachen, ISBN 3-8322-1979-X

Acknowledgement

First, I would like to express my gratitude to Prof. Dr. Peter Hänggi for giving me the opportunity to work on this fascinating subject. I profited a lot from his broad knowledge and experience. This work would have been impossible without his constant support. For his collaboration and for many fruitful discussions, comments, and hints, I would like to thank Dr. Sigmund Kohler. Furthermore, I am grateful to Prof. Dr. Gert-Ludwig Ingold for being very helpful with his expertise in the field of mesoscopic transport and for his steady support during this work.

I would also like to thank Prof. Dr. Ulrich Eckern and Dr. habil. Volkhard May for acting as referees of this thesis.

Over the last years, I enjoyed many valuable and inspiring scientific discussions with former and present colleagues in Augsburg, especially Dr. Sébastien Camalet, Dr. Ralf Eichhorn, Dr. Karen Fonseca Romero, Dr. Igor Goychuk, Andreas Hoffmann, Prof. Dr. Peter Reimann, Michael Schindler, Gerhard Schmid, Dr. Peter Schwab, Michael Straß, Prof. Dr. Peter Talkner, Dr. Michael Thorwart, and André Wobst.

A special mention goes to André as co-developer of PyX, a Python module with which the figures in the present work have been produced. I had a lot of fun working with him on this project.

For the careful proofreading of the manuscript and improving the English of this thesis, I would like to thank Dr. Sigmund Kohler and Michael Straß.

Financial support by the DFG through the Sonderforschungsbereich 486 "Manipulation von Materie auf der Nanometerskala" and the Graduiertenkolleg GRK283 "Nichtlineare Probleme in Analysis, Geometrie und Physik", the Volkswagen Stiftung in the framework of the program "Physics, Chemistry and Biology with Single Molecules" is gratefully acknowledged.

published by Shaker Verlag, Aachen, ISBN 3-8322-1979-X

published by Shaker Verlag, Aachen, ISBN 3-8322-1979-X